Regulation of Zebrafish Gastrulation Movements by *slb/wnt11*

Dissertation

zur Erlangung des akademischen Grades

Doctor rerum naturalium

(Dr. rer. nat.)

vorgelegt

der Fakultät Mathematik und Naturwissenschaften

der Technischen Universität Dresden

von

Dipl.-Biochem. Florian Ulrich

geboren am 17.12.1975 in Braunschweig

Gutachter: Dr. Carl-Philipp Heisenberg

Prof. Dr. Herwig O. Gutzeit

Prof. Dr. Stephen Wilson

Eingereicht am: 30.06.2005

I gazed down in the river's mirror
And watched its winding strum.
The water smooth ran like a hymn
And like a harp did hum.
Lay down your weary tune, lay down,
Lay down the song you strum,
And rest yourself 'neath the strength of strings
No voice can hope to hum.

Let me drink from the waters where the mountain streams flood
Let me smell of wildflowers flow free through my blood
Let me sleep in your meadows with the green grassy leaves
Let me walk down the highway with my brother in peace.
Let me die in my footsteps
Before I go down under the ground.

Oh, the benches were stained with tears and perspiration,
The birdies were flying from tree to tree.
There was little to say, there was no conversation
As I stepped to the stage to pick up my degree.
And the locusts sang off in the distance,
Yeah, the locusts sang such a sweet melody.
Oh, the locusts sang off in the distance,
Yeah, the locusts sang and they were singing for me.

Songs and Words by Bob Dylan

Acknowledgements

These years of doing my PhD were an extremely happy and lucky time in my life. Therefore, my thankfulness goes to everyone who directly or indirectly contributed to my PhD work.

First of all, I would like to thank the Brand, Oates, Dahmann and Heisenberg Labs for their continuous support and stimulating discussions and a nice working atmosphere. Special thanks go to Mathias Koeppen and Andy Oates for a continuous friendly and helpful input of new ideas and to Heather Thompson for pointing out the dominant-active rab5 to me, which has become an essential part of this thesis.

I would like to thank Prof. Herwig O. Gutzeit and Suzanne Eaton for their time and feedback in my thesis advisory committee. I would also like to thank Prof. Gutzeit for giving me the opportunity to give a talk during the International Meeting “Cells V” in Budweis.

Special thanks goes and belongs to the people with whom I cooperated in various parts of my project. First, I would like to thank David Soll and his whole lab for a very nice and stimulating atmosphere and many suggestions during my time in Iowa City. Special thanks go to Ed Voss and Paul “The Hammer” Heid for a really successful team work. You guys did an incredibly hard and good work.
I would like to thank Prof. Daniel J. Müller, Pierre-Henri Puech, Michael Krieg and Anna Taubenberger for a nice and friendly collaboration, which is still ongoing.
I am especially thankful to Viktor Schnabel for a continuous, friendly and reliable support in the analysis and quantification of many different data obtained during the second half of my PhD.

I thank Dr. Laurel Rohde for correcting this thesis and always very nice discussions; and I would like to thank Prof. Herwig Gutzeit and Prof. Stephen Wilson for reviewing my thesis.

I am very grateful to Carl-Philipp Heisenberg for designing the initial experiments before I started my PhD, and his continuous support throughout the entire thesis. I am totally sure that his effective, nice and always creative feedback made it possible for me to conduct my thesis project in the most successful way I could have imagined.

And, of course, I thank all my relatives and friends, especially my parents, grandmother and uncle for their continuous personal support and interest in my proceedings here in Dresden, which was often a true relief when times became stressful.

Parts of this thesis have already been published:

Ulrich, F.; Concha, M. L.; Heid, P. J.; Voss, E.; Witzel, S.; Roehl, H.; Tada, M.; Wilson, S. W.; Adams, R. J.; Soll, D. R.; Heisenberg, C.-P. 2003. *slb/wnt11* Controls Hypoblast Cell Migration and Morphogenesis at the Onset of Zebrafish Gastrulation. *Development* **130**: 5375 – 5834.

Ulrich, F.; Heisenberg, C.-P. 2005. Gastrulation in Zebrafish. In: Gong, Z; Korzh, V. (Ed.): Fish Development and Genetics - The Zebrafish and Medaka Models. *World Scientific Publishing*, *Singapore*.

Summary

During zebrafish gastrulation, highly coordinated cellular rearrangements lead to the formation of the three germ layers, ectoderm, mesoderm and endoderm. Recent studies have identified *silberblick* (*slb*/*wnt11*) as a key molecule that regulates gastrulation movement through a conserved pathway, which shares significant similarity with a signalling pathway that establishes epithelial planar cell polarity (PCP) in *Drosophila* (Heisenberg *et al*., 2000; Veeman *et al*., 2003), suggesting a role for cell polarity in regulating gastrulation movements.

However, the cellular and molecular mechanisms by which *slb*/*wnt11* functions during zebrafish gastrulation are still not fully understood.

In the first part of the thesis, the three-dimensional movement and morphology of individual cells in living embryos during the course of gastrulation were recorded and analysed using high resolution confocal microscopy. It was shown that in *slb*/*wnt11* mutant embryos, hypoblast cells within the forming germ ring display slower, less directed migratory movements at the onset of gastrulation, which are accompanied by defects in the orientation of cellular processes along the individual movement directions of these cells. The net movement direction of the cells is not changed, suggesting that *slb*/*wnt11*-mediated orientation of cellular processes serves to facilitate and stabilize cell movements during gastrulation.

By using an *in vitro* reaggregation assay on mesendodermal cells, combined with an analysis of the endogenous expression levels and distribution of E-cadherin in zebrafish embryos at the onset of gastrulation, E-cadherin mediated adhesion was found to be a downstream mechanism regulating *slb*/*wnt11* function during gastrulation. Interestingly, the effects of *slb*/*wnt11* on cell adhesion appear to be dependent on Rab5-mediated endocytosis, suggesting endocytic turnover of cell-cell contacts as one possible mechanism through which *slb*/*wnt11* mediates its effects on gastrulation movements.

Table of Contents

1. Abbreviations

SI units and symbols of standard multiples (m, μ, etc.) are not listed here; more specific abbreviations are explained in the text.

‘	minutes
2D	two-dimensional
3D	three-dimensional
A	area
APC	Adenomatous Polyposis Coli
APS	Ammonium Peroxodisulfate
Ar	Argon
BSA	Bovine Serum Albumine
Ca	Calcium
$CaCl_2$	Calcium Chloride
CamKII	Calmodulin dependent Kinase II
Cap1	Cyclase-associated protein 1
cDNA	complementary DNA
CE	convergent extension
cont	control
Cyc	Cyclops
da-Rab5	dominant activated Rab5
DEL	deep layer
DIAS	Dynamic Image Analysis System
DIG	Digoxygenin
dlx	distal-less
DMEM	Dulbecco’s Modified Eagle Medium
DMSO	dimethyle sulfoxide
DNA	Desoxyribonucleic Acid
dn-dyn	dominant negative Dynamin 2

Drok	*Drosophila* rho associated kinase
Dsh	Dishevelled
EDTA	ethylene diamine tetra acetate
e.g.	exemplum gratii (Lat.): for example
EGF-CFC	Epidermal Growth Factor and Cripto/FRL-1/Cryptic like
EVL	enveloping layer
FAK	Focal Adhesion Kinase
FGF	Fibroblast Growth Factor
flh	floating head
Fox	Forkhead-Box
Fz	Frizzled
GAP-43	Growth-Associated Protein 43
GDP	Guanosine Diphosphate
GFP	Green Fluorescent Protein
gsc	goosecoid
GSK	Glycogen Synthase Kinase
GTP	Guanosine Tris Phosphate
H_2O	dihydrogen oxide
He	Helium
HA	Haemagglutinin
hgg	hatching-gland gene
HRP	horse radish peroxidase
Hyb	Hybridization Medium
IgG	Immunoglobulin G
ISH	In Situ Hybridization
IQGAP	Calmodulin-binding and Ras GTPase Activating Protein
JNK	c-Jun N-terminal Kinase
KCl	Potassium Chloride
kny	knypek
LEF	Lymphoid Enhancer Factor

LRP	Low Density Lipoprotein-receptor Related Protein
MAB	Maleic Acid Buffer
$MgSO_4$	Magnesium Sulfate
mH_2O	millipore water
MIB	medio-lateral intercalation behaviour
MO	Morpholino Oligonucleotide
M_r	(relative) Molecular Weight
*m*RNA	messenger RNA
MTOC	microtubule organizing center
NA	numerical aperture
NaCl	sodium chloride
$NaHCO_3$	sodium hydrogen carbonate
Na_2HPO_4	disodium hydrogen phosphate
NaH_2PO_4	sodium dihydrogen phosphate
NaN_3	sodium azide
Ne	Neon
ntl	no tail
no	notochord
oep	one-eyed pinhead
p	probability value (t-test)
Papc	Paraxial protocadherin
PBS	Phosphate Buffered Saline
PCP	planar cell polarity
PFA	Para Formaldehyde
PI3K	Phospho-Inositide-3-Kinase
PKC	Protein Kinase C
PP2A	Protein Phosphatase 2A
ppl	prechordal plate
ppt	pipetail
Quo	Quattro

r	correlation coefficient (statistical analysis)
RGD	Arginine-Glycine-Aspartate
rnd	roundness
RN-tre	Related to the N-terminus of the tre oncogene
Rok2	Rho-associated kinase 2
rpm	revolutions per minute
RT	room temperature
SDS	sodium dodecyl sulfate
slb	silberblick
Smad	*C. elegans sma* and Mothers Against Decapentaplegic related
sqt	squint
Stbm	Strabismus
TARAM	TGFβ-Activin-related Receptor Expressed in Axial Mesoderm
TCF	T-Cell Factor
TGFβ	Transforming Growth Factor β
Ti	Titanium
SSC	Sodium Chloride Solution Supplemented with Citrate
TMR	tetramethyle rhodamine
TEMED	N,N,N',N'-Tetramethylethylendiamine
tri	trilobite
V	volume
vs	versus
wnt	Wingless- and Int-1 related
wt	wildtype
YFP	Yellow Fluorescent Protein
YSL	Yolk-Syncytial Layer

2. Material and Methods

2.1 Reagents and Buffers

Agarose solutions

1% agarose in E3 for mounting live embryos

2% agarose in E3 for cell culture and whole mount antibody stainings

Blocking buffer (for antibody stainings)

goat serum	10%
DMSO	1% (only for whole mount stainings)
NaN_3	5.0 mM

in PBSTT

stored at room temperature

Blocking buffer (for western blots)

BSA	3% (w/v)
NaN_3	5.0 mM

in PBST

Cell culture medium

DMEM	62.5 mL
Penicillin/Streptomycin	1.0 mL
Transferrin-Insulin-Selenium-X	1.0 mL
L-Glutamate 200 mM	1.0 mL

add mH_2O to 100 mL

stored at 4 °C

E2 medium

KCl	0.5 mM
NaCl	15.0 mM
$CaCl_2$	2.7 mM
$MgSO_4$	1.0 mM
$NaHCO_3$	0.7 mM
Hepes	10.0 mM

pH 6.5

stored at room temperature

E3 medium

NaCl	5.0 mM
KCl	0.2 mM
$CaCl_2$	0.3 mM
$MgSO_4$	0.3 mM
Methylene Blue	0.2 ‰ (v/v)

pH 6.5

stored at room temperature

Ginzburg Fish Ringer's solution (0.5x)

NaCl	58.0 mM
KCl	1.8 mM
$CaCl_2$	2.7 mM
$NaHCO_3$	1.3 mM

pH 7.2

stored at room temperature

Hyb$^+$ solution

formamide	50% (v/v)
SSC medium	5x
Tween-20	0.1%
Torula RNA	5 mg/mL
Heparin	50 μg/mL

pH 6.0 (adjusted adding 92 μL 1 M citric acid per 10 mL Hyb$^+$)

stored at - 20 °C

MABT

NaCl	150 mM
Maleic acid	100 mM

pH 7.5

stored at room temperature

PBST

0.1% (v/v) Tween-20 in PBS

PBSTT

0.1% (v/v) Tween-20

0.05% (v/v) Triton X-100

in PBS

PBT

0.5% (v/v) Triton X-100 in PBS

PFA (2%)

PFA	2% (w/v)
Na_2HPO_4	81 mM
NaH_2PO_4	19 mM

pH 7.4
stored at - 20 °C

Pronase solution

2 mg/mL Pronase
in E2 medium
stored at - 20 °C

SSC (20x)

NaCl	300 mM
Na-Citrate	300 mM

pH 7.0
stored at room temperature

SSCT (2x)

SSC (20x)	10 % (v/v)
Tween-20	0.1% (v/v)

stored at room temperature

SSCT (0.2x)

SSC (20x)	1 % (v/v)
Tween-20	0.1% (v/v)

stored at room temperature

SDS Sample Buffer (5x)

SDS	15.0 g
Tris 2 M pH 6.8	15.6 mL
Glycerol 87%	57.5 g
β-Mercaptoethanol	16.6 mL

add *m*H_2O to 100 mL total volume

stored at - 20 °C

Separating Acrylamide Gel (7.5%)

Acrylamide/Bisacrylamide	3.0 mL
Tris 1.5 M pH 8.8/0.4% SDS	3.0 mL
mH$_2$O	6.0 mL
APS 10%	80 μL
TEMED	8 μL

Stacking Acrylamide Gel (1.6%)

Acrylamide/Bisacrylamide	0.8 mL
Tris 1 M ph 6.8/0.4% SDS	0.8 mL
mH$_2$O	4.4 mL
APS 10%	40 μL
TEMED	15 μL

Tris-Glycin Buffer

Glycin	192 mM
Tris	25 mM
SDS	0.035 %

2.2 Morpholino Sequences

rab5c	5'-CGCTGGTCCACCTCGCCCCGCCATG-3' against the 5'-untranslated region of zebrafish rab5c (I. Castanon, personal communication)
e-cadherin	5'-ATC CCA CAG TTG TTA CAC AAG CCA T-3' against the ATG up to base pair 25; Babb and Marrs, 2004

2.3 Staging and Maintenance of Embryos

All zebrafish strains were maintained as previously described (Heisenberg *et al.*, 1996), and embryos were staged according to morphological criteria (Kimmel *et al.*, 1995). Wild-type embryos were taken from AB, Gol*, TL, Tübingen and Wik backgrounds; for mutant analysis, embryos from homozygous *slb*^{tx226} carriers in a TL background were used. To reduce background variability during antibody stainings, these carriers were only compared to wild-type TL embryos. For cell culture, heat shock treatment and western blotting, embryos were kept in E2 medium; for all other applications, E3 medium was used.

Transgenic gscGFP embryos were a gift from Henry Roehl (Sheffield, UK; http://www.shef.ac.uk/bms/research/roehl) and had been produced in the TL background as described (Gilmour *et al.*, 2002). Transgenic embryos carrying a wnt11-HA transgene under the control of a heatshock promotor ('*slb-hswnt11-HA*') were obtained from Vinzenz Link (MPI-CBG, Dresden) and produced similarly in a homozygous *slb*^{tx226} background (Gilmour *et al.*, 2002). Heat shocking embryos for 20' at 39 °C and keeping them 30' at 28 °C in E2 medium was suffient to efficiently induce wnt11-HA expression, as determined on western blots (Vinzenz Link, pers. communication).

2.4 In situ hybridisation

DIG labelled antisense riboprobes were synthesized from cDNA in pBluescript (Stratagene, USA), using a DIG labelling kit (Roche Diagnostics, Germany), and taken up in 200 μL Hyb$^+$. Whole-mount *in situ* hybridization was performed as previously described (Barth and Wilson, 1995). Embryos were fixed in 4% PFA over night at 4 °C, dechoryonated manually in PBST and preincubated in Hyb$^+$ solution for 3 h at 65 °C, followed by hybridisation over night at 65 °C with the probe diluted in Hyb$^+$; the next day, probes were washed 10 minutes each with Hyb$^+$/2x SSCT 2:1, Hyb$^+$/2x SSCT 1:2, 2x SSCT, 30 minutes each in 0.2x SSCT, then 10 minutes each with 0.2x SSCT/MABT 2:1, 0.2x SSCT/MABT 1:2, MABT, followed by incubation with 2% Block solution in MABT (Roche Diagnostics, Germany) for 5 h at and incubation with an α-DIG antibody

(Roche Diagnostics, Germany) diluted 1:5000 in 2% Block/MABT o/n at 4 °C. The antibody was washed away 4x 30 minutes each with MABT. After keeping the embryos 5 minutes in 0.1M Tris buffer pH 9.5, the signal from the probes was detected using BM Purple detection solution (Roche diagnostics) for several hours at room temperature. After detection, the staining solution was washed away 3 times with PBST, followed by refixation with 4% PFA 30 minutes, one 5 minute wash with PBST. Embryos were incubated 1 h each with 30%, 50% and 70% glycerol in PBST and stored in 70% glycerol at 4 °C. The washing steps were done at 65 °C; from the 0.2x SSCT/MABT steps onwards, all washes were done at room temeperature. The following probe concentrations were used: *hatching gland gene 1* (*hgg1*), 1:200; *floating head* (*flh*), 1:200; *goosecoid* (*gsc*), 1:200; *no tail* (*ntl*), 1:300; *distal-less 3* (*dlx3*), 1:100. A more detailed description of the probes, including corresponding references, can be found in table 7.

2.5 mRNA synthesis and morpholino oligonucleotides

The *m*Message *m*Machine kit (Ambion, UK) was used to synthesize *m*RNA *in vitro*; cDNAs for cytosolic GFP, GAP43-GFP, Cyclops, Wnt11, Stbm-HA, Rab5c-YFP, Rab5c(Q81L)-YFP ('darab5c'), RN-tre and Dynamin2 (K44A) ('dn-dyn') were cloned into a pCS2$^+$ or pcDNA3.1 expression vector (for details about the constructs and vectors used, see table 8). Rab5c(Q81L)-YFP cDNA was directly made from wild type Rab5c-YFP cDNA in pCS2$^+$ by site-directed mutagenesis with the QuikChange Site Directed Mutagenesis Kit (Stratagene, USA), using the primers 5'- CAC GGC CGG ACT GGA GCG GTA TCA C-3' and 5'-GTG ATA CCG CTC CAG TCC GGC CGT G-3' (BioSpring, Germany).

Morpholinos were obtained from GeneTools (USA; see 2.2 for sequences). The *e-cadherin* MO has been described elsewhere (Babb and Marrs, 2004; Montero *et al.*, 2005). The fluorescein-coupled rab5c-MO was directed against the 5'-UTR of Rab5c and tested for specificity by co-injection with da-rab5c-YFP mRNA, which efficiently rescued the morphant phenotype (Irinka Castanon and Carl-Philipp Heisenberg, personal communication). Throughout this study, only the rab5c homologue was analysed, since only rab5c, but not rab5a and rab5b, was both expressed during gastrulation and showed

a clearly recognizable gastrulation phenotype when 'knocked-down' (Irinka Castanon and Steffen Scholpp, personal communication).

2.6 mRNA overexpression and scatter labelling

*m*RNA and morpholino oligonucleotides (MO) were injected as previously described (Montero *et al*., 2005). For ubiquitous overexpression, *m*RNA was injected into the yolk of zygote/one-cell stage embryos, whereas for scatter-labelling, single blastomeres of 4- to 32-cell stage embryos were injected. Live time-lapse analysis of cell morphologies was done using a mixture of 120 pg GAP43-GFP and 40 pg cytosolic GFP mRNA (resembling a ratio of 3:1), whereas transgenic *gsc*GFP embryos or embryos for cell culture were injected with 250 pL of 0.5% (w/v) tetramethylrhodamine-dextran or fluorescein-dextran with M_r=2·10^6 kDa (Molecular Probes, USA) in 0.2 M KCl. To mark endocytic vesicles, 2 nL of a 10 mg/mL solution of lysin-fixable tetramethyl-rhodamine-dextran with M_r = 3·1 0^3 kDa (Molecular Probes, USA) were injected between the blastomeres of sphere - dome stage embryos.

2.7 Antibody stainings on fixed embryos

Embryos were fixed 4 h at room temperature in 2% PFA. For whole mount antibody staining, embryos were dechoryonated manually in PBT, incubated additional 2 - 3 h at room temperature in PBT, washed 4x briefly in PBSTT and incubated over night in blocking buffer. Embryos were incubated 4 h at room temperature with the primary antibody, diluted in blocking buffer, washed 4x 30 min with PBSTT, followed by a 4 h incubation with a secondary antibody; after washing 4x 30 min with PBSTT, embryos were mounted on agarose coated dishes in PBSTT medium with the dorsal side facing up, and images were acquired using a 488, 543 and/or 633 nm laser line with a 63x water-immersion objective (NA 0.9) on a Leica TCS-SP2 confocal microscope.

α-E-cadherin (1:500 - 750) and/or α-HA (1:1000) were used as primary antibodies; Cy5-coupled α-rabbit IgG (1:1000) and/or Alexa Fluor 633-coupled α-rat IgG (1:1000) secondary antibodies were used to detect the signal (see 2.14 for a more detailed description of the antibodies used in this study).

2.8 Quantification of antibody stainings

Confocal images were analysed and quantified using ImageJ Version 1.29 - 1.32 (http://rsb.info.nih.gov/ij). Intracellular vesicles were scored on single z-planes by visual inspection. Every 'dot-like' structure that showed staining intensity clearly above background and was not continuous with the plasma membrane or overlapping with the nucleus was scored as a 'vesicle'. For co-localization experiments, double positive vesicles were only counted when they showed clear overlap and similar morphology. Since the overall intensity of the antibody staining decreased towards the interior of the embryo, exclusively epiblast cells were analysed on whole mount stainings. Epiblast and hypoblast cells exhibited a similar pattern of E-cadherin localization, as judged from initial antibody stainings on paraffin- or cryosectioned embryos (C.-P. Heisenberg, personal communication).

2.9 Live confocal imaging

Shield-stage embryos were manually dechorionated and mounted in 1% agarose in E3 fish medium. Life images were obtained at 20 °C with a 60x water-immersion objective (NA 1.2) on a BioRad Radiance 2000 Multiphoton Confocal Microscope setup. For dual channel confocal timelapses, 488 nm Ar Laser and 543 nm He/Ne laser lines were used simultaneously. The emitted light was splitted by a 560 nm dichroic mirror/long path filter. Image z-stacks were obtained by scanning areas of 204.8 µm x 204.8 µm (0.4 µm/pixel) with 166 lines per second and 1.5 µm steps over a total vertical distance of 66 µm. For each experiment, 12 - 20 image stacks were acquired in 4-minute time intervals.
For single channel timelapse recordings, z-stacks were acquired by scanning an area of 102.4 µm x 102.4 µm (0.2 µm/pixel) with 750 lines per second and 0.5 µm steps over a total vertical distance of 50 µm. Stacks were taken continuously with no time gap in between. A mode-locked infrared laser line between 890 and 910 nm with an average power of 500 mW was used, originating from a Mira 900 two photon Ti::Sapphire laser. A 532 nm laser source with 5 W output power was used as a pump laser (Coherent, California).

2.10 Live image analysis

The acquired confocal z-stacks were volume rendered in 3D over time using the program Volocity (Improvision, UK). For transgenic gscGFP embryos, cell movement was analyzed by manually determining the positions of the geometric centre of the cells (the cell centroid) in three dimensions.

For the analysis of cell morphology in the GFP injected embryos, cell borders were manually outlined, using a newly developed version of the 3D-DIAS software (Soll *et al.*, 2000; Heid *et al.*, 2002). Cell bodies were always traced separately from cellular processes. To distinguish processes from a general elongation of the cell body, every cellular extension that emerged from the cell body at an angle of less than 135° (which is the sum of a right angle and 45 °) and a width of more than 2 μm was defined as a pseudopodial extension, if it was less than 2 μm thick, it was deemed a filopod (Jacinto and Wolpert, 2001). Epiblast and prechordal plate precursor cells were identified according to their position and net movement direction. The cell traces were rendered in three dimensions and measured using newly developed JAVA-based 3D-DIAS software (Heid *et al.*, 2005), which allowed the quantification of several morphometric parameters such as the surface area A, volume V, centroid position and three dimensional roundness ($rnd = 6 \cdot V \cdot \pi \cdot 0.5 \cdot A^{-1.5}$). The Roundness is a parameter that basically measures how efficient a surface encloses a volume, with rnd = 0 for a thin rod and rnd = 1 for a perfect sphere (Soll, 1995). To account for the resolution limit in the z-direction and the imperfection of manual traces, processes that had less than 5% of the length of the corresponding cell body, were less than 2 µm long or had a volume $V < 1.25 \cdot 10^{-2}$ % and a roundness rnd > 0.7 were not analysed. The subsequent quantification of the obtained morphological data was carried out using Microsoft Excel and ProFit (Quantum Soft, Basel).

2.11 Statistical analysis

Paired or unpaired Student's t-test (Microsoft Excel) with a two-tailed distribution was used to analyse significance between two mean values. For all analyses, a normal

distribution of values was assumed. For analysis of correlation between process orientation and movement persistence, a special Microsoft Excel plug-in was used that tested a linear dependence between the parameters (Müller et al., 2002).

2.12 Western Blot Analysis

Embryos at the desired stage were either manually dechoryonated with watchmaker Nr. 3 forceps, or their chorions were removed by treatment with 2 mg/mL pronase in E2 medium for 8 - 10 min at room temperature, followed by 5 washes in fresh E2 to remove the pronase. The embryos were then deyolked in 0.5x Ginzburg Fish Ringer solution, supplemented with 2.7 mM Ca^{2+}, shaken for 5' at 1100 rpm and taken up in 1 µL SDS sample buffer per embryo, heated 5' at 80 °C, vortexed and centrifuged 15' at 14.000 rpm (V. Link, personal communication). 10 - 15 embryos per lane were loaded onto a stacking gel on top of a 7.5% polyacrylamide gel and electrophoresed using Tris-Glycin Buffer. 5 µL BenchMark Protein Ladder (Invitrogen, USA) served as a molecular weight marker. Proteins were transferred onto PVDF membranes (Millipore, USA) in a semi-dry apparatus using 2 mAh/cm^2 membrane. To test for eequal protein levels on the membrane, Directly after the transfer, the membranes were stained for 10 - 15 min at room temperature in Ponceau S solution directly after the transfer and washes 2 - 3 times with PBS. For detection of specific proteins, membranes were blocked 2 h at room temperature in blocking buffer, incubated over night at 4 °C with α-E-cadherin (1:10.000) or α-actin (1:500) antibodies (see 4.12 for a detailed description of antibodies), washed 6x 5' at room temperature with PBST, incubated 4 h at room temperature with HRP coupled α-rabbit (1:20.000) or α-goat (1:5.000) secondary antibodies in blocking buffer, washed 6x 5' at room temperature with PBST and detected on Hyperfilm X-ray films using the ECL kit (Amersham, UK).

2.13 Cell culture

Cell culture was done similar to Montero *et al.* (2003). For ubiquitous induction of mesendodermal cell fates, wt and *slb*/*wnt11* mutant embryos were injected with 100 pg *cyclops m*RNA. The amount was high enough to ensure expression of no tail and

goosecoid, as determined by ISH analysis (B. Kilian, L. Carvalho, E.-M. Schoetz, C. P. Heisenberg, pers. comm.). For functional tests, 10 pg *slb/wnt11 m*RNA, 8 ng *e-cadherin* MO or 8 ng *rab5c* MO were additionally injected. To label the cells for fluorescence or confocal microscopy, 500 pL of a 0.25 % (w/v) high-molecular weight tetramethyl-rhodamine- or fluorescein-dextran solution (Molecular Probes, USA) or an additional 75 pg of GAP43-GFP *m*RNA, respectively, was injected into the embryos. Dome stage embryos were dechoryonated 10 min at room temperature with 2 mg/mL pronase and washed 5x in E2 medium. Cells were dissociated from these embryos by incubation with trypsin/EDTA (Invitrogen, USA) for 3' at 37 °C. After stopping the reaction by adding 10% (v/v) chicken serum (Invitrogen, USA), cells were spun down 3 min with 1000 rpm and taken up in Ca^{2+} containing cell culture medium. Cells were adjusted to a concentration of $2 \cdot 10^5$ cells/ml. 100 μL of the cell suspension was plated on plastic wells coated with 2.8μg fibronectin/mm^2. Cultures were incubated for 6 - 8 h at 25 °C and 2% CO_2, and images were taken with a 488 nm laser line on an inverted Zeiss LSM confocal microscope. 'Hanging drop' cultures were done as described in Ehrlich *et al.* (2002). For the co-cultures in substrate-free medium, equal numbers of two differentially labelled embryos were mixed before dissociating the cells; cells were taken up in Ca^{2+} containing medium as described before, and a 20 μL drop of cell suspension was hung upside down from the lid of a small petri dish, which had been filled with PBS to prevent the drop from drying out. Images were done after 6 - 8 h incubation at room temperature on a Zeiss Inverted epifluorescence microscope.

2.14 Antibodies

Name	antigen	antibody	species	source	reference
E-cadherin	peptide, extracellular domain of zebrafish E-cadherin	polyclonal serum	rabbit	Marrs lab	Babb and Marrs, 2004
HA	HA peptide	monoclonal, IgG_1	rat	Roche, clone 3F10	Wilson *et al.*, 1984
Actin	peptide, C-terminus of human actin	polyclonal serum affinity purified	goat	Santa Cruz, sc-1615	-
Cy5 coupled	heavy and light	polyclonal serum	goat	Jackson	-

GαM	chains of mouse IgG	affinity purified coupled to Cy5 dye		Immunoresearch 115-175-003	
Cy5 coupled GαR	heavy and light chains of rabbit IgG	polyclonal serum affinity purified coupled to Cy5 dye	goat	Jackson Immunoresearch 111-175-003	-
Alexa Fluor 633 coupled GαR	heavy and light chains of rat IgG	polyclonal serum affinity purified coupled to Alexa Fluor 633 dye	goat	Molecular Probes, A-21094	-
HRP coupled GαG	goat IgG	polyclonal serum coupled to HRP	donkey	Santa Cruz, sc-2020	-
HRP coupled GαR	heavy and light chains of rabbit IgG	polyclonal serum affinity purified coupled to HRP	goat	Jackson Immunoresearch 111-035-003	-

2.15 Plasmids for mRNA injections and antisense riboprobes

Name	Gene	cloned into	application	source	reference
GFP	GFP (cytosolic)	pCS2	*m*RNA injection	Steve Wilson, UCL London	-
GAP43-GFP	enhanced GFP (cytosolic), membrane-bound	pCS2	*m*RNA injection	Miguel Concha, Univers. de Chile, Santiago de Chile	Okada *et al*., 1999
Cyclops	D. *rerio cyclops*	pCS2	*m*RNA injection	Anukampa Barth, UCL London	Rebagliati *et al*., 1998
Wnt11	D. *rerio wnt11*	pCS2	*m*RNA injection	Masazumi Tada, UCL London	Heisenberg *et al*., 2000
Rab5c-YFP	D. *rerio rab5C*	pCS2	*m*RNA injection	Irinka Castanon, MPI-CBG Dresden	Scholpp and Brand, 2004
daRab5c-YFP 'darab5'	D. *rerio rab5c* Q81L	pCS2	*m*RNA injection	Modified from Rab5c-YFP	Pelkmans *et al*., 2004
Stbm-HA	D. *rerio stbm*, C-terminal HA-Fusion	pCS2	*m*RNA injection	Lila Solnica-Krezel, VU, Tennessee	Jessen *et al*., 2002
Wnt11-HA	D. *rerio wnt11*, C-terminal HA-fusion	pCS2	*m*RNA injection	Masazumi Tada, UCL, London	-
RN-tre		pCS2	*m*RNA injection	Irinka Castanon, MPI-CBG Dresden	Scholpp and Brand, 2004
Dyn2 (K44A) 'dndyn'	H. *sapiens* dom.-neg. *dynamin2*	pcDNA3.1	*m*RNA injection	Irinka Castanon, MPI-CBG Dresden	Scholpp and Brand, 2004

gsc	D. *rerio goosecoid*	pBluescript	antisense riboprobe	Steve Wilson, UCL, London	Schulte-Merker *et al*., 1994
ntl	D. *rerio no tail*	pBluescript	antisense riboprobe	Steve Wilson, UCL, London	Schulte-Merker *et al*., 1994
hgg1	D. *rerio hatching gland gene 1*	pBluescript	antisense riboprobe	Steve Wilson, UCL, London	Thisse *et al*., 1994
dlx3	D. *rerio distal-less 3*	pBluescript	antisense riboprobe	Steve Wilson, UCL, London	Akimenko *et al*., 1994
flh	D. *rerio floating head*	pBluescript	antisense riboprobe	Steve Wilson, UCL, London	Talbot *et al*., 1995

3. Introduction

"It is not birth, marriage or death, but gastrulation, which is truly the most important time in your life." (Wolpert, 1991)

Gastrulation is an essential process in metazoan development, by which a seemingly unstructured blastula rearranges to form an embryo with a distinct head-to-tail, left-to-right and bottom-up morphology. During this process, the three germ layers, ectoderm, mesoderm and endoderm, are formed and progenitor cells are brought into the positions from where they will later form more complex tissues and organs (Stern, 2004):

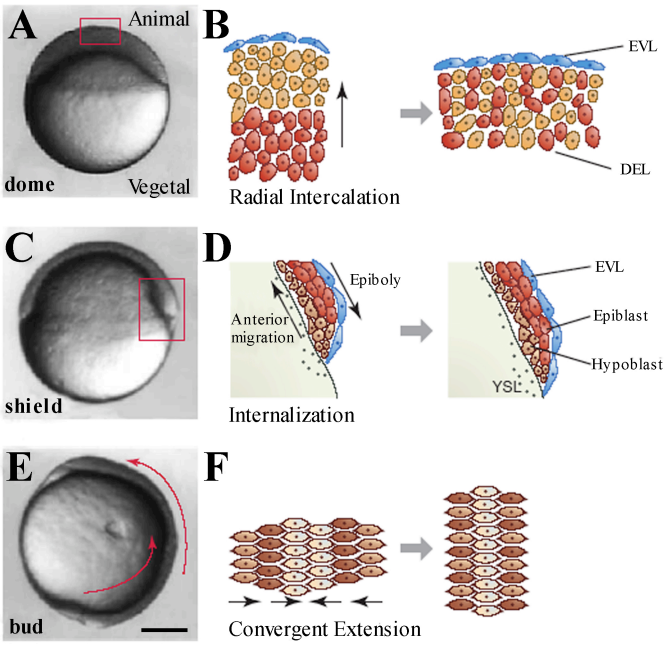

Figure 1. Gastrulation movements in zebrafish. (A) Live image of an embryo at 30% epiboly/dome stage. (B) Cartoon of the boxed area in (C) showing radial cell intercalations of blastodermal cells. (C) Live image of a shield stage embryo. (D) Cartoon of the boxed area in (C) displaying epiboly movements of ectodermal cells and the internalization and anterior migration of mesendodermal cells. (E) Embryo at bud stage - the end of gastrulation. (F) Cartoon showing the medio-lateral intercalation of cells during convergence and extension. (A), (C), (E) Lateral views. Black arrows in (B), (D), (F) demarcate the directions of cell or tissue movements. Red arrows in (E) display anteriorly directed cell movements during gastrulation. Scale bar in (E) = 100 μm. Modified from Montero and Heisenberg (2004).

The underlying principles of gastrulation movements are well conserved among vertebrates and have been extensively studied in *Xenopus laevis* and zebrafish. The initially spherical zebrafish embryo achieves its structure with distinct anterior-posterior and dorsal-ventral polarities by the complex interplay of five main types of cell movements and tissue rearrangements (see also suppl. Movie S1): epiboly, by which a multicellular blastoderm cap thins and spreads out to cover the entire yolk cell (figure 1 A,B); internalization of mesendodermal cell progenitors at the germ-ring, which forms at the margin of the spreading blastoderm (figure 1 C,D; suppl. Movie S2); the subsequent anterior migration of axial mesendodermal cells (figures 1 D; 2; suppl. Movie S2); convergence of embryonic cells towards the emerging dorsal axis and extension, by which this axis lengthens along its anterior-posterior extent (figure 1 E,F). These types of movement are closely linked to one another and cooperatively shape the early embryo (Warga and Kimmel, 1990; Kimmel *et al.*, 1995; Heisenberg and Tada, 2002; Ulrich and Heisenberg, 2005).

3.1 The cellular basis of gastrulation

Epiboly movements

Shortly after midblastula transition, the embryo consists of a mass of cells, the blastoderm, positioned on top of a big yolk cell; this stage is the so-called blastula stage. The blastoderm can be subdivided into an outer epithelium of enveloping layer (EVL) cells that cover the non-epithelial deep layer (DEL) cells, from which the embryo proper will form. Epiboly starts when EVL and DEL cells begin to spread over the yolk cell. In the DEL, epiboly is triggered by radial intercalations of cells deep within the blastula that move upwards into more superficial layers, thereby thinning the DEL along its 'inner-outer' extent and expanding its coverage over the yolk cell (figure 1 A,B). The EVL layer, by contrast, does not undergo radial cell intercalations. Instead, it connects at its leading edge to the yolk cell membrane and moves towards the vegetal pole of the

embryo to completely cover the yolk-cell at the end of gastrulation (Montero and Heisenberg, 2004).

Germ-ring formation and internalization

When epiboly has progressed to cover about half of the yolk cell (50% epiboly), the germ-ring starts to form and becomes apparent by an accumulation of cells at the blastoderm margin all around the circumference of the blastula (Warga and Kimmel, 1990). This accumulation is triggered by cells close to the margin of the blastoderm, which slow down their epibolic movements towards the vegetal pole of the embryo and, instead, move as a continuous stream of cells over the margin down towards the yolk cell. As a result, the blastoderm 'folds in' (Montero *et al.*, 2005). As soon as a recognizable germ-ring has formed, single mesendodermal progenitor cells within the blastoderm margin segregate or 'delaminate' from their neighbouring cells and become increasingly motile. These cells give rise to a distinct hypoblast (mesendodermal) layer positioned between the yolk cell and the overlying epiblast (ectodermal) layer. In the dorsal/axial region of the embryo, where hypoblast cells give rise to the future prechordal plate, delamination or ingression appears to be restricted to the marginal-most region of the germ-ring. Moreover, prechordal plate progenitors positioned at the tip of the germ-ring delaminate synchronously with direct neighbours showing similar cell behaviours (Warga and Nüsslein-Volhard, 1999; Montero and Heisenberg, 2004; Montero *et al.*, 2005). The 'folding-in' of cells during germ-ring formation is similar to the involution movements of the mesendodermal germ layer at the onset of *Xenopus* gastrulation (Winklbauer *et al.*, 1996). However, in contrast to *Xenopus*, germ-ring formation in zebrafish occurs before the internalization of mesendodermal progenitors and is at least partially independent of mesendoderm-inducing signals such as Nodal-related factors. This suggests that formation of the germ ring and the germ layers in zebrafish are separable events that involve different sets of cell fate inducing and morphogenetic signals (Montero and Heisenberg, unpublished; Montero *et al.*, 2005).

Prechordal plate migration

Once prechordal plate progenitor cells have delaminated, they move up towards the overlying epiblast, intercalate between each others at the forming interface between epiblast and hypoblast, and migrate along the epiblast in the direction of the animal pole of the gastrula (suppl. movie S2; figure 2). Therefore, the epiblast layer serves as a substrate on which prechordal plate progenitors move (Montero and Heisenberg, 2004; Montero *et al.*, 2005). Epiblast cells themselves undergo epiboly movements towards the vegetal pole of the gastrula. Therefore, cells of the prospective prechordal plate and the epiblast are moving on top of each other, but in opposite directions, implying that the movement of cells must be controlled in a highly dynamic manner, so that prechordal plate progenitors not only can compensate for the oppositely directed movement of the epiblast, but can also create some net movement towards the animal pole of the gastrula.

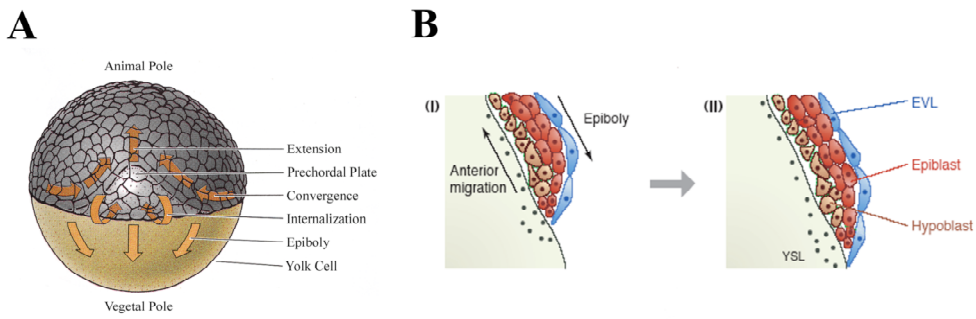

Figure 2. Internalization and anterior migration of mesendodermal cells. (A) Scheme of an embryo at the onset of gastrulation (dorsal view). Orange arrows display epibolic movements towards the vegetal pole, internalization of mesendodermal cells and movements of convergence and extension towards the animal pole. (B) Cartoon illustrating the different cell types and movements involved in mesendodermal cell internalization and migration at 60% (i) and 75% (ii) epiboly at the dorsal side of the germ-ring (lateral view). Modified from Gilbert (2003) and Montero and Heisenberg (2004).

The cellular requirements for the migration of hypoblast cells are not yet fully understood. Prechordal plate progenitor cells move in a directed and highly coordinated way towards the animal pole of the embryo; they are elongated and polarized, with numerous filopod- and pseudopod-like protrusions pointing towards their movement

direction. These protrusions appear to directly project onto cells of the overlying epiblast, indicating that during their migration from the germ-ring towards the animal pole, prechordal plate progenitors are in direct contact with the overlying epiblast cells (Montero *et al.*, 2005). Interestingly, interfering with the protrusive activity of hypoblast cells leads to slower and less directed cell movements, without changes in the net movement direction. This suggests that cell polarization and protrusive activity serve to stabilize or 'fine-tune' directed movements, but not to enable them *per se.* (Montero *et al.*, 2003; Ulrich *et al.*, 2003; Montero *et al.*, 2005).

How the overall movement direction of prechordal plate progenitor cells is determined, is not yet understood. The directed movement of hypoblast cells is reminiscent of chemotactic cell movements, and members of the fibroblast growth factor (FGF) family have been proposed to act as guidance cues for mesodermal cells during gastrulation in chick embryos (Yang *et al.*, 2002). Potential guidance cues have not been identified in zebrafish, although activation of Jak/Stat signalling on the dorsal side of the embryo is cell-autonomously required for the anterior migration of prechordal plate progenitor cells and non-cell autonomously for the convergence of paraxial cells towards the dorsal midline. This raises the possibility that Jak/Stat signalling on the dorsal side produces a secreted and yet unknown factor, which could function both as an autocrine/paracrine signal to maintain motility of prechordal plate progenitor cells and as an attractive cue for paraxial mesendodermal cells towards the dorsal midline (Yamashita *et al.*, 2002; Miyagi *et al.*, 2004; Solnica-Krezel, 2005).

Alternatively, since hypoblast cells simultaneously internalize around the circumference of the germ-ring, prechordal plate progenitor cells could be pushed away from the germ-ring towards the animal pole by newly ingressing cells at the blastoderm margin rather than actively migrate into the anterior direction. This assumption is supported by studies showing that single wild-type cells transplanted into the germ-ring of *mzoep* mutants - which lack nearly all mesendodermal induction and internalization - are able to internalize, but hardly move towards the animal pole, pointing at the possibility that this movement requires the simultaneous ingression of other mesendodermal cells (Carmany-Rampey and Schier, 2001; Montero *et al.*, 2003).

Convergence and extension

At the same time as the germ ring forms and mesendodermal cells internalize, epiblast and hypoblast cells begin to converge towards the dorsal side of the gastrula, and the anterior-posterior body axis extends ('convergence and extension'; Myers *et al.*, 2002). Convergence movements first become apparent in the germ ring by a local thickening at the dorsal side that gives rise to the embryonic organizer, the so-called 'shield' (figure 1 C). Dependent on their position within the embryo, cells exhibit different degrees of convergence and extension. Cells at the ventral side of the gastrula do not converge, but rather migrate directly towards the vegetal pole of the embryo, where they contribute to tail formation. At the lateral side, cells move towards the dorsal midline as a migratory 'stream' of cells with increasing rates of translocation. Upon approaching regions closer to the dorsal axis, they participate in convergence and extension of paraxial tissues, while their movement becomes increasingly faster and more direct (Sepich *et al.*, 2000; Myers *et al.*, 2002). At the dorsal side of the embryo, convergence and extension movements are coupled through the medio-lateral intercalation of cells between each other, leading to a displacement of cells in the anterior-posterior direction. Therefore, convergence movements become translated into the extension of the embryonic body axis ('medio-lateral intercalation behaviour', MIB; figure 1 E,F; Concha and Adams, 1998; Glickman *et al.*, 2003). Importantly, in zebrafish, convergence alone can not account for extension of the embryonic axis, since *no tail*(*ntl*)$^{-/-}$ mutants, which display strongly reduced convergence movements, still extend their axis in the anterior-posterior direction. This indicates, that - in contrast to *Xenopus*, where medio-lateral intercalation is thought to provide the predominant driving force for convergent extension movements - MIB can not be the only mechanism by which the embryonic body axis forms in zebrafish. Alternative mechanisms that could account for the extension of axial tissues are directed movements and radial intercalations of hypoblast and epiblast cells during epiboly (Glickman *et al.*, 2003; Keller *et al.*, 2003).

During medio-lateral cell internalization in *Xenopus*, cells become polarized, with large lamelliform protrusions at their medial and lateral ends, and small filoform protrusions at

their anterior and posterior surfaces. The medial and lateral protrusions appear to exert traction on adjacent cells, and generate tension along the medio-lateral axis. The cells become elongated, oriented parallel to one another, and intercalate between each other along the medio-lateral axis (Keller, 2002; Keller *et al.*, 2003). Similarly, in zebrafish, epiblast and hypoblast cells align and elongate along the medio-lateral axis of the embryo, and this elongation seems to be required for the velocity and stability of their movements. Cells from both germ-layers also display multiple medio-laterally oriented protrusions that project onto neighbouring cells, but whether this protrusive activity is required to stabilize cell movements or to directly mediate them is not yet fully understood (Ulrich and Heisenberg, unpublished; Concha and Adams, 1998; Topczewski *et al.*, 2001; Jessen *et al.*, 2002; Marlow *et al.*, 2002; Kilian *et al.*, 2003; Ulrich *et al.*, 2003).

3.2 Molecular and cell biological mechanisms of gastrulation

Involution and mesendoderm induction

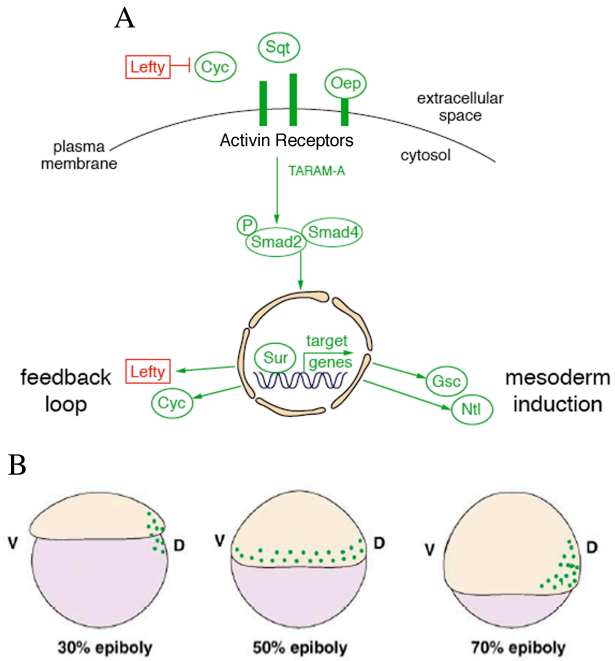

Figure 3. Nodal signaling during zebrafish gastrulation. (A) The nodal signaling pathway with members identified in zebrafish (see 1.2.1 for details). The secreted ligands Cyclops (Cyc) and Squint (Sqt) bind to activin-receptors with One-eyed pinhead (Oep) as an essential co-receptor. This leads to the activation of Smad proteins, which heteromerize and translocate to the nucleus, where they associate with transcriptional regulators such as Schmalspur (Sur). This upregulates the expression of mesoderm inducing signals like Goosecoid (Gsc) and No Tail (Ntl) and a molecular feedback loop involving the nodal ligand Cyc and the Lefty proteins, which serve as inhibitory factors. (B) Schematic zebrafish embryo during gastrulation, with green dots denoting *cyc*/*sqt* expression over the course of gastrulation. V - ventral side, D - dorsal side. Modified from Whitman (2001) and Kimelman and Schier (2002).

In zebrafish embryos, mesendodermal (hypoblast) fates in the germ-ring are specified by the Nodal signalling pathway. The *Nodal* gene was first isolated in mutagenized mice that exhibited severe gastrulation defects and was subsequently found to be expressed in the mouse gastrulation organizer, the node - hence its name (Conlon *et al.*, 1991; Zhou *et al.*, 1993). Nodal encodes a secreted molecule of the Transforming Growth Factor β (TGFβ) family, and Nodal related molecules have been identified in other vertebrates. In *Xenopus*, TGFβ like molecules such as activin have been proposed to serve as mesoderm inducers, and the Nodal factors *cyclops* (*cyc*) and *squint* (*sqt*) are required for germ-layer formation in zebrafish (Smith, 1995; Rebagliati *et al.*, 1998; Sampath *et al.*, 1998; Feldman *et al.*, 1998). It is now generally assumed that Nodals serve as mesendoderm inducers in all vertebrates; they exert additional roles in the regulation of left-right asymmetry and neural patterning (Burdine and Schier, 2000; Schier and Talbot, 2001; Schier, 2003).

The Nodal signalling pathway has been dissected both genetically and biochemically. In zebrafish, Cyclops or Squint bind to activin-receptors and EGF-CFC coreceptors like TARAM-A and *one-eyed pinhead* (*oep*), respectively (Gritsman *et al.*, 1999). The signal is transmitted intracellularly by phosphorylation of Smad2 and possibly Smad3. Following phosphorylation, they associate with Smad4 and translocate into the nucleus, where they interact with transcription factors such as FoxH1 (which is disrupted in zebrafish *schmalspur*/*sur* mutants) and regulate the transcription of specific target genes. Among these genes are determinants of mesendodermal fates, like *goosecoid* (*gsc*) or *no*

tail (*ntl*), *cyc* itself, and the *lefty* factors, which serve as secreted inhibitors of Nodal proteins (figure 3 A; Whitman, 2001; Schier, 2003). Ntl is sufficient, albeit not exclusively required, for the expression of *wnt11*, which encodes a secreted glycoprotein with important functions in morphogenesis and gastrulation (see also 3.2.2 and following chapters). Both *wnt11* and *ntl* display overlapping domains of expression at the onset of gastrulation (Makita *et al.*, 1998; Tada and Smith, 2001; Ulrich *et al.*, 2003).

The expression patterns of *sqt* and *cyc* indicate that they act as spatially restricted signals (Rebagliati *et al.*, 1998; Sampath *et al.*, 1998). In early blastula stages, *sqt* is expressed in dorsal marginal blastomeres and, slightly later, in the dorsal region of the yolk syncytial layer (YSL), an extraembryonic syncytium directly covering the yolk cell, which is a source of mesendoderm inducing signals (Mizuno *et al.*, 1996; Schier and Talbot, 2001). *cyc* is initially expressed in the late blastula stage. Shortly before the onset of gastrulation, both *cyc* and *sqt* transcripts are localized around the entire circumference of the margin, consistent with their roles in the formation of mesendodermal tissue in the whole embryo. At the onset of gastrulation, *cyc* is strongly expressed in internalizing dorsal mesendoderm, and *sqt* is expressed in a small group of dorsal marginal cells. As gastrulation proceeds, *sqt* expression ceases, while *cyc* continues to be expressed in axial mesendoderm throughout gastrulation (figure 4B; Schier and Talbot, 2001).

In the absence of Nodal signalling, zebrafish embryos lack all endodermal and most of mesodermal tissues; in zebrafish double mutant for the nodal factors *cyc* and *sqt* or the coreceptor *oep*, notochord markers like *floating head* (*flh*) and *ntl* and prechordal plate markers like *gsc* are not expressed, reflecting the transformation of the corresponding tissues into presumptive neurectoderm (Feldman *et al.*, 1998; Gritsman *et al.*, 1999; Schier and Talbot, 2001). Conversely, overexpression of Nodals in presumptive ectoderm induces cells to become mesendoderm (Schier and Shen, 2000; Whitman, 2001).

Nodal factors can act directly at a distance from the source of their production, and different levels of Nodal signalling can induce different cell fates (Schier, 2003).

Whereas *goosecoid* is only induced by high concentrations of *cyc* or *sqt*, lower levels of Nodal signalling are sufficient for *ntl* or *flh* expression. The concentration-dependent effects of Nodal signaling are also illustrated at the dorsal blastula margin in zebrafish, where cells give rise to prechordal plate anteriorly and notochord more posteriorly: prechordal plate progenitors reside closer to the margin, where Nodals are expressed, whereas notochord progenitors are located at a distance from the margin (Gritsman *et al.*, 2000). In addition, high levels of Nodals are required to induce endodermal fates, whereas most mesoderm still develops under conditions of reduced Nodal signalling (Stainier, 2002; Schier, 2003). At the onset of gastrulation, Nodals induce a mix of cells with either mesodermal, endodermal or mixed fates in the hypoblast, with a bias towards endodermal fates closest to the site of highest Nodal activity. Only after involution both germ-layers separate into morphologically distinct populations. By mid-gastrulation stage, endodermal cells gradually flatten and extend filopodial processes, forming a noncontiguous inner layer of cells at the yolk cell surface, while mesodermal cells form a coherent layer of rounder and more regularly shaped cells between endoderm and ectoderm (Warga and Nüsslein-Volhard, 1999).

Wnt signalling and the regulation of gastrulation movements

Wnt proteins constitute a family of secreted glycoproteins that can be found in species throughout the animal kingdom, ranging from *Hydra* to humans (Miller, 2001). During development, they are involved in a variety of processes, such as axis induction and patterning, tissue and organ morphogenesis, cell migration, polarity, division and axon guidance (Veeman *et al.*, 2003; Aulehla and Herrmann, 2004; Gong *et al.*, 2004; Walston *et al.*, 2004). In many cases, Wnt proteins signal through the so-called ***canonical*** pathway, originally found to specify segment polarity in *Drosophila* and mediate axis induction in *Xenopus*. In this pathway, the Wnt ligand binds to its transmembrane receptor Frizzled (Fz) and its LRP5/6 coreceptor, followed by activation of the cytoplasmic protein Dishevelled (Dsh). This leads to the inhibition of a "destruction complex" containing Adenomatous Polyposis Coli Protein (APC), Axin and Glycogen

Synthase Kinase 3 (GSK3), which in turn stabilizes β-Catenin and prevents it from degradation through a ubiquitin/proteasome dependent process. The stabilization of β-Catenin enables its translocation to the nucleus, where it associates with Lymphoid enhancer factor/T cell factor (Lef/Tcf) and participates in the transcriptional regulation of various target genes (figure 4 A; Cadigan and Nusse, 1997; Huelsken and Behrens, 2002; Veeman *et al.*, 2003; Tolwinski and Wieschaus, 2004).

In addition, both gain- and loss-of-function studies in vertebrates have revealed a class of Wnt proteins that do not function in embryonic patterning, but mainly regulate tissue rearrangements and cell migration during development. For example, while misexpression of Wnt1, Wnt3 or Wnt8 in *Xenopus* causes a β-catenin dependent duplication of the embryonic axis, overexpression of Wnt4, Wnt5 and Wnt11 mainly results in a disruption of morphogenetic movements without altering cell fates (Du *et al.*, 1995). In zebrafish, *wnt8* is required for mesodermal and neurectodermal patterning during early development (Lekven *et al.*, 2001). In contrast, a mutation in the zebrafish *pipetail(ppt)/wnt5* gene leads to defects in convergent extension movements in posterior parts of the embryo, and *silberblick(slb)/wnt11* is required for convergent extension movements along the entire anterior-posterior axis as well as prechordal plate migration during gastrulation. Both genes act redundantly in the anterior hypoblast (Rauch *et al.*, 1997; Heisenberg *et al.*, 2000; Kilian *et al.*, 2003; Ulrich *et al.*, 2003). Loss of *wnt4* function has not yet been analyzed in zebrafish, but *wnt4* misexpression can induce cell movement defects during gastrulation without disturbing embryonic patterning. Furthermore, *wnt4* is required for the regulation of apical cell migration in the *Drosophila* ovary. These observations suggest a function for *wnt4* in the regulation of cell movements and tissue rearrangements during embryonic development (Ungar *et al.*, 1995; Cohen *et al.*, 2002).

Interestingly, in *Xenopus*, Wnt5a is also capable of interfering with dorsal-ventral patterning of the gastrula through activation of the canonical Wnt signalling pathway (He *et al.*, 1997; Sumanas *et al.*, 2000; Umbhauer *et al.*, 2000), and maternally provided Wnt11 is required for the β-catenin dependent induction of the dorsal axis (Tao *et al.*,

2005). The involvement of *wnt11* and *wnt5* in embryonic patterning of other organisms is less clear, although massive *wnt11* overexpression or loss of maternal *wnt5* function have both been reported to interfere with dorsal-ventral patterning, and *wnt5* has been proposed to antagonize the canonical Wnt/β-catenin pathway both in zebrafish and cultured mammalian cells (Makita *et al.*, 1998; Topol *et al.*, 2003; Westfall *et al.*, 2003).

Besides *slb*/*wnt11* and *ppt*/*wnt5*, the mutants *knypek* (*kny*/*glypican4*/*6*) and *trilobite* (*tri*/*strabismus*) were recovered in saturation screens for early zebrafish development (Driever *et al.*, 1996; Haffter *et al.*, 1996; Heisenberg *et al.*, 1996; Solnica-Krezel *et al.*, 1996; Heisenberg and Nüsslein-Volhard, 1997; Heisenberg *et al.*, 2000). These mutants all show defective gastrulation movements and genetically and functionally interact with each others (Topczewski *et al.*, 2001; Jessen *et al.*, 2002; Kilian *et al.*, 2003), suggesting that these components function in a common signalling pathway (figure 4 B; Veeman *et al.*, 2003). In this pathway, Wnt5 and Wnt11 likely use Frizzled2 (Fz2) and Frizzled7 (Fz7), respectively, as receptors: loss-of-function of *fz2* and *wnt5* produces similar defects in convergence and extension in zebrafish, and Wnt5 and Fz2, but not Fz1, can functionally interact in zebrafish. Fz7 directly binds to and functionally interacts with Wnt11 in *Xenopus* (Slusarski *et al.*, 1997; Djiane *et al.*, 2001; Kilian *et al.*, 2003). As in the canonical Wnt pathway, Fz proteins transduce their signalling functions via Dsh to downstream components. Molecular and functional studies of these downstream elements in zebrafish and *Xenopus* revealed a complex, non-linear network of interacting components. One branch of this signalling module involves the modulation of intracellular Ca^{2+} levels, since overexpression of Wnt5 and Fz2 in zebrafish embryos stimulates intracellular Calcium release in a G protein coupled manner, which is thought to activate Ca^{2+} sensitive enzymes including Ca^{2+}/calmodulin dependent protein kinase II (CamKII) and protein kinase C (PKC) (Slusarski *et al.*, 1997; Kühl *et al.*, 2000). Other components that mediate signalling downstream of Fz include Daam1 - which links activated RhoA and Rac to Dsh in *Xenopus* - and Cdc42 (Djiane et al., 2000; Habas *et al.*, 2001; Choi and Han, 2002; Habas *et al.*, 2003; Penzo-Mendez *et al.*, 2003). The functions of RhoA, Rac and Cdc42 in vertebrate gastrulation are not fully understood, probably

because of their widespread role in the regulation of membrane traffic, cytoskeletal rearrangements and cell-cell adhesion (van Aelst and Symons, 2002). RhoA regulates cytoskeletal rearrangements downstream of *slb*/*wnt11* via Rho-associated kinase 2 (Rok2), suggesting a role for Wnt11 signalling in the regulation of the actin cytoskeleton (Marlow *et al.*, 2002). Paraxial protocadherin (Papc) functionally interacts with Wnt/Fz signalling, suggesting a cross-talk between Wnt11 signalling and mediators of adhesive contacts. In addition, other adhesion molecules like integrins and cadherins are involved in the regulation of normal gastrulation movements (figure 5; Marsden and DeSimone, 2003; Montero and Heisenberg, 2003; Medina *et al.*, 2004; Unterseher *et al.*, 2004).

Interestingly, several components used in this signalling module have homologues that function in the *Drosophila* planar cell polarity (PCP) pathway, which mediates the correct orientation of ommatidia in the eye, the polarized outgrowth of sensory bristles in the thorax and the polarization of cells in the wing epithelium (Adler and Lee, 2001; Adler, 2002). Initial evidence for a conservation of both pathways comes from the analysis of the *slb*/*wnt11* mutant embryo and the functional characterization of *dsh* in *Xenopus* and zebrafish. Defective gastrulation movements in the *slb*/*wnt11* mutant can be rescued by a truncated *dsh* construct that is homologous to the *dsh* version required for PCP signalling in *Drosophila*. Furthermore, a dominant negative *dsh* that specifically interferes with PCP in *Drosophila* is able to disrupt gastrulation movements and cell polarity in *Xenopus* and zebrafish (Heisenberg *et al.*, 2000; Wallingford *et al.*, 2000).

Since this pathway utilizes domains of Dsh which are different from those regulating canonical wnt signalling, and since this pathway is independent from the β-catenin dependent transcription of target genes, it is termed the ***non-canonical*** or Wnt/PCP pathway. However, it should be noted that this distinction is not totally strict: Both canonical and non-canonical pathways can antagonize each other's function, and cell movement can be regulated through a pathway which involves components of both canonical and non-canonical pathways (Cohen *et al.*, 2002; Topol *et al.*, 2003; Westfall *et al.*, 2003).

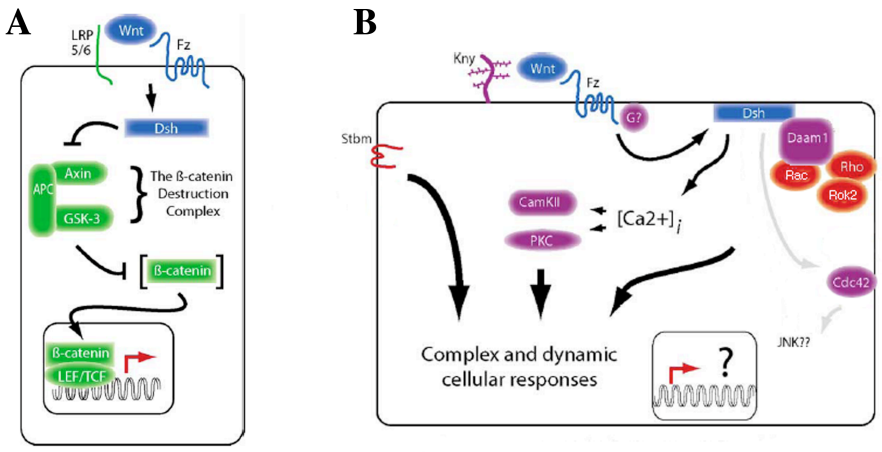

Figure 4. Canonical and non-canonical Wnt pathways. (A) Canonical Wnt signalling requires the Frizzled and LRP5/6 coreceptors and leads to the activation of Dishevelled, which inhibits the activity of the so-called β-catenin destruction complex, a complex of proteins including APC, Axin, and GSK-3 that otherwise phosphorylates β-catenin and targets it for destruction by the ubiquitin-proteasome pathway. These and other mechanisms allow Wnt ligands to both stabilize β-catenin and promote its entry into the nucleus, where it associates with other transcription factors such as proteins of the LEF/TCF family and regulates the expression of target genes. (B) Non-canonical Wnt signaling requires Frizzled receptors and the proteoglycan coreceptor Knypek. Like Wnt/β-catenin signaling, this pathway involves Dishevelled. A main branch downstream of Dishevelled involves small GTPases of the Rho family, and activation of Rho requires the bridging molecule Daam1. Non-canonical signalling can also stimulate calcium flux and the activation of the calcium-sensitive kinases PKC and CamKII. Gene transcription does not seem to be involved in non-canonical Wnt signalling, although it can also not be definitely excluded. Modified from Veeman *et al*. (2003).

Given the molecular conservation of non-canonical Wnt signalling and PCP signalling in *Drosophila*, it is tempting to speculate that Wnt11 regulates cell migration and tissue rearrangements through the modulation of cell polarity, which is essential for cells to migrate (Lauffenburger and Horwitz, 1996). However, the cellular and molecular mechanisms by which the Wnt/PCP pathway functions in vertebrates are largely unknown. While planar cell polarity in the *Drosophila* wing epithelium is manifested by the outgrowth of a single actin- and tubulin-filled, distally pointing hair at the distal vertex of each wing cell (Eaton, 1997; Adler, 2002), the precise cellular basis that gives

rise to defective gastrulation movements in Wnt/PCP mutants of the zebrafish is not yet understood. It has been speculated that the movement defects observed in these mutants are due to a failure of cells to elongate along the medio-lateral axis of the embryo, which is thought to constitute a prerequisite for cell intercalation behavior driving convergent extension (Topczewski *et al.*, 2001; Marlow *et al.*, 2002). However, it is not known if the lack of medio-lateral cell elongation in these embryos is a mere secondary consequence of these cells not being able to move dorsally and intercalate or if the Wnt/PCP pathway directly affects the polarization of these cells. Furthermore, it is not clear to which extent the elongation of cells during vertebrate gastrulation can be compared to the polarization of *Drosophila* wing epithelial cells. The formation of a single wing hair at the distal vertex of such a cell is preceded by the asymmetric localization of PCP pathway components along the cell membrane. In contrast, no definitive asymmetric membrane localization of homologous proteins in vertebrate cells has yet been observed (Rothbacher *et al.*, 2000; Axelrod, 2001). One possible reason for this could be that the organization of the tissues in which the Wnt/PCP pathways functions is rather different between *Drosophila* and vertebrates. While wing cells are organized in a tight, stationary epithelium with little space between single cells, mesendodermal cells in gastrulating *Xenopus* and zebrafish appear more loosely associated and show extensive movements relative to each other and on the substrate to which they attach (Keller *et al.*, 2000; Glickman *et al.*, 2003). Therefore, although several components of the PCP pathways are conserved between *Drosophila* and vertebrates, the functions of these pathways in *Drosophila* planar cell polarization and vertebrate gastrulation movements could be rather different.

Non-canonical Wnt signalling and the regulation of cytoskeletal rearrangements

One possible mechanism, by which non-canonical Wnt signalling regulates cell movements during gastrulation is through the modulation of cytoskeletal rearrangements. The actin-regulatory proteins Cyclase-Associated Protein 1 (Cap1) and Quatro (Quo) are required for the anterior migration of prechordal plate progenitor cells (Daggett *et al.*,

2004). Furthermore, Cdc42 acts downstream of Fz7 to regulate cell rearrangements in *Xenopus* animal caps, and this function has been proposed to be mediated by the actin cytoskeleton (Djiane *et al.*, 2000). During the establishment of planar cell polarity in *Drosophila* wing epithelia, actin becomes localized along an apical microtubule web, that lies at the level of apical cell junctions, towards the distal vertex of each wing cell, where it becomes a major component of the emerging wing hair (Eaton, 1997). PCP components like the small GTPases RhoA and Rac and the Rho effector *Drosophila* rho-associated kinase (Drok) restrict the outgrowth of actin-filled prehairs to one per wing cell. Widerborst, the B' regulatory subunit of Protein Phosphatase IIA (PP2A) organizes tissue polarity proteins into proximal and distal cortical domains, thus determining wing hair orientation. Interfering with *widerborst* function leads to a disruption of the planar microtubule web and defective polarisation of wing hair outgrowth. These experiments suggest a link between PCP signalling and the cytoskeleton (Eaton *et al.*, 1996; Strutt *et al.*, 1997; Winter *et al.*, 2001; Hannus *et al.*, 2002).

In *Xenopus*, Rac and RhoA mediated cytoskeletal rearrangements are required downstream of Wnt/Fz signalling for convergence and extension movements of mesodermal cells during gastrulation. Furthermore, in zebrafish, abolishing the activity of Widerborst (B' subunit of PP2A, s. a.) leads to defects in gastrulation movements. The Drok homologue Rok2 functions downstream of *slb*/*wnt11* to mediate the elongation, medio-lateral alignment and movement stability of mesodermal cells during zebrafish gastrulation. These observations suggest a link between cytoskeletal rearrangements and non-canonical Wnt signalling (Hannus *et al.*, 2002; Marlow *et al.*, 2002; Habas *et al.*, 2003). The cytoskeleton could instructively determine cell shape and/or the outgrowth of cellular protrusions by recruitment of actin to sites of process outgrowth, or it could act in a more permissive way, e.g. by regulating the strength of the actin cortex at the cell surface, which would then secondarily allow the remodelling of cell shape and the outgrowth of cellular protrusions.

Alternatively, the regulation of cytoskeletal rearrangements could be coupled to the regulation of processes such as endocytosis. Actin is recruited to endocytic patches in mammalian cells, and polymerisation of F-actin is thought to drive the fission of vesicles

from the plasma membrane into the cell (Merrifield *et al.*, 2002; Kaksonen *et al.*, 2003; Ayscough, 2004). Endocytic transport of membrane and adhesion receptors such as integrins from the rear of a cell to its front has been proposed to regulate cell motility in neutrophils; interestingly, the release of integrins from their substrates requires intracellular calcium transients, suggesting a connection between calcium signalling, endocytosis and cell motility (Lawson and Maxfield, 1995; Bretscher, 1996).

Non-canonical Wnt signalling and the regulation of cell adhesion

The regulation of cell adhesion is vital for cells to rearrange into distinct tissues during development, and there are several lines of evidence that non-canonical Wnt signalling modulates the adhesive behaviour of cells during gastrulation (Steinberg, 1996; Wedlich, 2002). Paraxial protocadherin (Papc) is expressed in mesodermal cells of *Xenopus* and zebrafish and is required downstream of non-canonical Wnt signalling for convergent extension movements (Kim *et al.*, 1998; Yamamoto *et al.*, 1998). More recent studies in *Xenopus* have shown that Papc functionally interacts with non-canonical Wnt signalling through RhoA, Rac and c-Jun N-terminal Kinase (JNK) to control convergence extension movements in mesodermal cells (figure 5; Unterseher *et al.*, 2004; Medina *et al.*, 2004). Interestingly, Papc is required for the separation of mesodermal and ectodermal cells at the onset of gastrulation, a function which was previously found to be mediated by Fz7 and PKC in a G-protein dependent manner. This points to a common role for protocadherin signalling via RhoA and non-canonical Wnt signalling through the regulation of intracellular Ca^{2+} levels, in controling the adhesive properties of tissues during gastrulation (Winklbauer *et al.*, 2001; Medina *et al.*, 2004).

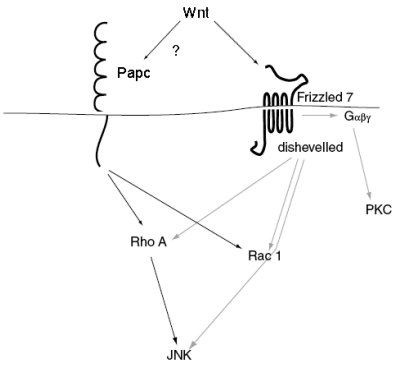

Figure 5. Crosstalk between Papc and non-canonical Wnt signalling during *Xenopus* gastrulation. Non-canonical Wnt ligands bind to Frizzled and possibly interact with Papc, although the link between Wnts and protocadherins remains enigmatic. Both Dishevelled and Papc functionally interact with RhoA and Rac, while JNK is probably activated through Dsh and RhoA. Both RhoA and Wnt/Ca^{2+} signalling through PKC are thought to regulate tissue separation during gastrulation. Modified from Unterseher *et al.* (2004).

In addition to *intra*cellular Ca^{2+} signals, recent reports suggest that *inter*cellular Ca^{2+} waves could play an important role in the coordination of individual cell behaviour within tissues undergoing gastrulation movements (Tada and Concha, 2001; Wallingford et al., 2001; Webb and Miller, 2003). Calcium waves are generated within dorsal tissues of gastrula embryos and propagate to surrounding cells over long distances. This dynamic event is closely associated with convergent extension of the dorsal tissues. In *Xenopus*, non-canonical Wnt signalling may be involved in the regulation of these Ca^{2+} waves, since their frequency was reduced upon misexpression of a dominant-negative form of XFz8 which strongly inhibits both canonical and non-canonical Wnt signalling (Wallingford *et al.*, 2001). The cellular function of these waves is less clear. Calcium has been implied in the regulation of actin dynamics or microfilament stability during neurite outgrowth as well as the stabilization of myosin thick filaments during the formation of striated muscle in *Xenopus* (Lankford and Letourneau, 1989; Neely and Gesemann, 1994; Ferrari *et al.*, 1998; Welnhofer et al., 1999). In Medaka, free Ca^{2+} in the cytoplasm, released from both an extracellular and intracellular pool, has been implied in the regulation of microfilament-driven contractions of the blastoderm, and during ooplasmic segregation, Ca^{2+} is required for the stability of the radial microtubule array that makes up the microtubule organizing center (MTOC) at the animal pole of the oocyte (Sguigna *et al.*, 1988; Abraham *et al.*, 1995). These observations suggest that Calcium could also serve to control gastrulation movements in zebrafish by controlling cytoskeletal rearrangements, although the molecular mechanism by which Calcium controls the cytoskeleton is not entirely clear. Besides regulating the stability or strength of

cytoskeletal elements, the microfilament-driven contractility of the actin cytoskeleton provides an attractive function for Ca^{2+} in this process (Webb and Miller, 2003). As an alternative possibility besides modulation of the cytoskeleton, Ca^{2+} could modulate cadherin- or protocadherin based cell-cell adhesion (Webb and Miller, 2003).

Recent reports have also stressed the importance of cell-substrate adhesion during gastrulation and its connection with non-canonical Wnt signalling. In *Xenopus* and zebrafish, fibronectin is an abundant component of the extracellular matrix and required for gastrulation movements (Winklbauer and Keller, 1996; Trinh and Stainier, 2004). Perturbation of Wnt/PCP pathway in *Xenopus* leads to defects in the polarized assembly of fibronectin fibrils on mesodermal tissue surfaces (Davidson *et al.*, 2004; Goto *et al.*, 2005).

In addition, fibronectin blocking antibodies or dominant-negative inhibitors of integrin function disrupt convergent extension movements, medio-lateral cell elogation and intercalation behaviour in *Xenopus*, indicating that interactions between integrins and fibronectin are essential for the regulation of gastrulation movements (Marsden and DeSimone, 2003). Interestingly, during *Xenopus* gastrulation, C-cadherin functions downstream of integrin β1, and integrin β1 is able to modulate the adhesive state of C-cadherin. This suggests that integrin signalling promotes cell rearrangements through the modulation of cadherin based cell-cell adhesion (Montero and Heisenberg, 2003; Marsden and DeSimone, 2003).

Interestingly, in that study, C-cadherin based adhesion is independent of cadherin or integrin expression levels. Several mechanisms could explain these observations. One possibility is that integrin signalling regulates the stability of adherens junctions by phosphorylation of cadherins or associated proteins, such as β-catenin (Gumbiner, 2000). Alternatively, integrins could regulate the endocytosis and recycling of C-cadherin at the plasma membrane without interfering with the total levels of C-cadherin. The endocytic turnover of cadherins has been proposed to regulate the stability of cell-cell contacts, and clathrin-mediated endocytosis of C-cadherin is required for the elongation of activin-treated animal caps in *Xenopus* (Le *et al.*, 1999; Jarrett *et al.*, 2002).

In *Xenopus*, integrin signalling recruits Dsh to the plasma membrane, and Dsh localization at the plasma membrane activates non-canonical Wnt signalling. Together with the observation that cadherin function is downstream of integrin activity, this suggests that integrin (and possibly integrin-fibronectin interactions) and non-canonical Wnt signalling cooperate in the regulation of cadherin-mediated cell adhesion to mediate gastrulation movements (Rothbacher *et al.*, 2000; Marsden and DeSimone, 2001; Marsden and DeSimone, 2003). In *Drosophila* ovaries, Wnt4 has been proposed to facilitate apical cell migration by regulating Focal Adhesion Kinase (FAK) activity via Fz, Dsh and PKC, suggesting another link between non-canonical Wnt signalling and the regulation of cell-substrate adhesion (Cohen *et al.*, 2002; Veeman *et al.*, 2003).

The involvement of cadherin-mediated cell-cell adhesion for the regulation of gastrulation movements is also supported by previous studies in *Xenopus*. Both interfering with cadherin function or increasing C-cadherin adhesive activity inhibits mesodermal cell movement, suggesting that cadherin levels have to be tightly regulated to enable proper cell movements (Kühl *et al.*, 1996; Lee and Gumbiner, 1995; Zhong *et al.*, 1999). Furthermore, blocking the function of different *Xenopus* cadherin molecules impairs the separation behaviour between involuted mesodermal progenitors and the blastocoel roof, indicating that cadherin-mediated cell-cell adhesion is required for germ-layer separation at the onset of *Xenopus* gastrulation (Wacker *et al.*, 2000). As tissue separation at the onset of gastrulation is also mediated by non-canonical Wnt signalling, cadherin mediated cell-cell adhesion could be involved in or interact with the non-canonical Wnt signalling pathway. Interestingly, overexpression of wnt5a decreases cadherin mediated adhesion between mesodermal cells in *Xenopus* reaggregation assays, suggesting that non-canonical Wnt signalling can regulate cadherin-mediated cell-cell adhesion (Torres *et al.*, 1996).

Local recruitment of adhesive contacts can be a potent mechanism to regulate the strength of cell adhesion and cell-cell rearrangements. The compaction of early mouse embryos, leading to the formation of the trophectodermal epithelium, is a good example. In this

context, E-cadherin–mediated adhesion is rapidly activated in response to a cellular signal (Vestweber *et al.*, 1987) through the recruitment of pre-existing E-cadherin at the cell surface to regions of cell contact (Fleming and Johnson, 1986; Vestweber *et al.*, 1987). Moreover, during convergence and extension movements in *Xenopus*, cells continuously rearrange their positions relative to each others, and this requires the rapid breakage of existing and the formation of new cell-cell contacts (Gerhart and Keller, 1986). A similar rearrangement of mesendodermal cells can be observed at the onset of zebrafish gastrulation, when freshly internalized cells build up the prospective prechordal plate. These cells rapidly modulate their shape and frequently change their contacts to other cells, which becomes most obvious at the interface between prechordal plate and epiblast (suppl. movie S2; Montero *et al.*, 2005).

Junctional rearrangements have also been proposed as a driving force for *Drosophila* germ band extension (GBE). In this process, cells locally rearrange and intercalate within each other, leading to a medio-lateral narrowing and an anterior-posterior elongation of the embryonic body axis, which requires the remodelling of cell-cell contacts through the polarized recruitment of Myosin II. Interestingly, the regulatory light chain of Myosin II has been implicated as a target of Drok in Drosophila and Rok2 in zebrafish. Since Drok functions within the Drosophila PCP pathway and Rok2 is downstream of *slb*/*wnt11* function in zebrafish, non-canonical Wnt/PCP signalling could function through the localized remodelling of cell-cell junctions (Winter *et al.*, 2001; Marlow *et al.*, 2002; Bertet *et al.*, 2004; Zallen *et al.*, 2004; Lecuit, 2005).

How the adhesive activity of cadherins at sites of cell-cell contacts is regulated on a molecular and cell biological level, is not entirely clear. Catenins bind to the cytoplasmic domain of cadherins and to actin, providing a link between cadherins and the cytoskeleton and thus provide strength to the adhesive contact. Cell adhesion could therefore be modulated through the regulated assembly and disassembly of the cadherin-catenin-complex. However, cadherin expression normally is the rate limiting step in the formation of cadherin-catenin complexes, and in many cases, when cadherin adhesion activity at the cell surface is acutely and rapidly modulated in response to developmental

signals, no alterations in the composition of the cadherin–catenin complex can be detected (Weidner *et al.*, 1990; Brieher and Gumbiner, 1994; Shibamoto *et al.*, 1994; Gumbiner, 2000).

Phosphorylation of the cadherin-catenin complex is another possible mechanism to regulate cell-cell adhesion (Daniel and Reynolds, 1997). Tyrosine phosphorylation of β-catenin correlates with inhibition of cadherin-mediated adhesion resulting from kinase activation (Shibamoto *et al.*, 1994). However, there are many potential substrates for kinases and phosphatases in the plasma membrane and cytoskeleton, and it has not been shown that phosphorylation of β-catenin is required for the observed effects on cell adhesion (Gumbiner, 2000).

Members of the Rho family of small GTPases have been implicated in the regulation of cell-cell contacts (Kaibuchi *et al.*, 1999). Rac can stabilize adherens junctions in mammalian cells through the accumulation of E-cadherin, β-catenin and actin at sites of cell-cell contact, and it also regulates the recruitment of actin to adherens junctions in *Drosophila* epithelia. Similar effects have been observed in a few cases for RhoA and Cdc42 (Eaton *et al.*, 1995; Braga *et al.*, 1997; Takaishi *et al.*, 1997). It is not known how Rho GTPases can exert their functions in these contexts, but they could indirectly regulate cadherin-mediated adhesion through effects on the actin cytoskeleton (Hall, 1998). In contrast, Cdc42 and Rac could directly regulate the cadherin complex through their effector IQGAP1, which can compete with the E-cadherin-β-catenin complex for the binding of α-catenin (Kaibuchi *et al.*, 1999). Rac and Cdc42 were found to inhibit IQGAP1 binding to β-catenin, and to restore adhesion, consistent with the role in stabilizing adherens junctions (Gumbiner, 2000).

How cadherins are recruited to sites of cell-cell contact is not well understood. During *Drosophila* germ band extension, it has been proposed that E-cadherin is transported laterally within the plasma membrane towards sites of cell-cell contacts, where it then clusters with other E-cadherin molecules (Gumbiner, 2000; Bertet *et al.*, 2004; Lecuit, 2005). How the transport of E-cadherin to cell-cell contact sites is regulated, is not

known, but Myosin II could either mediate the clustering by a local reorganization of the actin cytoskeleton, or locally interact with regulators of E-cadherin stability (Bertet *et al.*, 2004; Lecuit, 2005).

Alternatively, Myosin II could control the endocytosis of E-cadherin through its effects on the actin cytoskeleton, since actin is required for the fission of endocytic vesicles into the cells (Merrifield *et al.*, 2002; Kaksonen *et al.*, 2003; Ayscough, 2004). Endocytosed E-cadherin would then traffic towards sites of cell-cell contact. Indeed, clathrin-mediated endocytosis via rab5, a central regulator of clathrin-mediated endocytosis, and recycling of E-cadherin have been proposed to enable the dynamic regulation of adhesive contacts (Le *et al.*, 1999; Zerial and McBride, 2001). Interestingly, clathrin mediated endocytosis of C-cadherin is necessary for the elongation of *Xenopus* mesodermal animal cap explants, suggesting a role for the endocytic turnover of cadherins in regulating cell movements and tissue rearrangements (Jarrett *et al.*, 2002). That way, the breakage and formation of cell-cell contacts, mediated or enabled by the dynamic turnover of adhesive contacts, could be regulating cell migration and/or tissue rearrangements (Bryant and Stow, 2004). Indeed, previous studies have reported the polarized delivery of endocytic markers towards the leading edge of migrating chick fibroblasts (Hopkins *et al.*, 1994). In crawling neutrophils, $\alpha_v\beta_3$ integrin anchors the cells to an extracellular vitronectin substrate. This binding can be released upon elevation of intracellular Ca^{2+} levels, and $\alpha_v\beta_3$ integrin is subsequently found in intracellular vesicles that accumulate at the leading edge of the cells. When intracellular Ca^{2+} was artificially depleted, the cells stopped moving, and essentially all integrin molecules were found on the surface of the cell at its rear, being attached to the substrate vitronectin (Lawson and Maxfield, 1995; Bretscher, 1996). These experiments support a model in which adhesion molecules are continuously transferred fro the rear of the cell to its front for reuse. If they cannot be released from the substratum, cell-substratum contacts persist at the rear of the cell, which cannot then move forward.

Interestingly, Cdc42 and Rac regulate the endocytosis of E-cadherin through the modulation of IQGAP1 and the actin cytoskeleton *in vitro* (Izumi *et al.*, 2004). Other

studies have reported the effects of rac1 on E-cadherin endocytosis in cultured keratinocytes. Moreover, signalling to actin via protein kinase C regulates the endocytosis and the recycling of E-cadherin (Alexander *et al.*, 1998; Le *et al.*, 2002). From these experiments, it is still not clear if the effects on E-cadherin endocytosis are directly mediated, or if E-cadherin internalization occurs as a mere secondary consequence of the regulation of the actin cytoskeleton, which would in turn regulate the budding of endocytic vesicles into the cell (Ayscough, 2004). Since Rho GTPases, protein kinase C isoforms and regulation of the actin cytoskeleton have all been implicated in non-canonical Wnt signalling, and since cadherin endocytosis is required for gastrulation movements in *Xenopus*, there is the intriguing possibility that non-canonical Wnt-signalling could regulate gastrulation movements through the endocytic turnover of cadherins, thus enabling the local rearrangements of cells during gastrulation. However, functional evidence for an involvement of cadherin endocytosis in non-canonical Wnt signalling during gastrulation is still lacking, although an enhancement of intracellular E- or N-cadherin staining has been observed upon stimulation with Wnt11 in mammalian or avian cell culture (Eisenberg *et al.*, 1997; Ouko *et al.*, 2004).

3.3 Questions and aims of this thesis

The central aim of this study was to understand the cellular and molecular mechanisms by which non-canonical Wnt signalling via *slb*/*wnt11* mediates gastrulation movements in zebrafish.

To address the function of non-canonical Wnt signalling in cell movement and morphology during gastrulation, an assay was developed which allowed for the analysis and comparison of cell movement and morphology between wild-type and *slb*/*wnt11* mutant embryos *in vivo*. Prospective ectodermal and mesendodermal cells were labelled with various dyes, and their movement and morphology were followed over time by single- and two-photon confocal time-lapse microscopy. The obtained data were quantified by custom-built software which allowed for the analysis of various cell-shape and movement parameters. This part of the project was partially done in collaboration

with the research group of David Soll (Keck Imaging Facility, University of Iowa, Iowa City, USA).

To address one candidate mechanism by which non-canonical Wnt signalling regulates cell movement during gastrulation, the adhesiveness of mesendodermal cells from wild-type and *slb*/*wnt11* mutant embryos was analysed and compared in an *in vitro* reaggregation assay. To relate the findings to the endogenous situation in zebrafish, the *in vitro* observations were complemented by the analysis of the endogenous expression and distribution of E-cadherin in wild-type and *slb*/*wnt11* mutant embryos. As a potential mechanism underlying the regulation of cell adhesion downstream of *slb*/*wnt11*, endocytosis was blocked or enhanced, and its influence on endogenous E-cadherin distribution, cell adhesion and cell migration was analysed.

4. Results

slb/*wnt11* regulates cell movements during gastrulation in zebrafish embryos by the so-called non-canonical Wnt pathway. In *Drosophila*, a homologuos pathway is involved in the regulation of planar cell polarity, suggesting a role for cell morphology in the regulation of gastrulation movements downstream of sslb/wnt11 function (Heisenberg *et al.*, 2000; Veeman *et al.*, 2003). However, not much is known yet about the molecular and cellular functions of *slb*/*wnt11* during gastrulation.

To elucidate the cellular and molecular mechanisms by which *slb*/*wnt11* regulates gastrulation movements, movement and morphology of cells from wild-type embryos were first analysed in comparison to cells from *slb*/*wnt11* mutant embryos. This study was then complemented by addressing the mechanisms that could regulate the cellular and molecular function of *slb*/*wnt11* during zebrafish gastrulation.

4.1 Function of slb/wnt11 *in tissue positioning*

Zebrafish embryos mutant for *slb*/*wnt11* display a broadened neural plate and a shortened and broadened notochord at the end of gastrulation; furthermore, the prechordal plate is elongated and shifted posteriorly relative to the neural plate (Heisenberg and Nüsslein-Volhard, 1997; Heisenberg *et al.*, 2000). During gastrulation, *wnt11 m*RNA is expressed in the paraxial head mesoderm and the anterior lateral neurectoderm and is required for convergence and extension movements in paraxial and axial tissues in a non-cell autonomous manner (Heisenberg and Nüsslein-Volhard, 1997; Heisenberg *et al.*, 2000). At the onset of gastrulation, *wnt11 m*RNA is detectable around the circumference of the germ-ring with slightly reduced expression on the dorsal side, the region of the forming shield. Within the germ-ring, *slb*/*wnt11* is expressed predominantly in epiblast cells (ectodermal germ layer), whereas ingressing hypoblast cells (mesendodermal germ layer) show no detectable levels of *slb*/*wnt11* transcripts (Makita *et al.*, 1998; Ulrich *et al.*, 2003). These data suggest that *slb*/*wnt11*, expressed in epiblast cells, might be involved in

the control of cell movements in the germ-ring that mediate the ingression of hypoblast cells at the onset of gastrulation.

To examine if *slb*/*wnt11* is required for the movements of ingressing hypoblast cells during early stages of gastrulation, wild-type and *slb* mutant embryos were fixed in time intervals of 45 min, starting at the onset of gastrulation, and the positions of axial tissues in these embryos were determined by *in situ hybridization* (ISH) using riboprobes against *hatching gland gene 1* (*hgg1*) and *floating head* (*flh*), which specifically label the prospective prechordal plate (ppl) and notochord (no), respectively (Thisse *et al*., 1994; Talbot *et al*., 1995). To determine if differences between wt and *slb* mutant embryos were specifically due to the absence of *slb*/*wnt11* function, *slb* mutant embryos that had been injected with 5 pg *wnt11 m*RNA - an amount with which the *slb* phenotype could be efficiently rescued at the end of gastrulation - were also analyzed.

In wt embryos, the prechordal plate moved rapidly anteriorly towards the animal pole during the first 2-3 h of gastrulation (figure 6 A-D), whereas in slb mutants, prechordal plate cells were less advanced towards the animal pole already 45 min after the onset of gastrulation. This positioning defect became stronger during the course of gastrulation; in addition, the notochord was broadened and shortened in *slb* mutants (Figure 6 E-H). Both phenotypes could be rescued by *wnt11* overexpression (Figure 6 I-L), indicating that *wnt11* is specifically required for the shape and positioning of axial mesendodermal tissues at the onset of gastrulation.

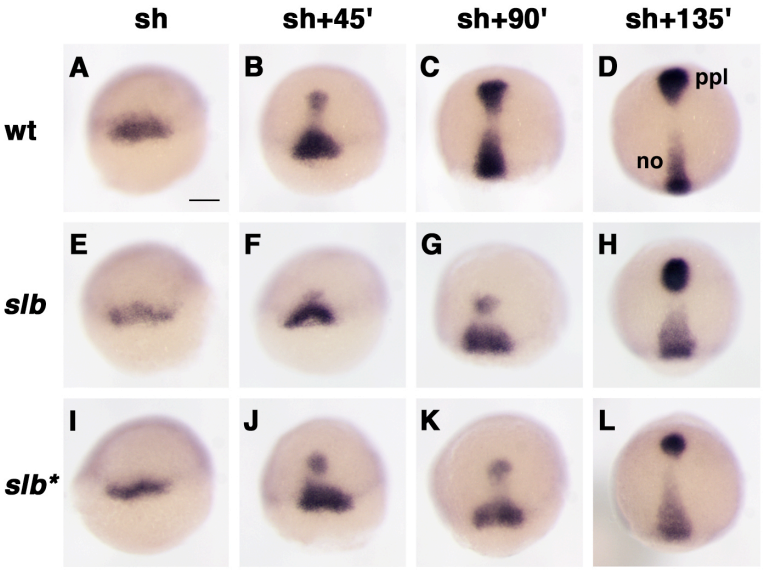

Figure 6. Extension of axial mesendodermal tissues (prechordal plate and notochord) is reduced in *slb* embryos throughout early stages of gastrulation. Embryos were fixed at various times after shield stage (sh) and stained for the expression of *hatching gland gene 1* (*hgg1*) and *floating head* (*flh*) to mark the positions of the

prechordal plate (ppl) and the notochord (no), respectively. Shape and position of prechordal plate and notochord in wild-type embryos (wt, A-D), *slb*/*wnt11* mutants (*slb*, E-H) and *slb* mutants overexpressing 5 pg *slb*/*wnt11* mRNA (*slb**, I-L) at the indicated time intervals. Anterior to the top, dorsal views. Scale bar in (A) = 100 μm.

4.2 slb/wnt11 *is required for speed and directionality of prechordal plate precursors*

To obtain a more dynamic picture of the requirement for *slb*/*wnt11* in positioning of axial tissues at the germ ring, the positions of labelled cells from wt and *slb* mutant embryos at the onset of gastrulation were recorded by three dimensional confocal microscopy, and their speed and directionality were analysed over time. To unambigously mark prechordal plate precursor cells, embryos carrying a transgene for cytosolic Green Fluorescent Protein (GFP) under the control of the *goosecoid* (*gsc*) promotor were observed. These embryos express GFP during gastrulation specifically in anterior axial mesendodermal cells at the dorsal side (Schulte-Merker *et al*., 1994). The embryos were injected with tetramethyle rhodamine (TMR), coupled to a high molecular weight form of dextran, into single blastomeres of 8 - 16 cell stage embryos, yielding a mosaique or "salt and pepper" pattern of labelling during their development (Abdelilah *et al*., 1994; Helde *et al*., 1994). At the onset of gastrulation, prechordal plate progenitor cells expressed cytosolic GFP, whereas all other cells in the dorsal region, that were not expressing GFP but labelled with TMR could be recognized as cells of the prospective neurectoderm (epiblast). Transgenic wt- and *slb*-gscGFP embryos were subjected to dual-colour single photon confocal microscopy with the green channel recording GFP labelled cells and the red channel TMR positive cells. In time intervals of 4 min, an image stack was produced by optical sectioning through the embryos; together, these stacks formed a timelapse sequence (a "movie") of cell movements in three dimensions. The stacks were rendered using appropriate software, and the movement of individual cells was followed in three dimensions over time (for details, see Material and Methods).

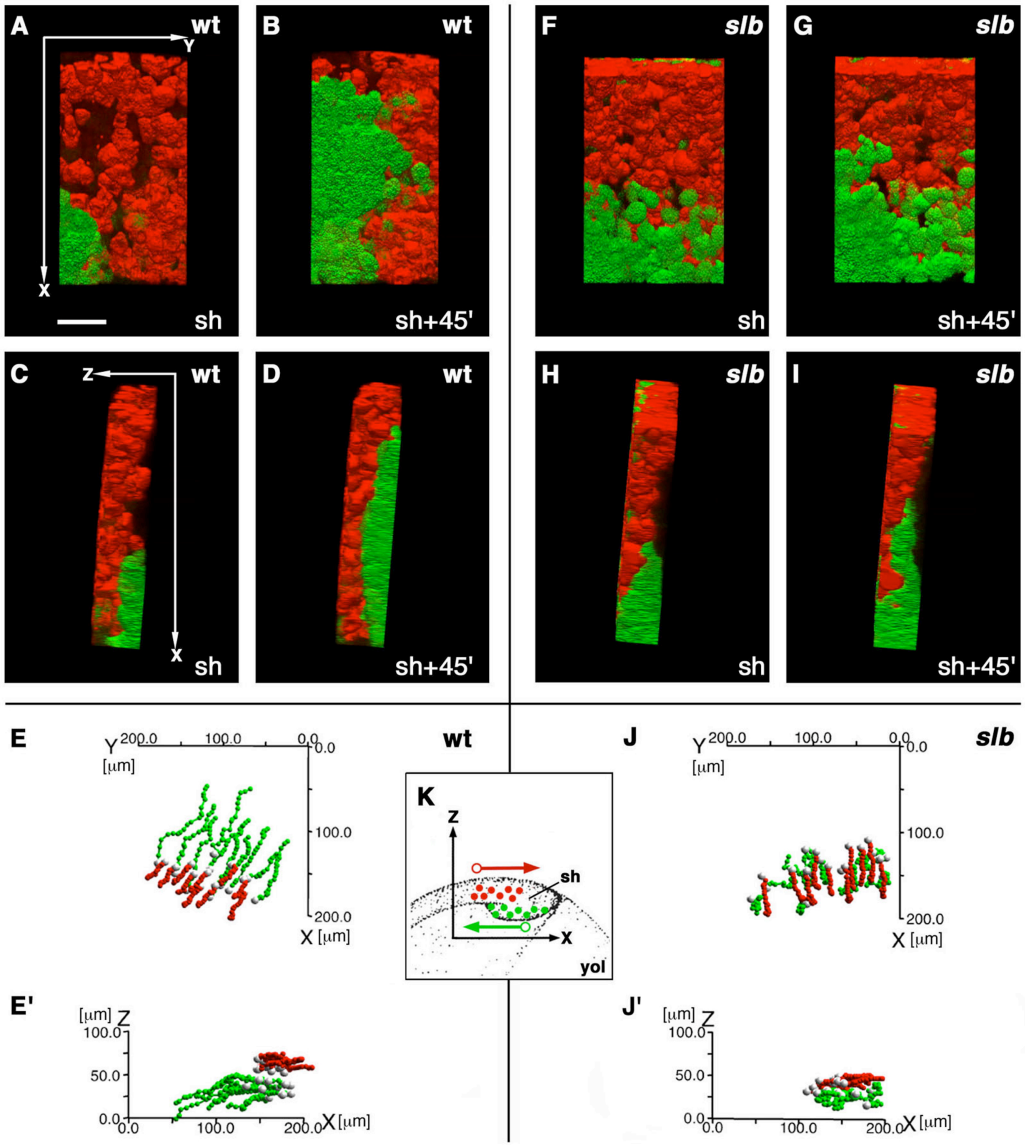

Figure 7. Movement of axial hypoblast (presumptive prechordal plate) cells in dorsal regions of the germ ring (shield) is disturbed in *slb*/*wnt11* mutant embryos at the onset of gastrulation. Embryos expressing GFP (green) under the control of the goosecoid (gsc) promotor in prechordal plate precursor cells were scatter labelled with rhodamine (red) in epiblast cells overlying the presumptive prechordal plate and followed in 3D over time by dual channel confocal microscopy.

(A-D,F-I) Prechordal plate precursor cells (green) and overlying epiblast cells (red) in wild-type (A-D) and slb (F-I) gscGFP embryos at shield stage (A,C,F,H) and 45 minutes (45') later (B,D,G,I). Ventral views

(A,B,F,G) and lateral views with ventral to the right and dorsal to the left (C,D,H,I). In all pictures, anterior is to the top and posterior to the bottom. The axes of orientation are shown in panels A and C. (E,E',J,J') Track diagrams showing the movements of prechordal plate precursor cells (green) and epiblast cells (red) in wild type (E,E') and *slb* gscGFP embryos (J,J') along the x (anterior-posterior) and y (mediolateral) axes (E,J) and along the x and z (dorsal-ventral) axes (E',J') of the embryo. The positions of the geometric centre of the cell (the centroid) were measured in 3D at 4-minute intervals and plotted as a single dot. Each line represents the track of one cell, with the first timepoint depicted in white. The net movement of the epiblast cells is along the +x (posterior) direction and that of prechordal plate precursor cells along the –x (anterior) direction. Note that the x, y and z axes depict the global coordinates within the gastrula, whereas in figs. 8, 9 and 11, these axes show the coordinates relative to the movement direction of individual cells. (K) Schematic diagram showing the orientation of the region analyzed in wild-type and *slb* embryos and the net movement direction of the cells (arrows) with respect to the x and z axes. The y axis is perpendicular to x and z and is not depicted in this diagram. Epiblast cells in red, hypoblast cells in green. Note that a left-handed coordinate system has been used. sh, shield; yol, yolk. Scale bar in (A) = 50 μm.

Figure 7 A-D and F-I show pictures of a representative wildtype and *slb* mutant embryo at the onset of gastrulation and 45 min later (see also supplementary movies S3 and S4). In wt embryos, hypoblast and epiblast cells move parallel to the surface of the yolk sac in a straight path in the anterior and posterior directions, respectively; both populations seem to "slide" alongside each other with no apparent disturbance between the cell layers. In contrast, in *slb* mutant embryos, prechordal plate cells move less straight anteriorly, and exhibit increased movements away from or towards the yolk cell (figure 7 E-E' and J-J'). *slb* prechordal plate progenitor cells move with a significantly lower velocity than wt cells, and the persistence of these movements - which is the direct distance between start and end of a cell track divided by the total distance that cell travels - is significantly decreased (figure 7 E-E', J-J'; table 1; Soll, 1995). This defect is restricted to hypolast cells, as epiblast cells from wt and *slb* embryos do not show any significant differences in speed and directionality (table 1). It is worth noting that although hypoblast cell movements are disoriented and slower, the net movement direction of these cells in the anterior direction is not changed (figure 7, suppl. movies S3 and S4).

cells from	speed (μm/min)	s. d. (μm/min)	p (t-test)	persistence (%)	s. d. (%)	p (t-test)
wt epiblast	0.67	0.25	$7.23 \cdot 10^{-1}$	74.46	8.61	$2.19 \cdot 10^{-1}$
slb epiblast	0.66	0.33		78.63	15.53	
wt hypoblast	1.24	0.23	$9.40 \cdot 10^{-4}$	84.35	6.52	$7.63 \cdot 10^{-18}$
slb hypoblast	1.06	0.22		37.54	20.77	

Table 01. Velocity and persistence in wt and *slb* mutant epiblast and hypoblast cells. n = 30 hypoblast and n = 20 epiblast cells from two different embryos each were analysed over 20 - 140 min (5 - 32 timepoints). See also figure 7. s. d., standard deviation. p-values were calculated with an unpaired Student's t-test.

These observations indicate that at the onset of gastrulation, *slb*/*wnt11* function is required to ensure proper speed and directionality in hypoblast cells. It is not required to enable mesendodermal cell movements *per se*, suggesting a role for *slb*/*wnt11* function in stabilizing cell movements, rather than allowing them to occur.

4.3 Function of slb/wnt11 in the regulation of cell morphology

To study the cellular mechanisms that underlie the cell movement defects in *slb* mutant embryos, individual cells were labelled with a mixture of cytosolic and membrane-bound GFP ('GAP43-GFP'; Okada *et al*., 1999) and the morphology and movement of hypoblast and epiblast cells was recorded with a confocal microscope *in vivo* over time.

To analyze single cells, wt and *slb* embryos were injected with *m*RNAs for cytosolic and membrane-bound GFP between the 2- and 16-cell stage and mounted for confocal analysis at shield stage, with the dorsal side facing the objective. For a three-dimensional analysis of cell movement and morphology over time, z-stacks were taken continuously over time with a two-photon confocal setup, which provides a detailed resolution of cells several layers deep in the tissue (Denk and Svoboda, 1997). The resulting timelapse movies were then rendered in three dimensions, and cell shape and motility were analysed over time. Since the net cell movement direction is not changed between wt and *slb* mutant embryos (see 4.2), individual cells of epiblast and hypoblast layers were distinguished by their overall movement direction towards the vegetal and animal pole, respectively.

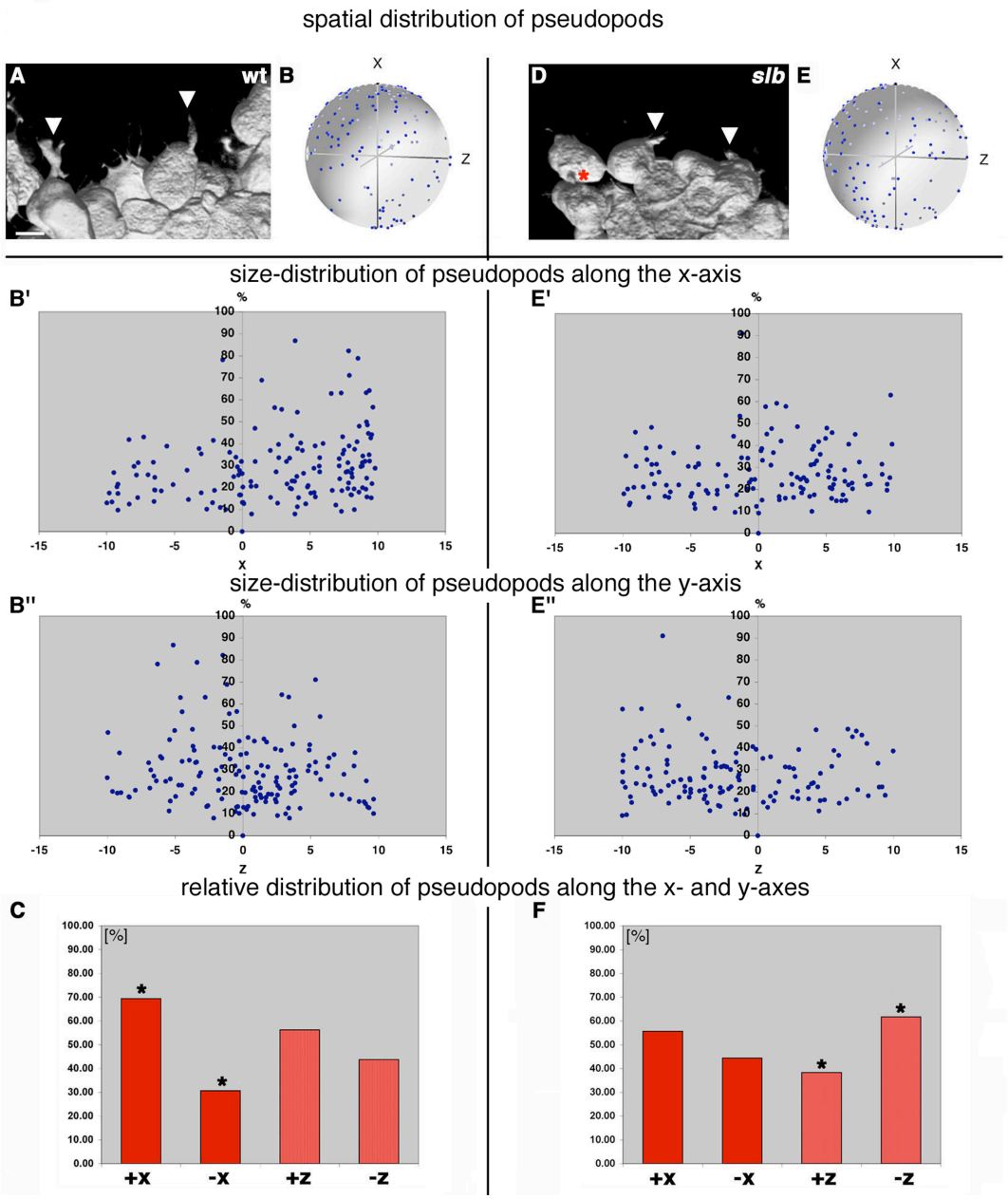

Figure 8. Distribution of pseudopodial processes in wildtype and *slb* prechordal plate precursor cells at the onset of gastrulation. Prechordal plate precursor cells were labelled with a mixture of cytosolic and membrane-bound GFP and visualised in 3D over time by two-photon confocal microscopy. (A,D) 3D images of prechordal-plate-precursor cells in a wild-type (A) and *slb* mutant embryo (D) moving from bottom (germ ring margin) to top (animal pole), at shield stage. Arrowheads point to thick, pseudopod-like processes, and the red asterisk in (D) marks a pseudopod projecting into the dorsal direction. (B,E)

Spherical plots showing the distribution of the outgrowth positions of pseudopods (blue dots) relative to the cell centroid and normalized to the movement direction of the cells (black dot) in wild-type (B) and *slb* mutant (E) embryos at shield stage. For these spherical diagrams, the 3D distribution of the positions where pseudopods emerged on the surface of each cell (blue dots) was measured relative to the centroid of the cell body. The distances between the positions of the pseudopod and the cell centroid were then calibrated to a constant value, leaving the orientation of the pseudopod positions unchanged. Plotted in 3D with the cell centroid at the origin, the pseudopod positions were, therefore, placed on the surface of a sphere centred around the origin. These spherical graphs were then turned so that the positions of each cell centroid for the following timepoint (black dot) were placed onto the x-axis. The pseudopod positions in 20 cells from five wild-type and five slb embryos at four consecutive timepoints (0, 2.5, 5 and 7.5 minutes) were plotted into one diagram. To enhance the 3D appearance of the plots, an artificial transparent sphere centred at the origin was added to each diagram. Note that the x, y and z axes in these diagrams show the coordinates relative to the movement direction of individual cells (+x axis), whereas in Fig. 7, these axes depict the global coordinates within the gastrula. (B',E') Distribution of pseudopod lengths from B and E, respectively, along the x-axis – the individual movement axis of the cells – or the z-axis (B'',E''). Each diagram shows pseudopod lengths relative to the body length of the corresponding cell (in %); the numbers on the ordinate axis correspond to arbitrary units, with x = 10 being the radius of the spheres in (B) and (E). (C,F) Distribution of the outgrowth positions of pseudopods in wild-type (C) and *slb* mutant (F) embryos. The columns show the relative distribution of pseudopods along (+x versus –x) or perpendicular (+z versus –z) to the individual movement direction of the cells, averaged over four consecutive timepoints (0, 2.5, 5 and 7.5 minutes), with the cell centroid at x = 0 and z = 0. *, $p < 0.05$, paired Student's t-test. Scale bar in A = 10 μm. **Note added in proof: the y-axis in B'' and E'' is meant to be the z-axis (type error).**

Figure 8 A,D show each one representative three-dimensionally rendered image of wt and *slb* prechordal plate cells, respectively, taken out of a longer timelapse sequence (see supplementary movie S5). In wt embryos, the anteriormost mesendodermal cells extend large pseudopod-like cellular processes in the anterior direction; in contrast, processes from *slb* mutant prechordal plate cells project less well into the anterior direction.

To gain a more detailed understanding of the three-dimensional morphology of the cells with respect to their movement direction, cells were manually outlined in three dimensions and their shape was analysed using custom-built 3D rendering software (Voss and Soll, unpublished; Soll *et al.*, 2000; Heid *et al.*, 2002). To address whether *slb*/*wnt11* regulates changes in specific cellular features – like the shape and/or orientation of

cellular protrusions - cell body and protrusions were traced and analyzed independently of each others. Since no molecular markers were available that would unambigously label pseudopod-like processes, cellular processes were defined according to morphological criteria. Only those protrusions that were sufficiently elongated, of a certain width and emanated under a specific angle from the cell body were counted as pseudopod-like processes (see Material and Methods for details). To obtain information about cell polarization in 3D, the positions, where pseudopodial protrusions emanated on the cell surface[1], were measured relative to the position of the cell body centroid (its geometrical centre; Soll, 1995; Heid *et al.*, 2002). The outgrowth positions of these protrusions were then projected onto the surface of a hypothetical sphere by assuming a constant net distance to the centroid while keeping the spatial orientation of protrusion outgrowth constant. To relate this orientation specifically to single cells, the positions were normalized to the individual movement direction of each cell, which was defined as the axis between the cell body centroids of two consecutive timepoints. This method of analysis resulted in spherical plots showing the outgrowth positions of pseudopod-like processes relative to the individual cell movement direction in wt and *slb* mutant embryos (figure 8 B, E). Figure 8 C,F and table 2 summarize the distribution of pseudopods along the x- and z-axis, i. e. the axis of individual cell movement and the axis perpendicular to it, respectively, for wt and *slb* embryos; the z-axis was chosen to point towards the yolk.
While in wt prechordal plate cells, pseudopodial processes preferably formed at positions along the individual movement direction of the cells, no such preferred orientation could be observed in *slb* embryos. In contrast, these cells oriented their processes preferably perpendicularly to their movement direction, pointing away from the overlying epiblast, whereas there was no such preference in wt embryos (figure 8 C,F; table 2). Moreover, in wildtype embryos, most of the elongated processes with a relative length of more than 50 % of the cell body pointed towards the +x-axis and thus towards the individual cell movement direction. No such distribution was seen in *slb*/*wnt11* mutant embryos (Figure 8 B'-B'', E'-E'’). Other parameters like average number, surface or volume of processes

[1] Although for this study, only the outgrowth positions of protrusions were quantified, the points to where these protrusions projected showed a similar spatial distribution relative to the cell movement direction.

were not significantly altered between wt and *slb* embryos (table 3), indicating that *slb*/*wnt11* is specifically required for the orientation of pseudopodial extensions along the individual movement direction of mesendodermal cells.

An analogous quantification was done for neurectodermal cells that were localized directly above or in front of the prechordal plate. Figure 9 A,D each show one snapshot of a representative timelapse sequence for wt and *slb* epiblast cells, respectively (see also supplementary movie S6). Pseudopods were localized towards and directly opposite the individual cell movement directions, but no significant difference in the distribution of processes along the individual cell movement axis could be observed, neither in wt nor *slb* embryos. However, in contrast to the wt case, *slb* epiblast cells displayed a preferred orientation of processes towards the underlying cell layer or substrate (figure 9 B,C,E,F; table 2). Neither in wt nor in *slb* is there any significant differential distribution of long processes along or perpendicular to the individual cell movement direction (figure 9 B'-B'', E'-E''), and other parameters like average number, surface and volume of processes - as in the case of hypoblast cells - also revealed no significant differences (table 3). In addition, surface and volume of the cell body are also not significantly changed in the absence of slb/wnt11 function (table 4).

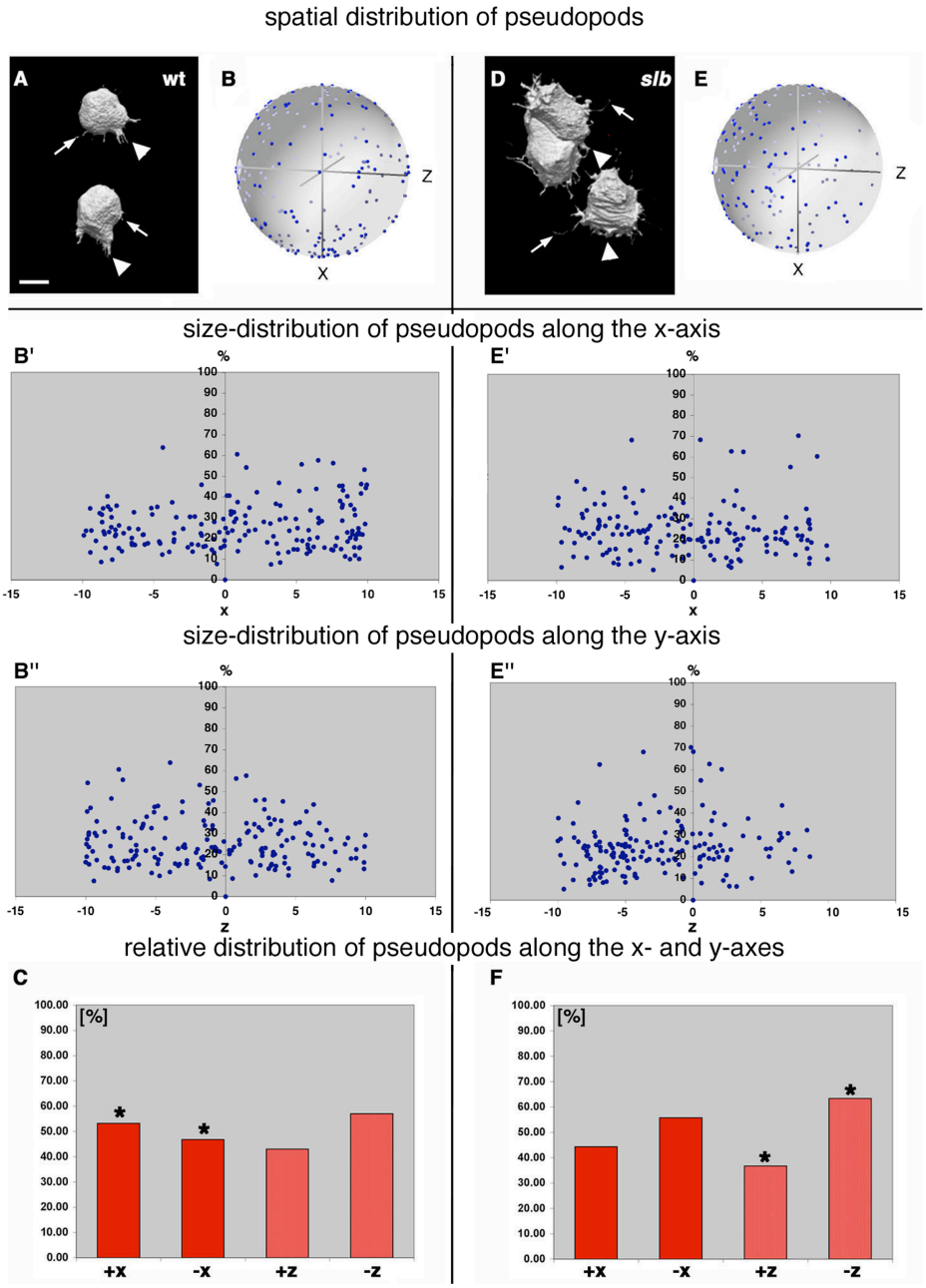

Figure 9.

Distribution of processes in wild-type and *slb* epiblast cells overlying the presumptive prechordal plate at the onset of gastrulation. Cells were labelled with a mixture of cytosolic and membrane-bound GFP and visualised in 3D over time by two photon confocal microscopy. (A,D) 3D images of typical epiblast cells in a wild-type (A) and *slb* mutant (D) embryo moving from top (animal pole) to bottom (germ ring margin) at shield stage. Arrowheads point to thick, pseudopod-like processes. Arrows mark smaller, filopod-like processes. In (A), the pseudopod emerging from the upper cell is branched. (B,E) Spherical plots showing the distribution of the outgrowth positions of pseudopods (blue dots) relative to the cell centroid and

normalized to the movement direction of the cells (black dot) in wild-type (B) and slb mutant (E) embryos at shield stage. The process positions of 20 cells (from four timepoints in wild type and the first three timepoints in *slb*) or from 11 cells (last timepoint in slb) from five wildtype and eight slb embryos at four consecutive timepoints (0, 2.5, 5 and 7.5 minutes) were plotted into one diagram. Note that the x, y and z axes in these diagrams show the coordinates relative to the movement direction of individual cells (+x axis), whereas in Fig. 7, these axes depict the global coordinates within the gastrula. (B',B'',E',E'') Distribution of pseudopod lengths from B and E, respectively, along the x-axis (B',E') – the individual movement axis of the cells – or the z-axis (B'',E''). Each diagram shows pseudopod lengths relative to the body length of the corresponding cell (in %); the numbers on the ordinate axis correspond to arbitrary units, with x = 10 being the radius of the spheres in (B) and (E). (C,F) Distribution of the outgrowth positions of pseudopods in wild-type (C) and slb embryos (F). The columns show the relative distribution of pseudopods along (+x versus –x) and perpendicular (+z versus –z) to the individual movement direction of the cells, averaged over four consecutive timepoints (0, 2.5, 5 and 7.5 minutes), with the cell centroid at x = 0 and z = 0. *, $p < 0.05$, paired Student's t-test. Scale bar in A = 10 μm. **Note added in proof: the y-axis in B'' and E'' is meant to be the z-axis (type error).**

cells from	+x in %	- x in %	s. d. in %	p-value	+z in %	-z in %	s. d. in %	p-value
wt epiblast	53.16	46.84	33.31	$3.98 \cdot 10^{-1}$	42.98	57.02	37.87	$1.01 \cdot 10^{-1}$
slb epiblast	44.27	55.73	30.60	$1.19 \cdot 10^{-1}$	36.71	63.29	36.48	$3.05 \cdot 10^{-3}$
wt hypoblast	69.33	30.67	37.59	$1.58 \cdot 10^{-5}$	56.23	43.77	39.58	$1.63 \cdot 10^{-1}$
slb hypoblast	55.63	44.38	36.26	$1.69 \cdot 10^{-1}$	38.33	61.67	38.99	$9.04 \cdot 10^{-3}$

Table 02. Distribution of pseudopodial processes towards ('+x'), against ('-x') or perpendicular to the individual cell movement direction ('+ z' or '-z'). The p-values were calculated through an unpaired Student's t-test. Only values below p = 0.05 were regarded as being significant. s. d., standard deviation. For each condition, n = 20 cells were analyzed over four timepoints each.

pseudo-pods	average number	s. d.	p-value	surface in μm^2	s. d. in μm^2	p-value	volume in μm^3	s. d. in μm^3	p-value
wt epiblast	2.26	1.91	$5.31 \cdot 10^{-2}$	59.34	39.78	$9.67 \cdot 10^{-1}$	28.29	28.02	$3.61 \cdot 10^{-1}$
slb epiblast	2.14	2.04		59.56	32.55		32.55	53.35	
wt hypoblast	1.89	1.39	$2.29 \cdot 10^{-1}$	90.50	81.35	$1.38 \cdot 10^{-1}$	58.31	80.30	$5.55 \cdot 10^{-1}$
slb hypoblast	1.64	1.22		81.45	83.20		55.67	107.37	

Table 03. Analysis of number and shape of pseudopodial processes emanating from epiblast or hypoblast cells with or without *slb*/*wnt11* function. p-values were calculated through an unpaired Student's t-test. s. d., standard deviation. For each condition, n = 20 cells were analyzed over four consecutive timepoints.

cell body	surface in μm^2	s. d. in μm^2	p-value	volume in μm^3	s. d. in μm^3	p-value
wt epiblast	1163	187		2974	687	
			$6.35 \cdot 10^{-1}$			$9.84 \cdot 10^{-1}$
slb epiblast	1176	172		2972	662	
wt hypoblast	1076	211		2876	869	
			$1.68 \cdot 10^{-1}$			$6.48 \cdot 10^{-2}$
slb hypoblast	1038	174		2600	596	

Table 04. Difference between morphological parameters of the cell body in the presence or absence of *slb*/*wnt11* function. The p-values were calculated through an unpaired Student's t-test. Only values below p = 0.05 were regarded as being significant. s. d., standard deviation. For each condition, n = 20 cells were analyzed over four timepoints each.

In principle, epiblast and hypoblast also displayed numerous thin, filopod-like extensions (see arrows in figure 9 A,D and Montero *et al.*, 2005). However, on hypoblast cells, they often appeared fuzzy, probably because the resolution of the microscope was not strong enough to resolve such fine structures several cell layers deep within the tissue, and in the epiblast, their number as well as their orientation was often very variable. Therefore, filopod-like processes were not included in the analysis, neither in the hypoblast nor in the epiblast.

Taken together, the morphological analysis of neurectodermal (epiblast) and prechordal plate (hypoblast) cells at the dorsal side of the embryo indicates that at the onset of gastrulation, *slb*/*wnt11* function is required in mesendodermal cells for the orientation of pseudopod-like processes towards the individual cell movement direction. Without *slb*/*wnt11*, neurectodermal and mesendodermal cells orient their processes perpendicular to their movement direction towards the underlying cells or substrate. The requirement for *wnt11* seems to be specific to the orientation of cellular processes, since neither their

shape and number nor the general shape of the cell body is changed between wt and *slb* epi- and hypoblast cells.

4.4 Link between cell morphology and movement

To test if the observed changes in the orientation of pseudopod-like processes of mesendodermal cells in *slb* mutants are linked to their defects in movement stability (see 4.1), the process orientation in wt and *slb* mesendodermal cells was determined relative to their movement persistence. The percentage of processes oriented in the individual movement direction of each cell over four consecutive timepoints was compared to the persistence of its movement path during that time sequence. Wildtype cells that have processes preferentially oriented towards their individual movement directions also show highly persistent movements, whereas in *slb/wnt11* mutant cells, a reduction in the percentage of processes oriented towards their individual movement direction is accompanied by less persistent movements (figure 10). Testing the correlation between process orientation and the stability of the movements reveals that both parameters are statistically linked to each others (r = 0.36; p = 0.02; Müller *et al.*, 2002), indicating that *slb/wnt11* mediated process orientation and movement stability depend on each other.

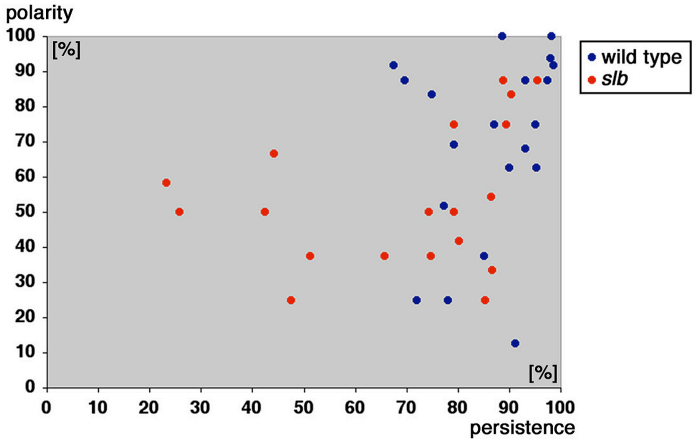

Figure 10. Scatter plot showing the relation between the orientation of hypoblast cell processes towards their individual movement directions (y-axis with % of processes in movement direction) in relation to the

degree of persistence of their movements (x-axis), determined for 5 consecutive timepoints (0', 2.5', 5', 7.5' and 10') in 20 wild type (blue dots) and 20 *slb* cells (red dots) from 5 embryos each. See also figure 8 for a description of the determination of process orientation.

4.5 Specificity of slb/wnt11 *function in regulating cell morphology*

To confirm that the defective process orientation along the individual movement direction in *slb* hypoblast cells at the onset of gastrulation (see 4.3; figure 8) is specifically caused by an absence of *slb*/*wnt11* function, 5 pg *wnt11 m*RNA was ubiquitously overexpressed in *slb* embryos, and the orientation of pseudopod-like processes in axial mesendodermal cells was scored relative to their individual movement direction. Only those *wnt11* overexpressing embryos that showed a morphologically recognizable rescue, i.e. a prechordal plate that was clearly more advanced towards the animal pole than in corresponding *slb* mutant embryos, were taken for analysis (see 4.1; figure 6). The positions where processes emanated were determined similar to the method used in figure 8, but to be able to quantify a larger number of cell, the analysis was conducted in two dimensions (along the anterior-posterior and left-right axis. At the onset of gastrulation, hypoblast cells from *slb* mutants overexpressing *wnt11 m*RNA preferentially oriented their processes towards the individual movement direction of the cells, similar to, but slightly weaker than, wt hypoblast cells. In contrast, uninjected slb embryos showed no such preference (table 5). The effects were even more pronounced at midgastrula stage (figure 11; table 5) showing that *slb*/*wnt11 m*RNA can indeed rescue the process orientation defect observed in mesendodermal cells of slb mutant embryos. Therefore, *slb*/*wnt11* specifically orients cellular processes in prechordal plate cells towards their individual movement directions.

Embryo	+ x in %	- x in %	s.d. in %	p-value
early wt	87	13	13	$7.4 \cdot 10^{-6}$
early *slb*	57	43	14	$2.9 \cdot 10^{-1}$
early *slb* rescue	61	39	23	$4.3 \cdot 10^{-2}$
late wt	87	13	15	$2.1 \cdot 10^{-7}$
late *slb*	66	34	21	$3.8 \cdot 10^{-3}$
late *slb* rescue	90	10	12	$9.6 \cdot 10^{-10}$

Table 05. Distribution of pseudopodial processes relative to the individual movement direction of single wild-type, *slb* and *slb*/*wnt11* injected *slb* prechordal plate precursor cells at the onset of gastrulation ('early') and mid-gastrulation ('late'). +x: processes pointing towards the individual movement direction; -x: processes pointing into the opposite direction. See figure 11 for a graphical representation of the data. s. d., standard deviation; to check, if the difference between +x- and -x-direction is significant, a paired Student's t-test was used ('p-value'). For each condition, 5 to 15 cells were analysed over 5 - 10 timepoints each.

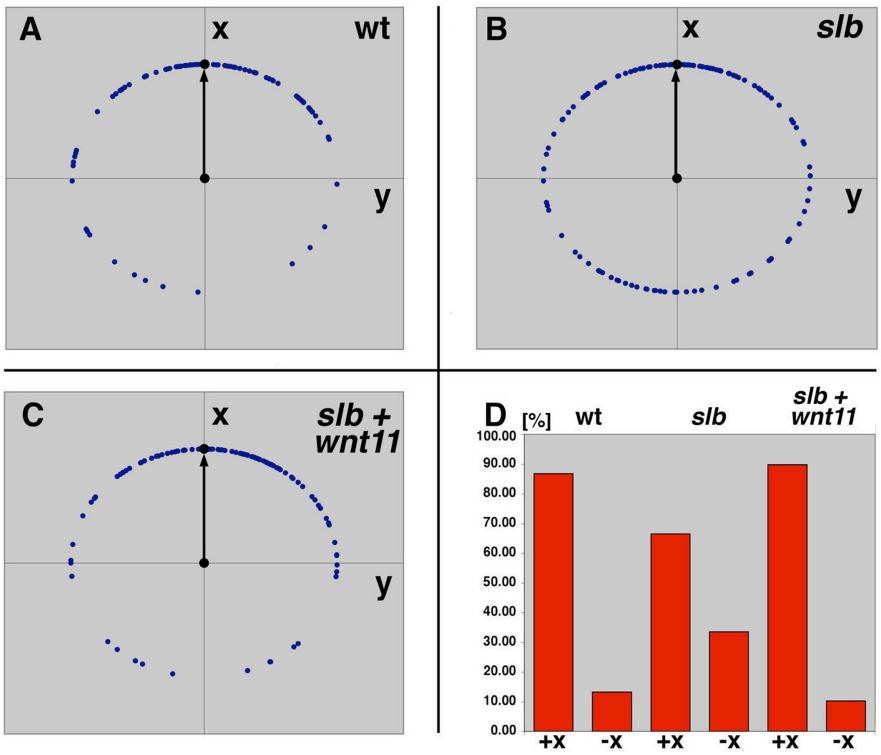

Figure 11. Two-dimensional distribution of pseudopodial processes in wild-type, *slb* and *slb*/*wnt11* injected *slb* prechordal plate precursor cells at midgastrulation stages. As in Figs 8 and 9, cells were

labelled with a mixture of cytosolic and membrane bound GFP and visualised over time by two-photon confocal microscopy. (A-C) Polar plots of the distribution of the outgrowth positions of pseudopods (blue dots) relative to the cell centroid and normalized to the movement direction of the cells (black arrows) in wild-type (A), *slb* (B) and *slb* embryos injected with 5 pg *slb/wnt11* mRNA (C) at 75% epiboly. These polar plots were made similar to the spherical plots shown in Fig. 8 and 9 (see above), except that the outgrowth positions of the pseudopods and the cell centroids were determined in two dimensions. For each genotype, the process positions in 5-10 cells over 5-15 consecutive timepoints (4-minute time intervals) from two embryos were analysed and plotted into one diagram. Note that the x and y axes show the coordinates relative to the movement direction of individual cells (+x direction) and do not resemble the global coordinates within the gastrula. (D) Relative distribution of the outgrowth positions of pseudopods (in %) along the individual movement direction of the cells (+x and –x) in wild-type, *slb* embryos and *slb* embryos injected with 5 pg *slb/wnt11 m*RNA, averaged over all timepoints analysed.

Taken together, these data indicate that *slb/wnt11* function is required at the onset of gastrulation for the orientation of cellular processes in hypoblast cells towards their individual movement directions. The aberrant orientation of these protrusions in *slb* mutant cells is accompanied by slower, less directed migratory cell movements. This suggests that *slb/wnt11* is needed for the orientation of cellular processes in hypoblast cells, and that their correct orientation facilitates and stabilises the movements of these cells.

4.6 Function of slb/wnt11 *in prechordal plate morphogenesis at the onset of gastrulation*

At the onset of gastrulation, cells at the tip of the germ-ring ingress to form the dorsal hypoblast (the prospective prechordal plate). The hypoblast contains both anterior mesodermal and endodermal precursors, while the epiblast is composed of neurectodermal and, at its most marginal extent, mesodermal progenitors. In addition, *slb/wnt11* is expressed in the most marginal cells of the epiblast, while hypoblast cells do not display any recognizable levels of *wnt11 m*RNA (Makita *et al.*, 1998; Ulrich *et al.*, 2003; Montero *et al.*, 2005). To observe if *slb/wnt11* functions in the dynamic rearrangement of these different populations of cells at the onset of gastrulation, wild

type and *slb* mutant embryos were injected with a mixture of cytosolic and membrane bound GFP, and the dynamic cellular rearrangements that build up the prospective prechordal plate at the dorsal side of the embryo were observed *in vivo* by two-photon confocal timelapse imaging. To address the cellular rearrangements that organize the axial hypoblast and epiblast cell layers relative to each others, the dorsal side of the germ-ring was imaged from lateral, and z-stacks were taken continuously over time. Figure 12 A,B,D,E shows movie snapshots of each one representative wt and *slb*/*wnt11* mutant embryo; exemplaric ectodermal (epiblast) and mesendodermal (hypoblast) cells are false-colored in green and red, respectively (see also supplementary movies S7 and S8). The corresponding tracks of wt and *slb*/*wnt11* mutant embryos in two dimensions are shown in figure 12 C,F.

In wildtype embryos, newly internalized mesendodermal (hypoblast) cells close to the yolk cell move up towards the interface between epiblast and hypoblast and keep their position at this interface before they eventually start to migrate towards the anterior direction (figure 12 A-C and supplementary movie S7). In contrast, hypoblast cells from *slb* mutant embryos fail to keep their position at the interface and even often appear to move in parallel with the overlying epiblast towards the vegetal pole (figure 12 D-F and supplementary movie S8). This suggests a function for *slb*/*wnt11* in the regulation of cell contacts at the interface between epiblast and hypoblast cells.

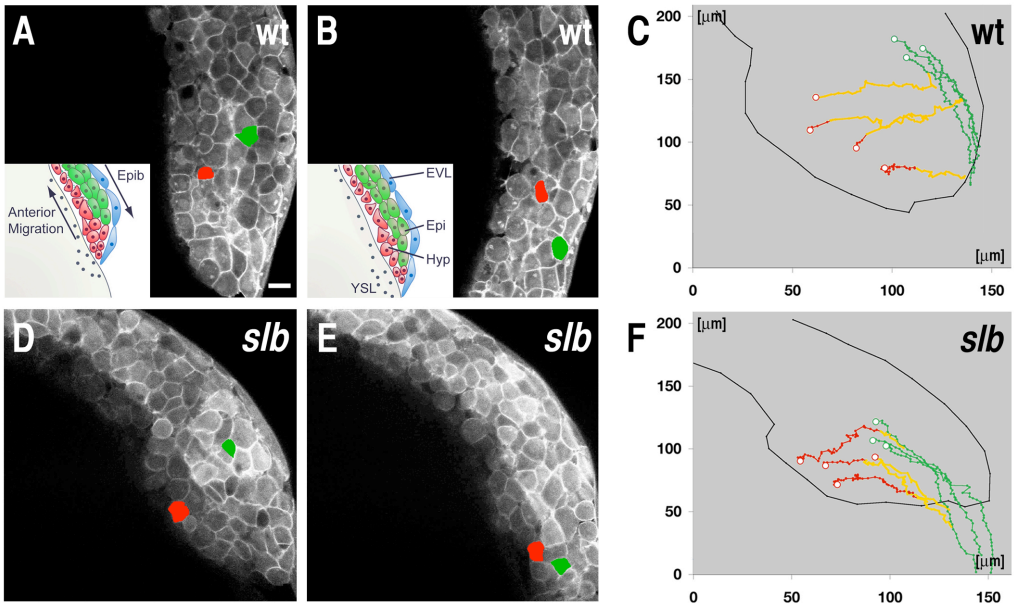

Figure 12. Cell movements within the axial germ ring (shield) at the onset of gastrulation. (A,B,D,E) Lateral views of the shield region of a wildtype (A,B) and *slb* mutant embryo (D,E) at 60% epiboly (A,D) and 90 min later (B,E). For the full sequence of images see supplementary movies (S7,S8). Single hypoblast and epiblast cells in panels (A,B,D,E) were labeled in red and green, respectively. Epiblast and hypoblast cells were identified by their different net movement and cell morphology (Montero *et al.*, 2005). Inlets in (A) and (B) show schematic representations of cell movements within the shield (EVL = Enveloping Layer; Epi = Epiblast; Hyp = Hypoblast; YSL = Yolk Syncytial Layer).
(C,F) Exemplary tracks of 4 hypoblast (red/yellow) and 3 epiblast cells (green) in a wildtype (C) and *slb* mutant embryo (F) taken from the same movies as shown in panels (A,B,D,E). The red tracks delineate hypoblast cell movement before they reach the epiblast, while the yellow tracks demarcate the movement after contact with the epiblast. White circles mark the starting points of the tracks. In total, 19 hypoblast and 15 epiblast cells from 3 wildtype embryos and 22 hypoblast and 15 epiblast cells from 3 *silberblick* embryos were tracked. Scale bar in (A) = 10 μm.

4.7 Effects of slb/wnt11 *on cell adhesiveness*

For cells to migrate, they have to tightly regulate their adhesive contacts with the substratum on which they move (Montero and Heisenberg, 2004). In *Xenopus*, non-canonical wnt-signalling has been shown to regulate the adhesion between mesodermal cells *in vitro*, and E-cadherin mediated adhesion between mesendodermal cells is required for their movement and spreading along the neurectoderm during zebrafish gastrulation (Montero *et al.*, 2005). Wnt11 signalling could therefore regulate cell movements during gastrulation by targeting E-cadherin mediated cell adhesion. To test this assumption, the aggregation behaviour of primary mesendodermal cells from wt and *slb/wnt11* mutant embryos in the presence or absence of E-cadherin on fibronectin was observed. Fibronectin is an abundant component of the extracellular matrix, which is required for gastrulation movements in both *Xenopus* and zebrafish (Marsden and DeSimone, 2003; Trinh *et al.*, 2004). To ubiquitously induce mesendodermal fates, the Nodal pathway was activated by *cyclops* overexpression, which normally induces mesendodermal fates at the onset of gastrulation (Whitman, 2001; Schier, 2003). Embryos were dissociated by treatment with trypsin and Ca^{2+} depletion shortly after the midblastula transition when the expression of target genes and mesendodermal markers such as *no tail* (*ntl*) and *goosecoid* (*gsc*) indicated the ubiquitous induction of

mesendodermal cell fates (B. Kilian, L. Carvalho, E.-M. Schoetz, personal communication[2]; Schulte-Merker *et al.*, 1994; Thisse *et al.*, 1994). These embryos also ubiquitously expressed *wnt11* - probably as a result of *ntl* activation, since the latter has been shown to be sufficient to induce *wnt11* in *Xenopus* and zebrafish (C.-P. Heisenberg, personal commmunication; Makita *et al.*, 1998; Tada and Smith, 2000).

Dissociated mesendodermal cells from wt and *slb*/*wnt11* mutant embryos were taken up in Ca^{2+} containing medium, plated on a fibronectin coated substrate, and their reaggregation behaviour was observed over time. These cells were also injected with *m*RNA for membrane-bound GFP ('GAP43-GFP'; Okada *et al.*, 1999) to highlight the plasma membrane. The cells were then observed with a confocal microscope (see Methods for more details). Already 6 h after plating, mesendodermal cells from wt embryos efficiently formed aggregates or 'clusters' of distinct sizes, many of which contained more than 10 cells. In contrast, *slb* mesendodermal cells appeared less efficient in clustering with many aggregates having less than 10 cells (figure 13 A,C). The large aggregates contained often around 100 cells and would have been very time-consuming to count or analyze. Therefore, the ratio of small clusters (less than 11 cells) vs. large clusters (more than 10 cells) was used to quantify the differences in aggregation behaviour between wt and *slb* mutant mesendodermal cells. This ratio was significantly higher in *slb*/*wnt11* mutant embryos compared to their wildtype counterparts (figure 13 A,C,E), indicating that *slb*/*wnt11* mediates the adhesion between mesendodermal cells plated on a fibronectin coat.

To address if the difference in clustering behaviour between wt and *slb* mutant cells is dependent on E-cadherin, E-cadherin protein levels were reduced in wt and *slb* cells by injection of 8 ng of an antisense morpholino oligonucleotide against E-cadherin into the embryo (figure 13 C-E; Babb and Marrs, 2004; Montero *et al.*, 2005). The difference in the ratio of small vs. large clusters which could be observed between uninjected wt and

[2] The expression of *no tail* and *goosecoid* in dome stage embryos that ubiquitously overexpressed cyclops was analysed several times by *in situ* hybridisation (ISH) by different members of the Heisenberg lab. In contrast to wildtype controls, cyclops injected embryos show a strong and ubiquitous upregulation of *gsc*, *ntl* and also *wnt11*.

slb cells was significantly reduced, albeit not totally diminished, indicating that the effects of *slb*/*wnt11* on the adhesion of mesendodermal cells are at least partially mediated by E-cadherin.

Since in this assay, cells are plated on a fibronectin coat, an interesting question remains whether the differences in adhesion between wt and *slb* mutant cells are also mediated by their interaction with the substrate on which they move. One possibility to address this question is to add RGD peptides to the culture medium to inhibit the binding of cells to fibronectin (Ruoslahti and Pierschbacher, 1987). In initial experiments, the difference in clustering behaviour between wt and *slb* mutant cells after 6h did not seem to be changed in the presence of 250 μM RGD peptides, but additional experiments have to be made and quantified to obtain a more reliable result.

Another interesting question is if the observed defect in aggregation in slb mutant cells is specifically caused by the absence of *slb*/*wnt11* function. This question was not yet addressed in the assay used here. However, in different assays, in which the cells were cultured over night, the diminished ability of *slb* mutant cells to aggregate could be restored upon overexpression of 10 pg *slb*/*wnt11* mRNA, suggesting that the loss of clustering ability is specifically due to the absence of *slb*/*wnt11* function (C.-P. Heisenberg, personal commmunication).

These results indicate that *slb*/*wnt11* is required for the regulation of adhesion between mesendodermal cells in culture, and that this function is at least partially mediated by E-cadherin, indicating that *slb*/*wnt11* regulates E-cadherin mediated cell adhesion.

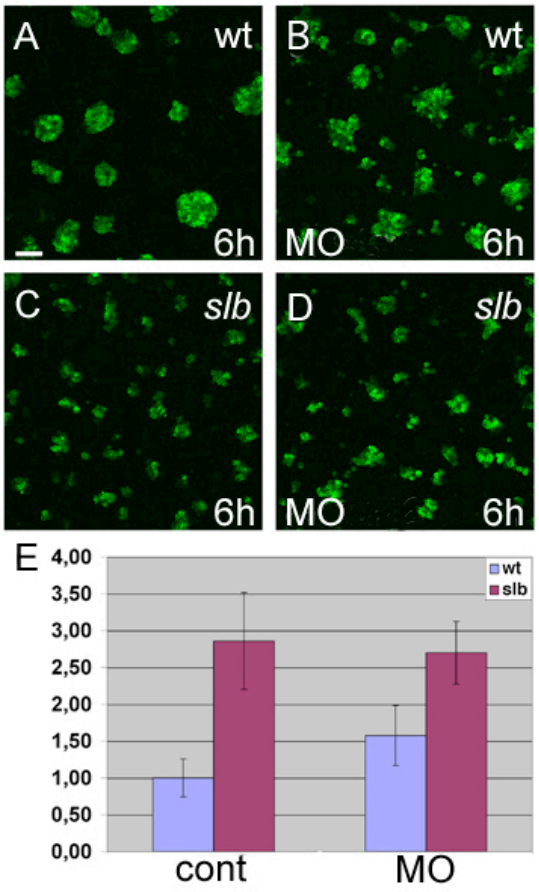

Figure 13. Adhesion between mesendodermal cells in culture. (A-D) Confocal images of primary mesendodermal progenitors labeled with Gap43-GFP from wild type (A,B) and *slb/wnt11* mutant embryos (C,D) plated on fibronectin after 6h in culture either un-injected (A,C) or injected with 8ng of e-cadherin-MO (B,D). (E) Ratios of small aggregates (≤ 10 cells) vs. large aggregates (>10 cells) after 6h in culture taken from wild type embryos and *slb/wnt11* mutants in the presence ('MO') and absence of E-cadherin ('cont'). Values were normalized to the uninjected wild type. Scale bar in (A) = 100 μm.

4.8 Effect of slb/wnt11 *function on subcellular E-cadherin localization*

Since E-cadherin is required *in vitro* for the function of *slb/wnt11* in mediating adhesion between mesendodermal cells, and since it is also needed for the spreading and movement of these cells during gastrulation *in vivo* (Montero et al., 2005), E-cadherin could act as a downstream target of *slb/wnt11* function in the regulation of cell adhesion

and migration during gastrulation. To address if Wnt11 controls the adhesion between mesendodermal progenitors by regulating the expression or subcellular distribution of E-cadherin within the early germ-ring, embryos were probed with an antibody directed against the extracellular domain of zebrafish E-cadherin (Babb and Marrs, 2004).

In wild-type embryos, E-cadherin staining could be predominantly observed at the plasma membrane and in vesicular structures in the cytosol; significantly less cytoplasmic staining was observed in *slb* mutant embryos (figure 14 A-C; table 06). In addition, the membrane staining appeared to be slightly weaker in wt embryos compared to *slb* embryos. However, the quantification of membrane intensity is still ongoing and therefore no definitive statement about E-cadherin membrane localization downstream of *slb/wnt11* function can be made here.

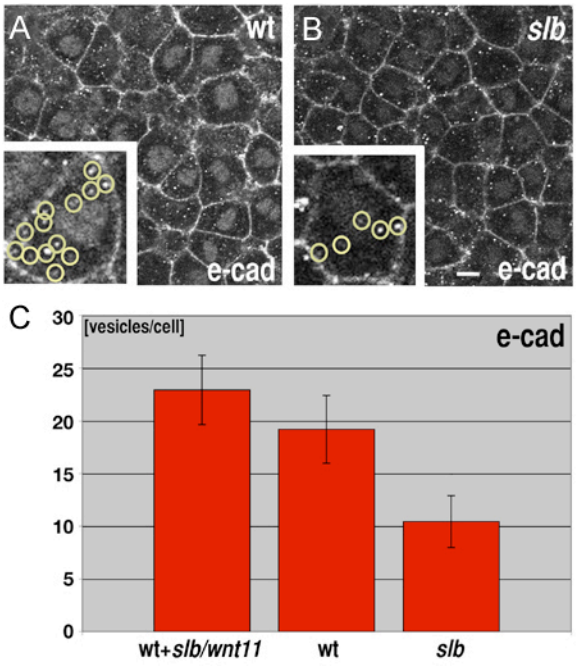

Figure 14. Expression and intracellular localization of E-cadherin within the germ ring at the onset of gastrulation. Confocal sections of shield stage epiblast cells at the dorsal region of the germ ring were chosen for analysis (see Methods for more details). (A,B) Face-on views of epiblast cells at shield stage (60% epiboly) stained with an antibody directed zebrafish E-cadherin in wild-type (A) and *slb* mutant embryos (B). The inlets show magnifications of single cells with E-cadherin positive vesicles circled. (C)

Quantification of the number of E-cadherin-positive cytoplasmic vesicles in wildtype (wt), wildtype injected with 125 pg *slb*/*wnt11 m*RNA and *slb* mutant epiblast cells. For each of the cases, n = 60 cells from 5 embryos were quantified; see also table 6. Scale bar in (B) = 5 μm (approximate value).

	dots/cell	**s. d.**	**wt + wnt11**	**wt**	**slb**
wt + *wnt11*	23	3	1.00	$1{,}95 \cdot 10^{-2}$	$3.27 \cdot 10^{-8}$
wt	19	3	$1{,}95 \cdot 10^{-2}$	1.00	$3.11 \cdot 10^{-6}$
slb	10	2	$3.27 \cdot 10^{-8}$	$3.11 \cdot 10^{-6}$	1.00

Table 06. E-cadherin positive cytoplasmic 'dots' per cell in *slb* mutant embryos, wt embryos and wt embryos injected with 125 pg *slb*/*wnt11 m*RNA. The three right-most columns display p-values, obtained by an unpaired Student's t-test, to show that the distribution of dots is significantly changed upon *slb*/*wnt11* function. s. d., standard deviation. For a graphical representation of the data, see figure 14.

A similar effect could be observed in *slb*/*wnt11* mutant embryos carrying a wnt11-HA transgene under the control of a heat shock promoter, that had been heat shocked for 20 minutes at 39 ºC and fixed 30 minutes later - which is the time when wnt11-HA expression could be first detected on a western blot (Vinzenz Link, personal communication). These embryos could be rescued by heat-induced overexpression of *slb*/*wnt11* (see table 07). After the heat shock, transgenic embryos showed an increased cytoplasmic E-cadherin staining with frequent disruptions of plasma membrane stainings. In contrast, similarly treated embryos with the same genetic background that did not carry a wnt11-HA transgene, had less E-cadherin staining in the cytoplasm and a seemingly more stable staining at the plasma membrane (figure 15 D,E). Furthermore, the differences in E-cadherin cytoplasmic distribution were not accompanied by recognizable changes in the overall expression levels of E-cadherin as determined on Western blots of early gastrula stage embryos (figure 15 A). As a control for general plasma membrane turnover downstream of *slb*/*wnt11* function, the five-pass transmembrane protein Strabismus, C-terminally fused to an HA tag ('stbm-HA'; Jessen *et al*., 2002), was overexpressed in wild type embryos, injected with 125 pg *slb*/*wnt11 m*RNA, and *slb* mutant embryos. Embryos were fixed at shield stage and subsequently stained with an α-HA antibody, but there was no upregulation of cytoplasmic staining in wildtype embryos

compared with *slb* mutants[3]. This staining behaviour could be consistently seen in all experiments carried out with Stbm-HA (S. Witzel, personal communication), although a definitive statement still awaits quantification. The results obtained from this experiment suggest that the enhanced cytoplasmic staining in wt embryos is specific for E-cadherin and not just the result of a generally enhanced membrane turnover (figure 15 B,C).

Taken together, these results indicate that *slb*/*wnt11* function specifically enhances E-cadherin staining in the cytoplasm, while it downregulates E-cadherin at the plasma membrane. The expression levels of E-cadherin in the whole embryo are not affected.

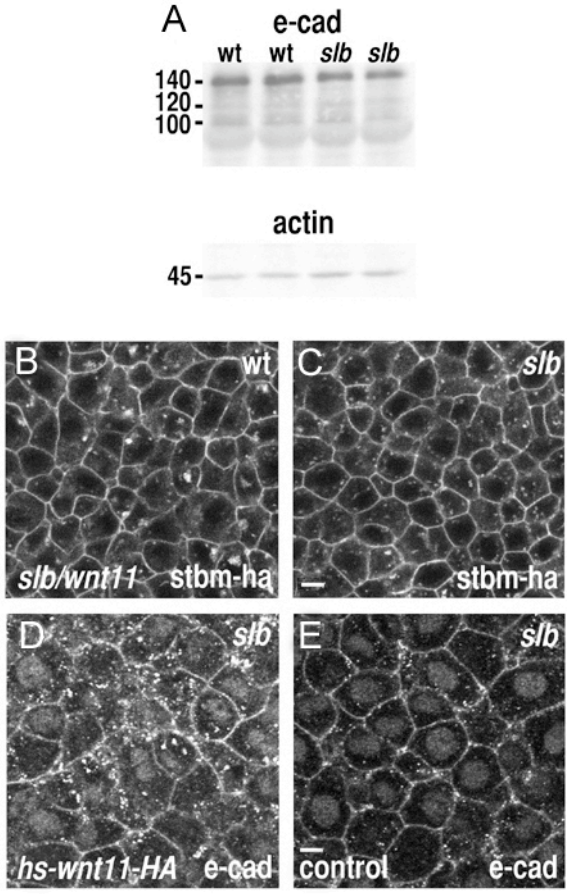

Figure 15. (A) Western blot analysis of E-cadherin expression in wildtype and *slb* mutant embryos at the onset of gastrulation. An Actin antibody was used as a loading control. (B-E) Confocal sections of shield

[3] However, it should be noted that stbm-HA cytoplasmic staining sometimes appeared slightly increased in *slb*/*wnt11* mutants (see figure 15 B,C).

stage epiblast cells at the dorsal region of the germ ring were chosen for analysis (see Methods for more details). (B,C) Face-on views of epiblast cells stained with an antibody directed against HA in a wildtype embryo injected with 125pg *slb/wnt11 m*RNA (B) and a *slb* mutant embryo (C). Both embryos were over-expressing 50pg *stbm-HA*. (D,E) Face-on views of epiblast cells stained with an antibody directed against zebrafish E-cadherin in a *slb hs-wnt11-HA* transgenic embryo and a *slb* non-transgenic control embryo 30' after heat-shock. Scale bars in (C) = 10 μm and (E) = 5 μm (approximate values).

4.9 Mechanism of slb/wnt11 *function in intracellular distribution of E-cadherin*

What could be the mechanism behind the observed differences in the intracellular E-cadherin staining pattern between wt and *slb* mutant embryos? To address the nature of the cytoplasmic vesicular staining of E-cadherin in wild-type embryos, rhodamine-dextran, which is readily endocytosed by gastrulating cells (Scholpp and Brand, 2004), was injected into the intercellular space of dome stage embryos (4.5 hpf); these embryos were fixed 1.5 h later at early shield stage (6 hpf) and stained for E-cadherin. At shield stage, a distinct portion of E-cadherin positive vesicles was found to colocalize with rhodamine-dextran (figure 16 A-C), indicating that E-cadherin positive vesicles indeed localized to endocytic compartments.

The GTPase Rab5 is a highly conserved key regulator of clathrin-mediated endocytosis and has previously been shown to play a central role in early endocytic trafficking in gastrulating zebrafish embryos (Zerial and McBride, 2001; Scholpp and Brand, 2004). To determine whether Rab5 is involved in endocytosis of E-cadherin, Rab5-mediated endocytosis was induced in *slb/wnt11* mutants by overexpressing an activated form of rab5c ('da-rab5c'; Pelkmans *et al.*, 2004). In *slb/wnt11* mutant embryos, only a small fraction of E-cadherin positive vesicles was found to be also positive for Rab5c-YFP (figure 16 D-F). However, upon expression of da-rab5c-YFP, the proportion of double positive vesicles was increased (figure 16 G-I), suggesting that activation of Rab5 is sufficient to induce E-cadherin cytoplasmic staining. Conversely, injecting *slb/wnt11* hs-wnt11-HA embryos with rab5c-MO (for details about rab5c-MO see Material and Methods) efficiently blocked the increase in cytoplasmic E-cadherin vesicles previously observed in un-injected, heat-shocked *slb/wnt11* hswnt11-HA transgenic embryos (figure

16 J-L). These observations suggest that Rab5 functions downstream of Wnt11 in regulating endocytosis of E-cadherin.

Figure 16. Endocytic function in E-cadherin localization. In (A-L), face-on-views of confocal sections of epiblast cells within the germ-ring at shield stage are shown (see Methods for more details). (A-C) Wildtype embryo injected with rhodamine-dextran at dome stage. (A) E-cadherin staining; (B) rhodamine-dextran labeling; (C) merged picture of (A) and (B). (D-F) *slb* mutant embryo injected with 100 pg rab5c-YFP *m*RNA. (D) E-cadherin staining; (E) Rab5c-YFP labeling; (F) merged picture of (D) and (E). (G-I) slb mutant embryo injected with 100 pg da-rab5c-YFP *m*RNA. (G) E-cadherin staining; (H) da-Rab5c-YFP labeling; (I) merged picture of (G) and (H). (J-L) *slb* hs-wnt11-HA transgenic embryo either un-injected (J) or injected with rab5c-MO (K) 30' after heat-shock; (L) shows the distribution of the fluorescent rab5c-MO in (K). Scale bar in (A) = 5 μm.

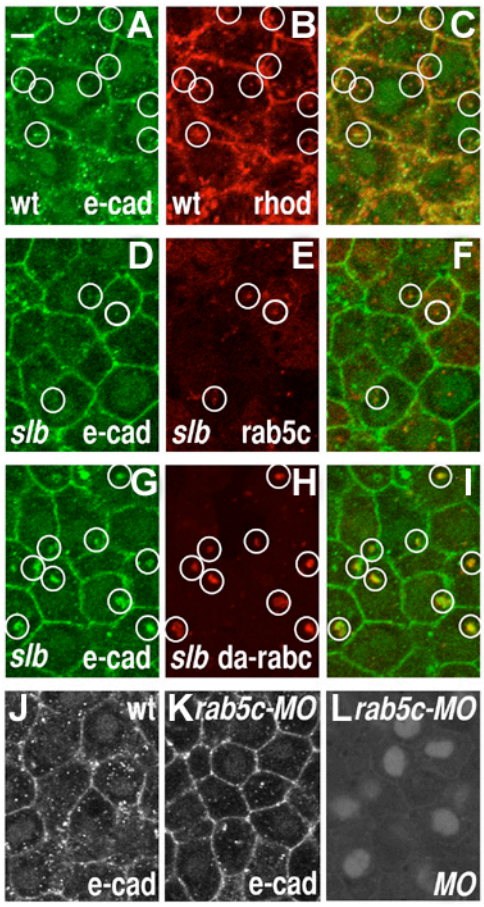

4.10 Function for rab5 mediated endocytosis in cell adhesion

To further address if, similar to loss of *slb/wnt11* function, reduced E-cadherin endocytosis is accompanied by a decrease in cell-cell adhesion, the cell aggregation behavior of wildtype and *rab5c-MO* injected mesendodermal cells in culture was compared. To specifically address if cell-cell adhesion is affected bei knockdown of rab5c, mesendodermal cells were cultured in substrate-free hanging-drops (details in Methods; Ehrlich *et al.*, 2002). After 6 - 8 h in culture, differently labelled wild-type cells clustered as randomly mixed populations of cells (Fig. 17 A,C,E), whereas wildtype cells mixed with *rab5c-MO* injected cells yielded smaller cell aggregates that consisted of tightly clustered wildtype cells surrounded by more loosely associated morphant cells (Fig. 17 B,D,F). According to the differential cell adhesiveness hypothesis (DAH), cell populatons with different adhesive properties sort out from each other, with the weaker adhesive cells being on the outside of aggregates with stronger adhesiveness (Steinberg, 1996). Since *rab5c* morphant cells apparently sort out from untreated wild-type cells (figure 17 B,D,F), thi suggests that Rab5-mediated endocytosis is required for the adhesion of mesendodermal cells in culture.

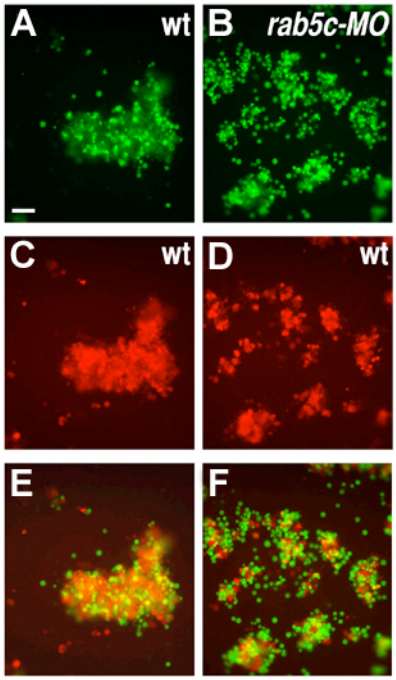

Figure 17. Function of Rab5 mediated endocytosis on cell adhesion. (A-F) Epifluorescence images of hanging-drop cultures with differentially labeled primary mesendodermal progenitors from a mix of two uninjected wildtype controls (A, green; C, red), and a mix of un-injected wildtype controls (D, red) and wildtype embryos injected with 8 ng of rab5c-MO (B, green) after 6 - 8 h in culture; panels (E,F) represent the merged pictures of (A,C) and (B,D), respectively. Scale bar in (A) = 50 μm.

4.11 Function of rab5 downstream of **slb/wnt11** *in gastrulation movements*

To finally test whether Rab5c functions downstream of *slb/wnt11* in mediating prechordal plate morphogenesis during gastrulation, wild type embryos were injected with 8 ng rab5c-morpholino or either a 50 pg of a dominant negative form of human Dynamin2 ('dn-dyn') or 200 pg RN-tre *m*RNA. Dynamin2 regulates the fission of clathrin-coated vesicles from the plasma membrane, which can be inhibited in a dominant-negative manner by overexpressing the mutant K44A ('dn-dyn'; van der Blieck *et al.*, 1993; Scholpp and Brand, 2004). RN-tre is a GTPase-activating-protein that specifically acts on Rab5 and converts it into the inactive Rab5-GDP form (Lanzetti *et al.*, 2000; Scholpp and Brand, 2004). Both 'dn-dyn' and RN-tre therefore function as inhibitors of Rab5- and Clathrin-mediated endocytosis (Pelkmans *et al.*, 2004; Scholpp and Brand, 2004). Embryos treated with rab5c morpholino, dn-dyn and RN-tre frequently showed a posteriorly displaced and elongated prechordal plate at the end of gastrulation, thus phenocopying the *slb/wnt11* mutant phenotype (figure 18 A-D; table 7). On the other hand, *slb/wnt11* mutant embryos injected with da-rab5c-YFP *m*RNA frequently formed a prechordal plate that was wild type in appearance, indicating a rescue of the mutant phenotype (figure 18 E,F; table 7).

These observations suggests that rab5-mediated endocytosis constitutes a downstream target mechanism by which *slb/wnt11* controls prechordal plate morphogenesis during gastrulation.

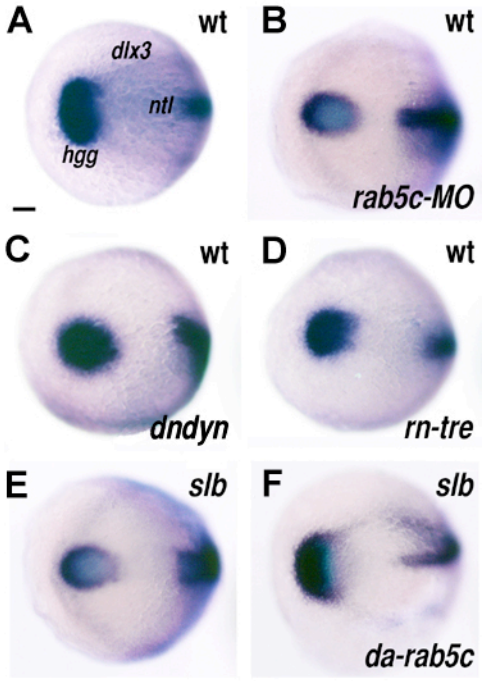

Figure 18. (A-F) Position of the prechordal plate stained for *hgg1* relative to the anterior edge of the neural plate, which was marked with *dlx3*, and the notochord expressing *ntl* at bud stage in a wildtype control embryo (A), a wildtype embryo injected with either 8ng rab5c-MO (B), 50pg dn-dyn mRNA (C) and 200pg RN-tre mRNA (D), in a *slb* mutant embryo (E) and a *slb* mutant injected with 150pg da-rab5c-YFP mRNA (F); see also table 7. Dorsal views with anterior to the left. Scale bar in (A) = 200 μm.

injected	genotype	wildtype (%)	*slb* (%)	abnormal (%)	total (n)
-	wt	100	0	0	72
rab5c MO	wt	43	51	6	120
rn-tre	wt	69	29	2	51
dn-dyn	wt	75	25	0	55
gfp	*slb*	4	96	0	48
da-rab5c	*slb*	40	60	0	58
heat shock	*slb* cont	9	91	0	99
heat shock	*slb wnt11HA*	76	24	0	87

Table 07. Phenocopy and rescue of the *slb*/*wnt11* phenotype at the end of gastrulation (see also figure 18). 8ng of rab5c morpholino (MO) and 200pg, 100pg and 150pg of rn-tre, cytoplasmic gfp and da-rab5c *m*RNA, respectively, were injected into one-cell stage embryos; 50pg dn-dyn *m*RNA was injected into one-two cell stage embryos. Heat shocks were performed 20 min at 39 °C on early shield stage *slb* embryos either with or without a hsp-wnt11HA transgene ('*slb* cont' or '*slb wnt11HA*', respectively; see Methods for further details). Embryos classified as '*slb'* displayed an elongated, posteriorly displaced prechordal plate at the end of gastrulation (bud stage), and embryos classified as 'abnormal' showed other variable defects in morphogenesis of prechordal plate and notochord.

5. Discussion

In this study, the movement and morphologies of individual cells in three-dimensions were recorded and analyzed during the onset of gastrulation by using two-photon confocal imaging and computer-assisted image analysis. In *slb* mutant embryos, axial hypoblast (mesendodermal progenitor) cells within the forming germ-ring migrate towards the animal pole in a slower, less directed way than in wildtype embryos. These aberant cell movements are accompanied by defects in the orientation of cellular protrusions along the individual movement direction of these cells rather than defects in the net movement direction, indicating that *slb/wnt11* regulates the stabilization of cellular movements within the germ-ring, but does not enable them *per se*.

By analyzing the cellular and molecular functions of *slb/wnt11* at the onset of gastrulation, *slb/wnt11* is found to regulate the adhesion of mesendodermal progenitor cells. Moreover, Wnt11 activity in gastrulation is mediated by the GTPase Rab5, since blocking Rab5-mediated endocytosis in wild type embryos phenocopies *slb* mutants, and enhancing Rab5-mediated endocytosis effectively rescues the *slb* mutant phenotype. In addition, E-cadherin is required downstream of *slb/wnt11* for mesendodermal cell adhesion, and is endocytosed via Rab5 in response to Wnt11 signals. These data suggest that E-cadherin plays an important role in the regulation of cell adhesion downstream of Wnt11 signalling during gastrulation, and that this process is mediated by Rab5-based endocytosis.

5.1. Cellular function of slb/wnt11 at the onset of gastrulation

The main finding in the first part of this study is that *slb/wnt11* is required for both cellular process orientation and directed cell movements of hypoblast cells at the onset of gastrulation. To obtain insight into the relationship of process orientation and cell movement in single cells, an assay was developed that allowed for the comparison of dynamic changes in process orientation with changes in the direction of cell movements (figures 8; 9). In wild-type prechordal plate progenitors (axial hypoblast), process

orientation and individual movement direction are aligned, whereas in *slb* mutant cells, no such alignment is observed. The misalignment of process orientation and movement direction in *slb* mutants is linked to less efficient movements of hypoblast cells towards the animal pole (figures 6; 7; 10). How do these findings relate to previous studies that implicate *slb/wnt11* function and non-canonical Wnt signalling in the regulation of convergence and extension (CE) movements at later stages of gastrulation (reviewed by Tada *et al.*, 2002; Wallingford *et al.*, 2002)?

In this study, *slb/wnt11* function was analyzed in cells that were morphogenetically distinct from cells undergoing convergence and extension (CE) movements. Prospective prechordal plate cells in the region of the forming germ ring at the onset of gastrulation do not show medio-lateral cell intercalation behaviour nor elongate along their medio-lateral axes (Miguel Concha and Carl-Philipp Heisenberg, personal communication), as described for cells undergoing CE movements (Concha and Adams, 1998; Myers *et al.*, 2002; Glickman *et al.*, 2003). Instead, they move in a straight path towards the animal pole, similar to the behaviour of cells exhibiting directed migration on a substrate (figure 7; Warga and Kimmel, 1990). Consequently, *slb/wnt11* is required for the orientation of cellular processes along the movement axis of individual cells, a feature that is associated commonly with migrating cells *in vitro* and *in vivo* (Lauffenburger and Horwitz, 1996).

By contrast, the cellular functions of non-canonical Wnt signalling in controlling cell movements during CE have not been fully addressed. Reduced medio-lateral cell elongation in different mutant and morphant phenotypes of the Wnt/PCP pathway has been associated with slower, less persistent cell movements at late stages of gastrulation (Wallingford *et al.*, 2000; Topczewski *et al.*, 2001; Keller, 2002; Jessen *et al.*, 2002; Marlow *et al.*, 2002). However, the specific changes in cell elongation have not been correlated with the dynamic changes in the individual movement directions of these cells. Moreover, these cells have been analysed mainly in two dimensions (along the anterior-posterior and dorsal-ventral axis). This limits the view on those cells and, consequently, the interpretation of these observations, because cells undergoing CE movements can also exhibit distinctive movements along the dorsal-ventral axis (Glickman *et al.*, 2003). Future studies that compare the role of non-canonical Wnt signalling in cellular dynamics

during early versus late stages of gastrulation are needed to reveal the common and divergent aspects of Wnt/PCP signalling during the course of gastrulation.

Interestingly, although prospective prechordal plate (hypoblast) cells move slower with more frequent changes in their movement trajectory ('less persistent movement'), and do not orient their processes along their individual movement direction, their net movement direction appears to be unaffected (figure 7; supplementary movies S3 and S4). This indicates that the role of *slb*/*wnt11*-mediated orientation of cellular processes is to facilitate and stabilise these movements, rather than to determine the overall movement direction. Abolishing process formation in gastrulating cells by inhibiting the function of phosphoinositide-3 kinases (PI3Ks) also destabilizes cell movements without changing the net movement direction (Montero *et al.*, 2003), challenging the common view that process formation is in general necessary to enable cell movements (Lauffenburger and Horwitz, 1996; Montero *et al.*, 2003).

Which other mechanisms could enable the movement of mesendodermal (hypoblast) cells in zebrafish? The directed migration of hypoblast cells towards the animal pole of the embryo appears reminiscent of chemotactic behaviour, and Jak/Stat signalling has been implied in the production of a putative secreted convergence factor which would act as a guidance cue for mesendodermal progenitors in a cell autonomous and non-autonomous manner (Yamashita *et al.,* 2002; Miyagi *et al.*, 2004; Solnica-Krezel, 2005). However, definitive evidence for any molecule acting as a chemoattractant or -repellant has been lacking so far, although typical chemotactic ligands such as Slit and Ephrin are present in the embryo (Oates *et al.*, 1999; Yeo *et al.*, 2001). It also appears unlikely that *slb*/*wnt11* in zebrafish provides such a guidance signal, since defective gastrulation movements in *slb* mutants can be rescued by ubiquitous overexpression of *slb*/*wnt11* (figure 6; Heisenberg *et al.*, 2000).

Rather, prechordal plate progenitor (hypoblast) cells could be pushed away at the germ-ring by newly ingressing cells at the germ-ring margin. Since mesendodermal progenitors simultaneously internalize around the entire circumference of the germ-ring margin, the only possible direction for prechordal plate progenitors would be towards the animal pole

(Montero *et al.*, 2003; Montero *et al.*, 2005). If the direction of cell migration is determined independently of cell polarization and process formation, the alignment of processes in the individual cell movement direction could serve as a 'fine-tuning' mechanism for the cells to facilitate their movement and explore their cellular environment. Similar observations have been made by recent studies in zebrafish and *Xenopus* showing that in both gain- and loss-of-function situations for different components of the Wnt/PCP pathway, a reduction in cell elongation and/or polarization leads to less stable and slower cell movements during gastrulation, but does not interfere with the net movement direction of these cells (Wallingford *et al.*, 2002; Tada *et al.*, 2002).

5.2 Potential target processes of slb/wnt11 *function at the onset of gastrulation*

How does *slb/wnt11* control the orientation of cellular processes and directed cell movements in the germ ring at the onset of gastrulation? The observation that *slb/wnt11* is expressed within the epiblast, although predominantly required in the hypoblast, indicates that *slb/wnt11*, produced in epiblast cells, directly or indirectly influences hypoblast cell movement and morphology. A discrimination between a direct or indirect function of *slb/wnt11* in controlling hypoblast morphogenesis is difficult, partly because antibodies are lacking which would unambigously detect the distribution of endogenous Wnt11 protein. However, the Wnt11-receptor Fz7 is expressed in prechordal plate cells, and secreted Wnt11 activity is sufficient to bind and recruit Fz7 and Dsh to the plasma membrane in a cell non-autonomous, suggesting a more direct function for *slb/wnt11* (Witzel and Heisenberg, unpublished).

Wnt11, secreted by epiblast cells, could regulating rearrangements of the cytoskeleton that modulate the formation and orientation of processes in hypoblast cells. *slb/wnt11* could exert its function either permissively, by allowing these cells to extend and stabilise cellular protrusions in their preferred orientation, or it might function instructively, by determining the orientation of these processes. The observation that ubiquitous overexpression of *slb/wnt11* rescues the cell morphology and movement phenotype of *slb*

mutans argues in favour of a more permissive function of *slb/wnt11* in this process (figures 6; 11). Findings from recent studies in zebrafish, which show that Rok2, known to directly regulate cytoskeletal elements such as myosin in *Drosophila*, is a downstream component of the *slb/wnt11* signalling pathway support a function of *slb/wnt11* in regulating cytoskeletal dynamics (Marlow *et al*., 2002).

Alternatively, *slb/wnt11* could also indirectly affect morphogenesis of hypoblast tissue by regulating the adhesiveness of hypoblast cells, which would have a secondary effect on process orientation and directed cell movement. Support for a role of *slb/wnt11* in regulating cell adhesion comes from recent studies in *Xenopus,* which show that the presumptive receptor for Wnt11, Fz7, is required for the effective separation of mesoderm from ectoderm at the onset of gastrulation. Furthermore, Wnt11 signalling has been shown to decrease adhesive contacts between cultured mouse endothelial cells by modulating intracellular E-cadherin distribution (Winklbauer *et al*., 2001; Ouko *et al*., 2004).

Prospective prechordal plate (hypoblast) cells, once internalized, move towards the overlying epiblast and subsequently use the epiblast as a substrate to migrate towards the animal pole (figure 12; supplementary movie S7; Montero *et al*., 2005). In contrast, hypoblast cells from *slb/wnt11* mutants, although they can still move normally towards the epiblast, move down with the overlying epiblast towards the vegetal pole (figure 12; supplementary movie S8). Since the epiblast 'substrate' itself moves towards the vegetal pole, hypoblast cells must exhibit a movement component in parallel to the epiblast that compensates this opposite-directed movement. It is conceivable that hypoblast cells, in order to achieve that goal, have to tightly regulate their adhesive properties and have to be able to quickly remodel their adhesive contacts. Indeed, in wildtype embryos, hypoblast cells at the interface to the epiblast layer quickly modulate their shape and contacts to the epiblast cells (supplementary movies S2; S7). In addition, without adhesion molecules such as E-cadherin, hypoblast cells do not move properly towards the animal pole and fail to extend cellular processes in the direction of their movement (Babb

and Marrs, 2004; Montero *et al.*, 2005), suggesting a role for E-cadherin mediated cell-cell adhesion during prechordal plate morphogenesis.

The assumption that *slb/wnt11* function regulates adhesiveness within mesendodermal cells at the onset of gastrulation is strongly supported by *in vitro* studies, where primary mesendodermal cells are dissociated by Ca^{2+} depletion and their reaggregation behaviour is observed for several hours in Ca^{2+} containing medium on a fibronectin coated surface (figure 13; Montero *et al.*, 2003). Fibronectin is an abundant component of the extracellular matrix in *Xenopus* and is required for gastrulation movements in zebrafish (Winklbauer and Keller, 1996; Trinh and Stainier, 2004). *slb/wnt11* is required for the adhesion between mesendodermal cells, and this function is partially - although not exclusively - mediated by E-cadherin (figure 13). Among the other candidates that could mediate cell adhesion downstream of *slb/wnt11* independently of E-cadherin are other cadherins, like N-cadherin, and protocadherins, like Paraxial Protocadherin (Papc). N-cadherin is expressed during later stages of gastrulation in zebrafish, and convergence movements during development of the neural tube are disrupted in zebrafish embryos mutant for *parachute/n-cadherin* (Lele *et al.*, 2002), but neither the involvement of N-cadherin in gastrulation movements nor its interaction with *slb/wnt11* has yet been analyzed. Papc has recently been reported to bind to Fz7 and functionally interact with non-canonical Wnt signalling to coordinate convergent extension movements via RhoA, Rac1 and JNK, known modulators of the cytoskeleton and cell-matrix contacts, in *Xenopus* (Medina *et al.*, 2004; Unterseher *et al.*, 2004). Furthermore, integrin-fibronectin bindings are required for mesodermal progenitor migration and convergent extension movements during *Xenopus* gastrulation. Interestingly, integrin-fibronectin interaction appear to regulate CE movements by modulating cadherin dependent cell-cell adhesion, although the molecular mechanisms underlying this regulation are still not known (Winklbauer and Keller, 1996; Marsden and DeSimone, 2001; Marsden and DeSimone, 2003). Integrin-fibronectin interactions are accompanied by a recruitment of the intracellular Wnt signalling mediator Dishevelled to the plasma membrane (Marsden and DeSimone, 2001; Marsden and DeSimone, 2003). Since Dsh translocates to the plasma

membrane when Wnt signaling is activated (Rothbacher *et al.*, 2000), this suggests a cross-talk between Wnt-, cadherin and integrin-function in the regulation of cell adhesiveness during gastrulation. Adding RGD peptides to mesendodermal cultures on fibronectin to address cell-substrate adhesiveness downstream of *slb*/*wnt11* function, effective inhibitors of integrin-fibronectin interactions (Ruohslahti and Pierschbacher, 1987), to the mesendodermal cells did not appear to change the difference in aggregation behaviour in the presence or absence of *slb*/*wnt11* function after several hours in culture (although these results have not yet been completely quantified yet). It should be noted, however, that abolishing integrin-fibronectin binding by RGD peptides does enhance the aggregation behaviour of mesendodermal cells from wildtype embryos observed during the first 2 - 3 h in culture, while at the same time, it does not change the aggregation behaviour of *slb*/*wnt11* cells (Puech *et al.*, 2005). This suggests that cell-substrate adhesion has an inhibitory effect on early mesendodermal cell re-aggregation and that *slb*/*wnt11* function has an additional role in mediating cell-substrate adhesion in early steps of mesendodermal cell reaggregation.

How could E-cadherin exert its effect on cell migration and cell adhesion in mesendodermal cells? Analysis of the endogenous distribution of E-cadherin indicates that its protein levels are not globally up- or downregulated in the embryo (figure 14). Instead, it appears to relocate into the cytosol dependent of *slb*/*wnt11* function. This enhanced cytoplasmic localization appears unlikely to be a secondary readout for general membrane localization, since other transmembrane proteins such as Strabismus did not show an enhanced cytoplasmic staining upon activation of Wnt11 (figure 15). When labelling the endocytic pathway with rhodamine-dextran, E-cadherin is found to colocalize more strongly with rhodamine positive vesicles upon enhancing Wnt11 activity. This effect can be reverted by depletion of rab5c, indicating that rab5c mediated endocytosis is necessary to mediate the cytosolic localization of E-cadherin downstream of *slb*/*wnt11* function. Moreover, activation of rab5c within the germ-ring of *slb* embryos leads to a nearly complete localization of E-cadherin into rab5c positive endosomes, indicating that rab5c activity is sufficient to trigger cadherin endocytosis (figure 15). A

similar effect of Wnt11 can be seen in avian or mammalian cells, where stimulation with Wnt11 leads to an enhanced cytoplasmic staining of endogenous N-cadherin or E-cadherin, respectively (Eisenberg *et al.*, 1997; Ouko *et al.*, 2004). However, a functional relationship of the intracellular distribution of cadherins downstream of *slb/wnt11* function with rab5 mediated endocytosis has so far not been tested in these systems.

How could Wnt11 regulate the endocytosis of E-cadherin? One possibility is that Rab5 activity is directly regulated. Wnt11 could signal to Rab5 via known regulators and effectors of Rab5, such as the Rabaptin5-Rabex-5 complex and early endosomal antigen 1 (EEA1) (Zerial and McBride, 2001). However, the endogenous function(s) of these molecules and potential regulation by upstream signals have not yet been analyzed in zebrafish. It is also not known, if Rab5 mediates its effect exclusively via the clathrin-mediated pathway, or if other endocytic routes, like caveolae mediated endocytosis, are also involved. E-cadherin has been shown to colocalize with caveolin-1, an abundant component of caveolae, in metastatic cells (Lu *et al.*, 2003). Furthermore, zebrafish embryos depleted of caveolin-1 are shorter and display a broadened notochord and narrow somites during somitogenesis, a phenotype reminiscent of defects in convergent extension movements, suggesting a requirement for caveolin-mediated endocytosis in gastrulation (Smart *et al.*, 2004). An alternative possibility is that Wnt11 increases endocytosis more indirectly, for example through its downstream signaling mediators RhoA and Rok2 (Habas et al., 2001; Marlow et al., 2002) to promote actin-myosin contractility, which would secondarily lead to a stimulation of endocytosis (Ascough, 2004).

Importantly, clathrin- and/or rab5-mediated endocytoses are required for gastrulation movements, and Rab5c functions downstream of *slb/wnt11* (figure 16; table 7). Moreover, rab5c function is required for cell adhesion, and Rab5c activity is sufficient to rescue the adhesion defect in mesendodermal cells from *slb/wnt11* mutant embryos. This indicates that rab5c mediated endocytosis, possibly of cadherin molecules, regulates the adhesive and the migratory potential of mesendodermal cells during gastrulation.

5.3 A model for slb/wnt11 *function in regulating gastrulation movements*

The findings of this study strongly suggest that Wnt11 controls mesendodermal cell adhesion through Rab5-mediated endocytosis and E-cadherin. Cell migration depends on dynamic modulation of adhesive contacts (Lauffenburger and Horwitz, 1996), and endocytosis and recycling of adhesion molecules is a prerequisite for junction formation and remodeling (Le *et al.*, 1999). Therefore, *slb/wnt11* could control prechordal plate progenitor migration by promoting cell adhesion through Rab5-mediated endocytosis of adhesion molecules including E-cadherin. However, the specific contribution of E-cadherin endocytosis for tissue morphogenesis during gastrulation remains to be determined. Previous work has shown that E-cadherin is the prime classical Cadherin expressed at the onset of zebrafish gastrulation, and that it is required for mesendodermal cell adhesion and migration (Babb and Marrs, 2004; Kane *et al.*, 2005; Montero *et al.*, 2005). This data, in combination with the findings that E-cadherin functions downstream of Wnt11 and is endocytosed in response to *slb/wnt11* and rab5c function, strongly suggest a role for E-cadherin endocytosis during gastrulation cell movements. However, it is unlikely that E-Cadherin will be the sole target of the Wnt11 driven endocytosis responsible for cell adhesion. In fact, the observation from this study that E-cadherin is partially, but not exclusively required for Wnt11 controlling mesendodermal cell adhesion, suggests that other molecules, perhaps protocadherins, must also be involved.

Interestingly, recent findings show that the PCP pathway controls the dynamic modulation of adhesion contacts during *Drosophila* imaginal disc development by regulating endocytosis and/or recycling of E-cadherin adhesion complexes (A. Classen and S. Eaton, personal communication). Considering that several zebrafish homologues of the *Drosophila* PCP pathway also genetically interact with and/or are part of the Wnt11 signaling pathway during gastrulation (Tada *et al.*, 2002; Veeman *et al.*, 2003), this raises the intriguing possibility that Wnt/Fz-mediated E-cadherin endocytosis might represent an evolutionary conserved mechanism by which tissue morphogenesis is controlled in both vertebrates and invertebrates. Future studies are necessary to reveal possible conserved molecular control mechanisms by which Wnt/Fz signaling regulates

E-cadherin endocytosis and the specific contribution of this process for tissue morphogenesis.

6. Movie Legends

The corresponding movies are on the CD supplemented with this thesis.

Supplementary Movie S1. Zebrafish development from 2-cell stage to mid-somitogenesis. The living embryo was mounted laterally, with the future dorsal side on the right and the anterior part on the top left. The time intervals between single frames is approximately 70 seconds (35 seconds per number displayed in the top right corner). Frame size: approx. 750 x 750 μm. Reproduced from Karlström and Kane (1996).

Supplementary Movie S2. Time-lapse of the cell movements within the germ ring margin at the region of the shield from the beginning of gastrulation onwards, recorded with a two-photon microscope. Cells were labelled with a mixture of cytosolic and membrane bound GFP. The movie was recorded for a total of 123 minutes at 2.6-minute time intervals. Sagittal views. Frame size: 206 x 206 μm. Reproduced from Montero *et al*. (2005).

Supplementary Movie S3. Time-lapse showing the movement of epiblast cells in red (labelled with rhodamine) and hypoblast cells in green (labelled with GFP) in wild type embryos for 45 minutes at the onset of gastrulation. Hypoblast (prospective prechordal plate) cells are moving from the bottom (germ ring) to the top (animal pole), while epiblast (prospective ectoderm) cells are moving in the opposite direction. Dorsal (start of movie), ventral (middle) and lateral (end) views. Frame size: 205 x 205 μm.

Supplementary Movie S4. Time-lapse showing the movement of epiblast cells in red (labelled with rhodamine) and hypoblast cells in green (labelled with GFP) in *slb*/*wnt11*

mutant embryos for 45 minutes at the onset of gastrulation. Hypoblast (prospective prechordal plate) cells are moving from the bottom (germ ring) to the top (animal pole), while epiblast (prospective ectoderm) cells are moving in the opposite direction. Dorsal (start of movie), ventral (middle) and lateral (end) views. Frame size: 205 x 205 μm.

Supplementary Movie S5. Time-lapse of wild-type and *slb*/*wnt11* mutant prechordal plate precursor cell movement at four consecutive timepoints (0, 2.5, 5, 7.5 minutes). Cells were labelled with a mixture of cytosolic and membrane-bound GFP and move from top (germ ring) to the bottom (animal pole). Frame size: approx. 75 x 75 μm.

Supplementary Movie S6. Time-lapse of wild-type and *slb*/*wnt11* mutant epiblast cell movement at four consecutive timepoints (0, 2.5, 5, 7.5 minutes). Cells were labelled with a mixture of cytosolic and membrane-bound GFP and move from top (animal pole) to the bottom (germ ring). Frame size: approx. 75 x 75 μm.

Supplementary Movie S7. Time-lapse showing the movement of ectodermal precursor (epiblast) cells and mesendodermal precursor (hypoblast) cells in the shield region of wild type embryos for 90 minutes at the onset of gastrulation. Exemplaric cells from hypoblast and epiblast are depicted in red and green, respectively. Hypoblast cells are moving from the germ ring (bottom) towards and along the epiblast in direction of the animal pole (top), while epiblast cells are moving in the opposite direction. Sagittal view. Frame size: 207 x 207 μm.

Supplementary Movie S8. Time-lapse showing the movement of ectodermal precursor (epiblast) cells and mesendodermal precursor (hypoblast) cells in the shield region of wild type embryos for 90 minutes at the onset of gastrulation. Exemplaric cells from hypoblast and epiblast are depicted in red and green, respectively. Hypoblast cells are moving from the germ ring (bottom) towards and along the epiblast in direction of the animal pole (top), while epiblast cells are moving in the opposite direction. Sagittal view. Frame size: 207 x 207 μm.

7. References

Abraham, V. C.; Miller, A. L.; Jaffe, L. F. 1995. Microtubule Arrays during Ooplasmic Segregation in the Medaka Fish Egg (*Oryzias latipes*). *Biol. Bull.* **188**: 136 - 145.

Abdelilah, S.; Solnica-Krezel, L.; Stainier, D. Y.; Driever, W. 1994. Implications for Dorsoventral Axis Determination from the Zebrafish Mutation *Janus*. *Nature* **370**: 468 - 471.

Adler, P. N.: Lee, H. 2001 Frizzled Signaling and Cell-Cell Interactions in Planar Polarity. *Curr. Opin. Cell Biol.* **13**: 635 - 640.

Adler, P. N. 2002. Planar Signaling and Morphogenesis in *Drosophila*. *Dev Cell* **2**: 525 - 535.

Akimenko, M. A.; Ekker, M.; Wegner, J.; Lin, W.; Westerfield, M. 1994. Combinatorial Expression of Three Zebrafish Genes Related to Distal-Less: Part of a Homeobox Gene Code for the Head. *J. Neurosci.* **14**: 3475 - 3486.

Alexander, J. S.; Jackson, S. A.; Chaney, E.; Kevil, C. G.; Haselton, F. R. 1998. The Role of Cadherin Endocytosis in Endothelial Barrier Regulation: Involvement of Protein Kinase C and Actin-Cadherin Interactions. *Inflammation* **22**: 419 - 433.

Aulehla, A.; Herrmann, B. G. 2004. Segmentation in Vertebrates: Clock and Gradient Finally Joined. *Genes Dev*. **18**: 2060 - 2067.

Axelrod, J. D. 2001. Unipolar Membrane Association of Dishevelled Mediates Frizzled Planar Cell Polarity Signalling. *Genes Dev*. **15**: 1182 - 1187.

Ayscough, K. R. 2004. Endocytosis: Actin in the Driving Seat. *Curr. Biol.* **14**: R124 -

R126.

Babb, S. G.; Marrs, J. A. 2004. E-Cadherin Regulates Cell Movements and Tissue Formation in Early Zebrafish Embryos. *Dev. Dyn.* **230**: 263 - 277.

Barth, K. A.; Wilson, S.W. 1995. Expression of Zebrafish *nkx2.2* Is Influenced by Sonic Hedgehog/Vertebrate Hedgehog-1 and Demarcates a Zone of Neuronal Differentiation in the Embryonic Forebrain. *Development* **121** : 1755 - 1768.

Bertet, C.; Sulak, L.; Lecuit, T. 2004. Myosin-Dependent Junction Remodelling Controls Planar Cell Intercalation and Axis Elongation. *Nature* **429**: 667 - 671.

Braga, V. M. ; Machesky, L. M. ; Hall, A. ; Hotchin, N. A. 1997. The Small GTPases Rho and Rac Are Required for the Establishment of Cadherin-Dependent Cell-Cell Contacts. *J. Cell Biol.* **137**: 1421 - 1431.

Bretscher, M. S. 1996. Moving Membrane up to the Front of Migrating Cells. *Cell* **85**: 465 - 467.

Brieher, W. M.; Gumbiner, B. M. 1994. Regulation of C-Cadherin Function during Activin-Induced Morphogenesis of *Xenopus* Animal Caps. *J. Cell Biol.* **126**: 519 - 527.

Bryant, D. M.; Stow, J. L. 2004. The Ins and Outs of E-Cadherin Trafficking. *Trends Cell Biol.* **14**: 427 - 434.

Burdine, R. D.; Schier, A. F. 2000. Conserved and Divergent Mechanisms in Left-Right Axis Formation. *Genes Dev.* **14**: 763 - 776.

Cadigan, K. M.; Nusse, R. 1997. Wnt Signalling - A Common Theme in Animal Development. *Genes Dev.* **11**: 3286 - 3305.

Carmany-Rampey, A.; Schier, A. F. 2001. Single-Cell Internalization during Zebrafish Gastrulation. *Curr. Biol.* **11**: 1261 - 1265.

Choi, S. C.; Han, J. K. 2002. *Xenopus* Cdc42 Regulates Convergent Extension Movements during Gastrulation through Wnt/Ca^{2+} Signaling Pathway. *Dev. Biol.* **244**: 342 - 357.

Cohen, E. D.; Mariol, M. C.; Wallace, R. M.; Weyers, J.; Kamberov, Y. G.; Pradel, J.; Wilder, E. L. 2002. DWnt4 Regulates Cell Movement and Focal Adhesion Kinase during *Drosophila* Ovarian Morphogenesis. *Dev. Cell* **2**: 437 - 448.

Concha, M. L.; Adams, R. J. 1998. Oriented Cell Divisions and Cellular Morphogenesis in the Zebrafish Gastrula and Neurula: a Time-Lapse Analysis. *Development* **125**: 983 - 994.

Conlon, F. L.; Barth, K. S.; Robertson, E. J. 1991. A Novel Retrovirally Induced Embryonic Lethal Mutation in the Mouse: Assessment of the Developmental Fate of Embryonic Stem Cells Homozygous for the 413.d Proviral Integration. *Development* **111**: 969 - 981.

Daggett, D. F.; Boyd, C. A..; Gautier, P.; Bryson-Richardson, R. J.; Thisse, C.; Thisse, B.; Amacher, S. L.; Currie, P. D. 2004. Developmentally Restricted Actin-Regulatory Molecules Control Morphogenetic Cell Movements in the Zebrafish Gastrula. *Curr. Biol.* **14**: 1632 - 1638.

Daniel, J. M.; Reynolds, A. B. 1997. Tyrosine Phosphorylation and Cadherin/Catenin Function. *Bioessays* **19**: 883 - 891.

Davidson, L. A.; Keller, R.; DeSimone, D. W. 2004. Assembly and Remodelling of the Fibrillar Fibronectin Extracellular Matrix during Gastrulation and Neurulation in *Xenopus laevis*. *Dev*. *Dyn*. **231**: 888 - 895.

Denk, W.; Svoboda, K. 1997. Photon Upmanship: Why Multiphoton Imaging Is More than a Gimmick. *Neuron* **18**: 351 - 357.

Djiane, A.; Riou, J.; Umbhauer, M.; Boucaut, J.; Shi, D. 2000. Role of Frizzled 7 in the Regulation of Convergent Extension Movements during Gastrulation in *Xenopus laevis*. *Development* **127**: 3091 - 3100.

Driever, W.; Solnica-Krezel, L.; Schier, A. F.; Neuhauss, S. C.; Malicki, J.; Stemple, D. L.; Stainier, D. Y.; Zwartkruis, F.; Abdelilah, S.; Rangini, Z.; Belak, J.; Boggs, C. 1996. A Genetic Screen for Mutations Affecting Embryogenesis in Zebrafish. *Development* **123**: 37 - 46.

Du, S. J.; Purcell, S. M. Christian, J. L.; McGrew, L. L. Moon, R. T. 1995. Identification of Distinct Classes and Functional Domains of Wnts through Expression of Wild-type and Chimeric Proteins in *Xenopus* Embryos. *Mol*. *Cell Biol*. **15**: 2625 - 2634.

Eaton, S.; Auvinen, P.; Luo, L.; Jan, Y. N.; Simons, K. 1995. Cdc42 and Rac1 Control Different Actin-Dependent Processes in the *Drosophila* Wing Disc Epithelium. *J*. *Cell Biol*. **131**: 151 - 164.

Eaton, S.; Wepf, R.; Simons, K. 1996. Roles for Rac1 and Cdc42 in Planar Polarization and Hair Outgrowth in the Wing of *Drosophila*. *J*. *Cell Biol*. **135**: 1277 - 1289.

Eaton, S. 1997. Planar Polarization of *Drosophila* and Vertebrate Epithelia. *Curr*. *Opin*. *Cell Biol*. **9**: 860 - 866.

Ehrlich, J. S.; Hansen, M. D.; Nelson, W. J. 2002. Spatio-temporal Regulation of Rac1 Localization and Lamellipodia Dynamics during Epithelial Cell-Cell Adhesion. *Dev Cell* **3**: 259 - 270.

Eisenberg, C. A.; Gourdie, R. G.; Eisenberg, L. M. 1997. Wnt-11 Is Expressed in Early Avian Mesoderm and Required for the Differentiation of the Quail Mesoderm Cell Line QCE-6. *Development* **124**: 525 - 536.

Feldman, B.; Gates, M. A.; Egan, E. S.; Dougan, S. T.; Rennebeck, G.; Sirotkin, H. I.; Schier, A. F.; Talbot, W. S. 1998. Zebrafish Organizer Development and Germ-Layer Formation Require Nodal-Related Signals. *Nature* **395**: 181 - 185.

Ferrari, M. B.; Ribbeck, K.; Hagler, D. J.; Spitzer, N. C. 1998. A Calcium Signaling Cascade Essential for Myosin Thick Filament Assembly in *Xenopus* Myocytes. *J. Cell Biol.* **141**: 1349 - 56.

Fleming, T. P.; Johnson, M. H. 1988. From Egg to Epithelium. *Annu. Rev. Cell Biol.* **4**: 459 - 485.

Geiger, B.; Volberg, T.; Ginsberg, D.; Bitzur, S.; Sabanay, I.; Hynes, R. O. 1990. Broad Spectrum pan-Cadherin Antibodies, Reactive with the C-Terminal 24 Amino Acid Residues of N-Cadherin. *J. Cell Sci.* **97**: 607 - 614.

Gerhart, J., and R. Keller. 1986. Region-Specific Cell Activities in Amphibian Gastrulation. *Annu. Rev. Cell Biol.* **2**: 201 - 229.

Gilbert, S. F. (Ed.) 2003. Developmental Biology, 7th Edition. S*inauer Associates, Sunderland.*

Gilmour, D. T.; Maischein, H. M.; Nüsslein-Volhard, C. 2002. Migration and Function of a Glial Subtype in the Vertebrate Peripheral Nervous System. *Neuron* **34**: 577 - 588.

Glickman, N. S.; Kimmel, C. B.; Jones, M. A.; Adams, R. J. 2003. Shaping the Zebrafish Notochord. *Development* **130**: 873 - 887.

Gong, Y.; Mo, C.; Fraser, S. E. 2004. Planar Cell Polarity Signalling Controls Cell Division Orientation during Zebrafish Gastrulation. *Nature* **430**: 689 – 693.

Goto, T.; Davidson, L.; Asashima, M.; Keller, R. 2005. Planar Cell Polarity Genes Regulate Polarized Extracellular Matrix Deposition during Frog Gastrulation. *Curr. Biol.* **15**: 787 - 793.

Gritsman, K.; Zhang, J.; Cheng, S.; Heckscher, E.; Talbot, W. S.; Schier, A. F. 1999. The EGF-CFC Protein One-eyed Pinhead Is Essential for Nodal Signaling. *Cell* **97**: 121 - 132.

Gritsman, K.; Talbot W. S.; Schier, A. F. 2000. Nodal Signalling Patterns the Organizer. *Development* **127**: 921 - 932.

Gumbiner, B. M. 2000. Regulation of Cadherin Adhesive Activity. *J. Cell Biol.* **148**: 399 - 403.

Habas, R.; Kato, Y.; He, X. 2001. Wnt/Frizzled Activation of Rho Regulates Vertebrate Gastrulation and Requires a Novel Formin Homology Protein Daam1. *Cell* **107**: 843 - 854.

Habas, R.; Dawid, I. B.; He, X. 2003. Coactivation of Rac and Rho by Wnt/Frizzled Signaling Is Required for Vertebrate Gastrulation. *Genes Dev.* **17**: 295 - 309.

Haffter, P.; Granato, M.; Brand, M.; Mullins, M. C.; Hammerschmidt, M.; Kane, D. A.; Odenthal, J.; van Eeden, F. J.; Jiang, Y, J.; Heisenberg, C.-P.; Kelsh, R. N.; Furutani-Seiki, M.; Vogelsang, E.; Beuchle, D.; Schach, U.; Fabian, C.; Nüsslein-Volhard, C. 1996. The Identification of Genes with Unique and Essential Functions in the Development of the Zebrafish, *Danio rerio*. *Development* **123**: 1 - 36.

Hall, A. 1998. Rho GTPases and the Actin Cytoskeleton. *Science* **279**: 509 - 514.

Hannus, M.; Feiguin, F.; Heisenberg, C.-P.; Eaton, S. 2002. Planar Cell Polarization Requires Widerborst, a B' Regulatory Subunit of Protein Phosphatase 2A. *Development* **129**: 3493 - 3503.

He, X.; Saint-Jeannet, J.P.; Wang, Y.; Nathans, J.; Dawid, I.; Varmus, H. 1997. A Member of the Frizzled Protein Family Mediating Axis Induction by Wnt-5A. *Science* **275**: 1652 - 1654.

Heid, P. J.; Voss, E.; Soll, D. R. 2002. 3D-DIASemb: a Computer-Assisted System for Reconstructing and Motion Analyzing in 4D Every Cell and Nucelus in a Developing Embryo. *Dev. Biol.* **245**: 329 - 347.

Heid, P. J.; Geiger, J.; Wessels, D.; Voss, E.; Soll, D. R. 2005. Computer-Assisted Analysis of Filopod Formation and the Role of Myosin II Heavy Chain Phosphorylation in Dictyostelium. *J. Cell Sci.* **118**: 2225 - 2237.

Heisenberg, C. P.; Brand, M.; Jiang, Y. J.; Warga, R. M.; Beuchle, D.; van Eeden, F. J.; Furutani-Seiki, M.; Granato, M.; Haffter, P.; Hammerschmidt, M.; Kane, D. A.; Kelsh, R. N.; Mullins, M. C.; Odenthal, J.; Nüsslein-Volhard, C. 1996. Genes Involved in Forebrain Development in the Zebrafish, *Danio rerio*. *Development* **123**: 191 - 203.

Heisenberg, C.-P.; Nüsslein-Volhard, C. 1997. The Function of *silberblick* in the Positioning of the Eye Anlage in the Zebrafish Embryo. *Dev. Biol.* **184**: 85 - 94.

Heisenberg, C. P.; Tada, M.; Rauch, G. J.; Saúde, L.; Concha, M. L.; Geisler, R.; Stemple, D. L.; Smith, J. C.; Wilson, S. W. 2000. *silberblick/wnt11* Mediates Convergent Extension Movements during Zebrafish Gastrulation. *Nature* **405**: 76 - 81.

Heisenberg, C.-P.; Tada, M. 2002. Zebrafish Gastrulation Movements: Bridging Cell and Developmental Biology. *Semin. Cell Dev. Biol.* **13**: 471 - 479.

Helde, K. A.; Wilson, E. T.; Cretekos, C. J.; Grunwald, D. J. 1994. Contribution of Early Cells to the Fate Map of the Zebrafish Gastrula. *Science* **265**: 517 - 520.

Hopkins, C. R.; Gibson, A.; Shipman, M.; Strickland, D. K.; Trowbridge, I. S. 1994. In Migrating Fibroblasts, Recycling Receptors are Concentrated in Narrow Tubules in the Pericentriolar Area, and then Routed to the Plasma Membrane of the Leading Lamella. *J. Cell Biol.* **125**: 1265 - 1274.

Huelsken, J.; Behrens, J. 2002. The Wnt Signalling Pathway. *J. Cell Sci.* **115**: 3977 - 3978.

Izumi, G.; Sakisaka, T.; Baba, T.; Tanaka, S.; Morimoto, K.; Takai, Y. 2004. Endocytosis of E-cadherin Regulated by Rac and Cdc42 Small G Proteins through IQGAP1 and Actin Filaments. *J. Cell Biol.* **166**: 237 - 248.

Jacinto, A.; Wolpert, L. 2001. Filopodia. *Curr. Biol.* **11**: R634.

Jarrett, O.; Stow, J. L.; Yap, A. S.; Key, B. 2002. Dynamin-Dependent Endocytosis Is Necessary for Convergent-Extension Movements in *Xenopus* Animal Cap Explants. *Int. J. Dev. Biol.* **46**: 467 - 473.

Jessen, J.; Topczewski, J.; Bingham, S.; Sepich, D. S.; Marlow, F.; Chandrasekhar, A.; Solnica-Krezel, L. 2002. Zebrafish *trilobite* Identifies New Roles for Strabismus in Gastrulation and Neuronal Movements. *Nat. Cell Biol.* **4**: 610 - 615.

Kaibuchi, K.; Kuroda, S.; Fukata, M.; Nakagawa, M. 1999. Regulation of Cadherin-Mediated Cell-Cell Adhesion by the Rho Family GTPases. *Curr. Opin. Cell Biol.* **11**: 591 - 596.

Kaksonen, M.; Sun, Y.; Drubin, D. G. 2003. A Pathway for Association of Receptors, Adaptors, and Actin during Endocytic Internalization. *Cell* **115**: 475 - 487.

Kane, D. A.; McFarland, K. N.; Warga, R. M. 2005. Mutations in Half Baked/E-Cadherin Block Cell Behaviors that are Necessary for Teleost Epiboly. *Development* **132**: 1105 - 1116.

Karlstrom, R. O.; Kane, D. A. 1996. A Flipbook of Zebrafish Embryogenesis. *Development* **123**: 1 - 461

Keller, R.; Davidson, L.; Edlund, A.; Elul, T.; Ezin, M.; Shook, D.; Skoglund, P. 2000. Mechanisms of Convergence and Extension by Cell Intercalation. *Philos. Trans. R. Soc. Lond. B Biol. Sci.* **355**: 897 - 922.

Keller, R. 2002. Shaping the Vertebrate Body Plan by Polarized Embryonic Cell Movements. *Science* **298**: 1950 - 1954.

Keller, R.; Davidson, L. A.; Shook, D. R. 2003. How We Are Shaped: the Biomechanics of Gastrulation. *Differentiation* **71**: 171 - 205.

Kilian, B.; Mansukoski, H. K.; Barbosa, F. C.; Ulrich, F.; Tada, M.; Heisenberg, C.-P. 2003. The Role of *ppt*/*wnt5* in Regulating Cell Shape and Movement during Zebrafish Gastrulation. *Mech. Dev*. **120**: 467 - 476.

Kim S. H.; Yamamoto, A.; Bouwmeester, T.; Agius, E.; Robertis, E. M. 1998. The Role of Paraxial Protocadherin in Selective Adhesion and Cell Movements of the Mesoderm during *Xenopus* Gastrulation. *Development* **125**: 4681 - 4690.

Kimelman D.; Schier, A. F. 2002. Mesoderm induction and patterning. *Res. Probl. Cell Differ*. **40**:15 - 27.

Kimmel, C. B.; Ballard, W. W.; Kimmel, S. R.; Ullmann, B.; Schilling, T. F. 1995. Stages of embryonic development of the zebrafish. *Dev. Dyn*. **203**: 253 - 310.

Kühl, M.; Finnemann, S.; Binder, O.; Wedlich, D. 1996. Dominant Negative Expression of a Cytoplasmically Deleted Mutant of XB/U-Cadherin Disturbs Mesoderm Migration during Gastrulation in *Xenopus laevis*. *Mech. Dev.* **54**: 71 - 82.

Kühl, M.; Sheldahl, L. C.; Park, M.; Miller, J. R.; Moon, R. T. 2000. The Wnt/Ca^{2+} Pathway: a New Vertebrate Wnt Signaling Pathway Takes Shape. *Trends Genet*. **16**: 279 - 283.

Lanzetti, L.; Rybin, V.; Malabarba, M. G.; Christoforidis, S.; Scita, G.; Zerial, M.; Di Fiore, P. P. 2000. The Eps8 Protein Coordinates EGF Receptor Signalling through Rac and Trafficking through Rab5. *Nature* **408**: 374 - 377.

Lauffenburger, D. A.; Horwitz, A. F. 1996. Cell Migration: A Physically Integrated Molecular Process. *Cell* **84**: 359 - 369.

Lankford, K. L.; Letourneau, P. C. 1989. Evidence that Calcium May Control Neurite Outgrowth by Regulating the Stability of Actin Filaments. *J. Cell Biol.* **109**: 1229 - 43.

Lawson, M. A.; Maxfield, F. R. 1995. Ca^{2+}- and Calcineurin-Dependent Recycling of an Integrin to the Front of Migrating Neutrophils. *Nature* **377**: 75 - 79.

Le, T. L.; Yap, A. S.; Stow, J. L. 1999. Recycling of E-Cadherin: a Potential Mechanism for Regulating Cadherin Dynamics. *J. Cell Biol.* **146**: 219 - 232.

Le, T. L.; Joseph, S. R..; Yap, A. S.; Stow, J. L. 2002. Protein Kinase C Regulates Endocytosis and Recycling of E-cadherin. *Am. J. Phys. Cell Physiol.* **283**: C489 - C499.

Lecuit, T. 2005. Adhesion Remodeling Underlying Tissue Morphogenesis. *Trends Cell Biol.* **15**: 34 - 42.

Lee, C. H.; Gumbiner B. M. 1995. Disruption of Gastrulation Movements in *Xenopus* by a Dominant-Negative Mutant for C-Cadherin. *Dev. Biol.* **171**: 363 - 373.

Lekven, A. C.; Thorpe, C. J.; Waxman, J. S.; Moon, R. T. 2001. Zebrafish Wnt8 Encodes Two Wnt8 Proteins on a Bicistronic Transcript and is Required for Mesoderm and Neurectoderm Patterning. *Dev. Cell* **1**: 103 - 114.

Lele, Z.; Folchert, A.; Concha, M.; Rauch, G. J.; Geisler, R.; Rosa, F.; Wilson, S. W.; Hammerschmidt, M.; Bally-Cuif, L. 2002. Parachute/N-cadherin Is Required for Morphogenesis and Maintained Integrity of the Zebrafish Neural Tube. *Development* **129**: 3281 - 3294.

Lu, Z.; Ghosh, S.; Wang, Z.; Hunter, T. 2003. Downregulation of Caveolin-1 Function by EGF Leads to the Loss of E-cadherin, Increased Transcriptional Activity of β-Catenin, and Enhanced Tumor Cell Invasion. *Cancer Cell* **4**: 499 - 515.

Makita, R.; Mizuno, T.; Koshida, S.; Kuroiwa, A.; Takeda, H. 1998. Zebrafish Wnt11: Pattern and Regulation of the Expression by the Yolk Cell and No Tail Activity. *Mech. Dev.* **71**: 165 - 176.

Marlow, F.; Topczewski, J.; Sepich, D. S.; Solnica-Krezel, L. 2002. Zebrafish Rho Kinase 2 Acts Downstream of *wnt11* to Mediate Cell Polarity and Effective Convergence and Extension Movements. *Curr. Biol.* **12**: 876 - 884.

Marsden, M.; DeSimone, D. W. 2001. Regulation of Cell Polarity, Radial Intercalation and Epiboly in *Xenopus*: Novel Roles for Integrin and Fibronectin. *Development* **128**: 3635 - 3647.

Marsden, M.; DeSimone, D. W. 2003. Integrin-ECM Interactions Regulate Cadherin-Dependent Cell Adhesion and are Required for Convergent Extension in *Xenopus*. *Curr. Biol.* **13**: 1182 - 1191.

Medina, A.; Swain, R. K.; Kuerner, K.-M.; Steinbeisser, H. 2004. *Xenopus* Paraxial Protocadherin Has Signaling Functions and Is Involved in Tissue Separation. *EMBO J.* **23**: 3259 - 3269.

Merrifield, C.; Feldman, M. E.; Wan, L.; Almers, W. 2002. Imaging Actin and Dynamin Recruitment during Invagination of Single Clathrin-Coated Pits. *Nat. Cell Biol.* **9**: 691 - 698.

Miller, J. R. 2001. The Wnts. *Gen. Biol.* **3**: REVIEWS3001.1 - 3001.15.

Miyagi, C.; Yamashita, S.; Ohba, Y.; Yoshizaki, H.; Matsuda, M.; Hirano, T. 2004. STAT3 Non Cell-Autonomously Controls Planar Cell Polarity during Zebrafish Convergence and Extension. *J. Cell Biol.* **166**: 975 - 981.

Mizuno, T.; Yamaha, E.; Wakahara, M.; Kuroiwa, A.; Takeda, H. 1996. Mesoderm Induction in Zebrafish. *Nature* **383**: 131 - 132.

Montell, D. J. 2003. Border-Cell Migration: the Race Is On. *Nat. Rev. Mol. Cell Biol.* **4**: 13 - 24.

Montero, J. A.; Kilian, B.; Chan, J.; Bayliss, P. E.; Heisenberg, C.-P. 2003. Phosphoinositide 3-Kinase Is Required for Process Outgrowth and Cell Polarization of Gastrulating Mesendodermal Cells. *Curr. Biol.* **13**: 1279 - 1289.

Montero, J. A.; Heisenberg, C.-P. 2003. Adhesive Crosstalk in Gastrulation. *Dev. Cell* **5**: 190 - 191.

Montero, J. A.; Heisenberg, C.-P. 2004. Gastrulation Dynamics: Cells Move into Focus. *Trends Cell Biol.* **14**: 620 - 627.

Montero, J. A.; Carvalho, L.; Wilsch-Bräuninger, M.; Kilian, B.; Mustafa, C.; Heisenberg, C.-P. 2005. Shield Formation at the Onset of Zebrafish Gastrulation. *Development* **132**: 1187 - 1198.

Müller, P.Y.; Janovjak, H.; Miserez, A. R.; Dobbie, Z. 2002. Processing of Gene Expression Data Generated by Quantitative Real-Time RT-PCR. *Biotechniques* **32**: 1372 - 1379.

Myers, D. C.; Sepich, D. S.; Solnica-Krezel, L. 2002. Convergence and Extension in Vertebrate Gastrulae: Cell Movements According to or in Search of Identity? *Trends Genet*. **18**: 447 - 455.

Neely, M. D.; Gesemann, M. 1994. Disruption of Microfilaments in Growth Cones Following Depolarization and Calcium Influx. *J. Neurosci*. **14**: 7511 - 20.

Niewiadomska, P.; Godt, D.; Tepass, U. 1999. DE-Cadherin Is Required for Intercellular Motility during *Drosophila* Oogenesis. *J. Cell Biol*. **144**: 533 - 547.

Oates, A. C.; Wollberg, P.; Pratt, S. J.; Paw, B. H.; Johnson, S. L.; Ho, R. K.; Postlethwait, J. H.; Zon, L. I.; Wilks, A. F. 1999. Zebrafish Stat3 Is Expressed in Restricted Tissues during Embryogenesis and Stat1 Rescues Cytokine Signaling in a STAT1-Deficient Human Cell Line. *Dev. Dyn*. **215**: 352 - 370.

Okada, A.; Lansford, R.; Weimann, J. M.; Fraser, S. E.; McConnell, S. K. 1999. Imaging Cells in the Developing Nervous System with Retrovirus Expressing Modified Green Fluorescent Protein. *Exp. Neurol*. **156**: 394 - 406.

Ouko, L.; Ziegler, T. R.; Gu, L. H.; Eisenberg, L. M.; Yang, V. W. 2004. Wnt11 Signaling Promotes Proliferation, Transformation, and Migration of IEC6 Intestinal Epithelial Cells. *J. Biol. Chem*. **279**: 26707 - 26715.

Pelkmans, L.; Burli, T.; Zerial, M.; Helenius, A. 2004. Caveolin-Stabilized Membrane Domains as Multifunctional Transport and Sorting Devices in Endocytic Membrane Traffic. *Cell* **118**: 767 - 780.

Penzo-Mendez, A.; Umbhauer, M.; Djiane, A.; Boucaut, J. C.; Riou, J. F. 2003. Activation of Gβγ Signaling Downstream of Wnt-11/Xfz7 Regulates Cdc42 Activity during *Xenopus* Gastrulation. *Dev. Biol*. 257: 302 - 314.

Puech, P.-H.; Taubenberger, A.; Ulrich, F.; Krieg, M.; Müller, D. J.; Heisenberg, C.-P. 2005. Measuring Cell Adhesion Forces of Primary Gastrulating Cells from Zebrafish using Atomic Force Microscopy. *J. Cell Sci.*, **in press**.

Rauch, G. J.; Hammerschmidt, M.; Blader, P.; Schauerte, H. E.; Strähle, U.; Ingham, P. W.; McMahon, A. P.; Haffter, P. 1997. Wnt5 Is Required for Tail Formation in the Zebrafish Embryo. *Cold Spring Harb. Symp. Quant. Biol.* **62**: 227 - 234.

Rebagliati, M. R.; Toyama, R.; Haffter, P.; Dawid, I. B. 1998. *cyclops* Encodes a Nodal-Related Factor Involved in Midline Signaling. *Proc. Natl. Acad. Sci. USA* **95**: 9932 - 9937.

Rothbacher, U.; Laurent, M. N.; Deardorff, M. A.; Klein, P. S.; Cho, K. W.; Fraser, S. E. 2000. Dishevelled Phosphorylation, Subcellular Localization and Multimerization Regulate Its Role in Early Embryogenesis. *EMBO J.* **19**: 1010 - 1022.

Ruohslahti, E.; Pierschbacher, M. D. 1987. New Perspectives in Cell Adhesion: RGD and Integrins. *Science* **238**: 491 - 497.

Sampath, K.; Rubinstein, A. L.; Cheng, A. M.; Liang, J. O.; Fekany, K.; Solnica-Krezel, L.; Korzh, V.; Halpern, M. E.; Wright, C. V. 1998. Induction of the Zebrafish Ventral Brain and Floorplate Requires Cyclops/Nodal Signalling. *Nature* **395**: 185 - 189.

Schier, A. F.; Shen, M. M. 2000. Nodal Signalling in Vertebrate Development. *Nature* **403**: 385 - 389.

Schier, A. F.; Talbot, W. S. 2001. Nodal Signalling and the Zebrafish Organizer. *Int. J. Dev. Biol.* **45**: 289 - 297.

Schier, A. F. 2003. Nodal Signalling in Vertebrate Development. *Ann. Rev. Cell Dev. Biol.* **19**: 589 - 621.

Scholpp, S.; Brand, M. 2004. Endocytosis Controls Spreading and Effective Signaling Range of Fgf8 Protein. *Curr Biol.* **14**: 1834 - 1841.

Schulte-Merker, S.; Hammerschmidt, M.; Beuchle, D.; Cho, K. W.; De Robertis, E. M.; Nüsslein-Volhard, C. 1994. Expression of Zebrafish goosecoid and *no tail* Gene Products in Wild-Type and Mutant *no tail* Embryos. *Development* **120**: 843 - 852.

Sepich, D. S.; Myers, D. C.; Short, R.; Topczewski, J.; Marlow, F.; Solnica-Krezel, L. 2000. Role of the Zebrafish *trilobite* Locus in Gastrulation Movements of Convergence and Extension. *Genesis* **27**: 159 - 173.

Sguigna, C.; Fluck, R.; Barber, B. 1988. Calcium Dependence of Rhythmic Contractions of the *Oryzias latipes* Blastoderm. *Comp. Biochem. Physiol. C.* **89**: 369 - 74.

Shibamoto, S.; Hayakawa, M.; Takeuchi, K.; Hori, T.; Oku, N.; Miyazawa, K.; Kitamura, N.; Takeichi, M.; Ito, F. 1994. Tyrosine Phosphorylation of β-Catenin and Plakoglobin Enhanced by Hepatocyte Growth Factor and Epidermal Growth Factor in Human Carcinoma Cells. *Cell Adhes. Commun.* **1**: 295 - 305.

Slusarski, D. C.; Corces, V. G.; Moon, R. T. 1997. Interaction of Wnt and a Frizzled Homologue Triggers G-Protein-Linked Phosphatidylinositol Signalling. *Nature* **390**: 410 - 413.

Smart, E. J.; De Rose, R. A.; Farber, S. A. 2004. Annexin 2-Caveolin 1 Complex Is a Target of Ezetimibe and Regulates Intestinal Cholesterol Transport. *Proc. Natl. Acad. Sci. U S A* **101**: 3450 - 3455.

Smith, J. C. 1995. Mesoderm-Inducing Factors and Mesodermal Patterning. *Curr. Opin. Cell Biol.* **7**:856 - 861.

Soll, D. 1995. The Use of Computers in Understanding How Animal Cells Crawl. *Int. Rev. Cytol.* **163**: 43 - 104.

Soll, D. R.; Voss, E.; Johnson, O.;Wessels, D. 2000. Three-Dimensional Reconstruction and Motion Analysis of Living, Crawling Cells. *Scanning* **22**: 249 - 257.

Solnica-Krezel, L.; Stemple, D. L.; Mountcastle-Shah, E.; Rangini, Z.; Neuhauss, S. C.; Malicki, J.; Schier, A. F.; Stainier, D. Y.; Zwartkruis, F.; Abdelilah, S.; Driever, W. 1996. Mutations Affecting Cell Fates and Cellular Rearrangements during Gastrulation in Zebrafish. *Development* **123**: 67 - 80.

Solnica-Krezel, L. 2005. Conserved Patterns of Cell Movements during Vertebrate Gastrulation. *Curr. Biol.* **15**: R213 - R228.

Stainier, D. Y. 2002. A Glimpse into the Molecular Entrails of Endoderm Formation. *Genes Dev.* **16**: 893 - 907.

Steinberg, M. 1996. Adhesion in Development: An Historical Overview. *Dev. Biol.* **180**: 377 - 388.

Stern, C. (Ed.) 2004. Gastrulation: From Cells to Embryo. *Cold Spring Harbor Laboratory Press,* New York.

Strutt D. I.; Weber, U.; Mlodzik, M. 1997. The Role of RhoA in Tissue Polarity and Frizzled Signalling. *Nature* **387**: 292 - 295.

Sumanas, S.; Strege, P.; Heasman, J.; Ekker, S.C. 2000. The Putative Wnt Receptor

Xenopus Frizzled-7 Functions Upstream of β-Catenin in Vertebrate Dorsoventral Mesoderm Patterning. *Development* **127**: 1981 - 1990.

Tada, M.; Smith, J. C. 2000. Xwnt11 Is a Target of *Xenopus* Brachyury: Regulation of Gastrulation Movements via Dishevelled, but not through the Canonical Wnt Pathway. *Development* **127**: 2227 - 2238.

Tada, M.; Concha, M. L. 2001. Vertebrate Gastrulation: Calcium Waves Orchestrate Cell Movements. *Curr. Biol.* **11**: R470 - R472

Tada, M.; Concha, M. L.; Heisenberg, C.-P. 2002. Non-Canonical Wnt Signalling and Regulation of Gastrulation Movements. *Semin. Cell Dev. Biol.* **13**: 251 - 260.

Takaishi, K.; Sasaki, T.; Kotani, H.; Nishioka, H.; Takai, Y. 1997. Regulation of Cell-Cell Adhesion by Rac and Rho Small G Proteins in MDCK Cells. *J. Cell Biol.* **139**: 1047 - 1059.

Talbot, W. S.; Trevarrow, B.; Halpern, M. E.; Melby, A. E.; Farr, G.; Postlethwait, J. H.; Jowett, T.; Kimmel, C. B.; Kimelman, D. 1995. A Homeobox Gene Essential for Zebrafish Notochord Development. *Nature* **378**: 150 - 157.

Tao, Q.; Yokota, C.; Puck, H.; Kofron, M.; Birsoy, B.; Yan, D.; Asashima, M.; Wylie, C. C.; Lin, X.; Heasman, J. 2005. Maternal Wnt11 Activates the Canonical Wnt Signaling Pathway Required for Axis Formation in *Xenopus* Embryos. *Cell* **120**: 857 - 871.

Thisse, C.; Thisse, B.; Halpern, M. E.; Postlethwait, J. H. 1994. *goosecoid* Expression in Neurectoderm and Mesendoderm Is Disrupted in Zebrafish *cyclops* Gastrulas. *Dev. Biol.* **164**: 120 - 129.

Tolwinski, N. S.; Wieschaus, E. 2004. A Nuclear Function for Armadillo/β-Catenin. *PloS Biol*. **2**: 486 - 493.

Topczewski, J.; Sepich, D. S.; Myers, D. C.; Walker, C.; Amores, A.; Lele, Z.; Hammerschmidt, M.; Postlethwait, J.; Solnica-Krezel, L. 2001. The Zebrafish Glypican Knypek Controls Cell Polarity during Gastrulation Movements of Convergent Extension. *Dev. Cell* **1**: 251 - 264.

Topol, L.; Jiang, X.; Choi, H.; Garrett-Beal, L.; Carolan, P. J..; Yang, Y. 2003. Wnt-5a Inhibits the Canonical Wnt Pathway by Promoting GSK-3-Independent β-Catenin Degradation. *J. Cell Biol*. **162**: 899 - 908.

Torres, M. A.; Yang-Snyder, J. A.; Purcell, S. M.; DeMarais, A. A.; McGrew, L. L.; Moon, R. T. 1996. Activities of the Wnt-1 Class of Secreted Signaling Factors Are Antagonized by the Wnt-5A Class and by a Dominant Negative Cadherin in Early *Xenopus* Development. *J. Cell Biol*. **133**: 1123 - 37.

Trinh, L. A.; Stainier, D. Y. 2004. Fibronectin Regulates Epithelial Organization during Myocardial Migration in Zebrafish. *Dev. Cell* **6**: 371 - 382.

Ulrich, F.; Concha, M. L.; Heid, P. J.; Voss, E.; Witzel, S.; Roehl, H.; Tada, M.; Wilson, S. W.; Adams, R. J.; Soll, D. R.; Heisenberg, C.-P. 2003. *slb/wnt11* Controls Hypoblast Cell Migration and Morphogenesis at the Onset of Zebrafish Gastrulation. *Development* **130**: 5375 - 5834.

Ulrich, F.; Heisenberg, C.-P. 2005. Gastrulation in Zebrafish. In: Gong, Z; Korzh, V. (Ed.): Fish Development and Genetics - The Zebrafish and Medaka Models. *World Scientific Publishing*, *Singapore*.

Umbhauer, M.; Djiane, A.; Goisset, C.; Penzo-Mendez, A.; Riou, J.F.; Boucaut,

J.C.; Shi, D.L. 2000. The C-terminal Cytoplasmic Lys-Thr-XXX-Trp Motif in Frizzled Receptors Mediates Wnt/β-Catenin Signalling. *EMBO J*. **19**: 4944 - 4954.

Ungar, A. R.; Kelly, G. M.; Moon, R. T. 1995. *wnt4* Affects Morphogenesis when Misexpressed in the Zebrafish Embryo. *Mech. Dev*. **52**: 153 - 164.

Unterseher, F.; Hefele, J. A.; Giehl, K.; De Robertis, E. M.; Wedlich, D.; Schambony, A. 2004. Paraxial Protocadherin Coordinates Cell Polarity during Convergent Extension via RhoA and JNK. *EMBO J*. **23**: 3259 - 3269.

Van Aelst, L.; Symons, M. 2002. Role of Rho Family GTPases in Epithelial Morphogenesis. *Genes Dev*. **16**: 1032 - 1054.

Van der Bliek, A. M.; Redelmeier, T. E.; Damke, H.; Tisdale, E. J.; Meyerowitz, E. M.; Schmid, S. 1993. Mutations in Human Dynamin Block an Intermediate Stage in Coated Vesicle Formation. *J. Cell Biol*. **122:** 553 - 563.

Veeman, M. T.; Axelrod, J. D.; Moon, R. T. 2003. A Second Canon. Functions and Mechanisms of β-Catenin-Independent Wnt Signaling. *Dev. Cell* **5**: 367 - 377.

Vestweber, D., Gossler, A.; Boller, K.; Kemler, R. 1987. Expression and Distribution of Cell Adhesion Molecule Uvomorulin in Mouse Preimplantation Embryos. *Dev. Biol*. **124**: 451 - 456.

Wacker, S.; Grimm, K.; Joos, T.; Winklabuer, R. 2000. Development and Control of Tissue Separation at Gastrulation in *Xenopus*. *Dev. Biol*. **224**: 428 - 439.

Wallingford, J. B.: Rowning, B. A.; Vogeli, K. M.; Rothbacher, U.; Fraser, S. E.; Harland, R. M. 2000. Dishevelled Controls Cell Polarity during *Xenopus* Gastrulation. *Nature* **405**: 81 - 85.

Wallingford, J. B.; Ewald, A. J.; Harland, R. M.; Fraser, S. E. 2001. Calcium Signaling during Convergent Extension in *Xenopus*. *Curr. Biol.* **11**: 652 - 661.

Wallingford, J. B.; Fraser, S. E.; Harland, R. M. 2002. Convergent Extension. The Molecular Control of Polarized Cell Movement during Embryonic Development. *Dev. Cell* **2**: 695 - 706.

Walston, T.; Tuskey, C.; Edgar, L.; Hawkins, N.; Ellis, G.; Bowerman, B.; Wood, W.; Hardin, J. 2004. Multiple Wnt Signalling Pathways Converge to Orient the Mitotic Spindle in Early *C. elegans* Embryos. *Dev. Cell* **7**: 831 - 841.

Warga, R. M.; Kimmel, C. B. 1990. Cell Movements during Epiboly and Gastrulation in Zebrafish. *Development* **108**: 569 - 580.

Warga, R. M.; Nüsslein-Volhard, C. 1999. Origin and Development of the Zebrafish Endoderm. *Development* **126**: 827 - 838.

Webb, S. E.; Miller, A. L. 2003. Calcium Signalling during Embryonic Development. *Nat. Rev. Mol. Cell Biol.* **4**: 539 - 551.

Wedlich, D. 2002. The Polarising Role of Cell Adhesion Molecules in Early Development. *Curr. Opin. Cell Biol.* **14**: 563 - 568.

Weidner, K.M.; Behrens, J.; Vandekerckhove, J.; Birchmeier, W. 1990. Scatter Factor: Molecular Characteristics and Effect on the Invasiveness of Epithelial Cells. *J. Cell Biol.* **111**: 2097 - 2108.

Welnhofer, E. A.; Zhao, L.; Cohan, C. S. 1999. Calcium Influx Alters Actin Bundle Dynamics and Retrograde Flow in *Helisoma* Growth Cones. *J. Neurosci.* **19**: 7971 - 82.

Westfall, T. A.; Brimeyer, R.; Twedt, J.; Gladon, J.; Olberding, A.; Furutani-Seiki, M.; Slusarski, D. C. 2003. Wnt-5/Pipetail Functions in Vertebrate Axis Formation as a Negative Regulator of Wnt/β-Catenin Activity. *J. Cell Biol.* **162**: 889 - 898.

Whitman, M. 2001. Nodal Signaling in Early Vertebrate Embryos: Themes and Variations. *Dev. Cell* **1**: 605 - 617.

Wilson, I. A.; Niman, H. L.; Houghten, R. A.; Cherenson, A. R.; Connolly, M. L.; Lerner, R. A. 1984. The Structure of an Antigenic Determinant in a Protein. *Cell* **37**: 767 - 778.

Winklbauer, R.; Keller, R. E. 1996. Fibronectin, Mesoderm Migration, and Gastrulation in *Xenopus*. *Dev. Biol.* **177**: 413 - 426.

Winklbauer, R. Nagel, M.; Selchow, A.; Wacker, S. 1996. Mesoderm Migration in the *Xenopus* Gastrula. *Int. J. Dev. Biol.* **40**: 305 - 311.

Winklbauer, R.; Medina, A.; Swain, R. K.; Steinbeisser, H. 2001. Frizzled-7 Signalling Controls Tissue Separation during *Xenopus* Gastrulation. *Nature* **413**: 856 - 860.

Winter, C. G.; Wang, B.; Ballew, A.; Royou, A.; Karess, R.; Axelrod, J. D.; Luo, L. 2001. *Drosophila* Rho-Associated Kinase (Drok) Links Frizzled-Mediated Planar Cell Polarity Signaling to the Actin Cytoskeleton. *Cell* **105**: 81 - 91.

Wolpert, L. 1991. The Triumph of the Embryo. *Oxford University Press, Oxford.*

Yamamoto, A.; Amacher, S. L.; Kim, S. H.; Geissert, D.; Kimmel, C. B.; De Robertis, E. M. 1998. Zebrafish Paraxial Protocadherin Is a Downstream Target of

Spadetail Involved in Morphogenesis of Gastrula Mesoderm. *Development* **125**: 3389 - 3397.

Yamashita, S.; Miyagi, C.; Carmany-Rampey, A.; Shimizu, T.; Fujii, R.; Schier, A. F.; Hirano, T. 2002. Stat3 Controls Cell Movements during Zebrafish Gastrulation. *Dev. Cell* **2**: 363 - 375.

Yang, X.; Dormann, D.; Münsterberg, A. E.; Weijer, C. J. 2002. Cell Movement Patterns during Gastrulation in the Chick Are Controlled by Positive and Negative Chemotaxis Mediated by FGF4 and FGF8. *Dev. Cell* **3**: 425 - 437.

Yeo, S. Y.; Little, M. H.; Yamada, T.; Miyashita, T.; Halloran, M. C.; Kuwada, J. Y.; Huh, T. L.; Okamoto, H. 2001. Overexpression of a Slit Homologue Impairs Convergent Extension of the Mesoderm and Causes Cyclopia in Embryonic Zebrafish. *Dev. Biol.* **230**:1 - 17.

Zallen, J.A.; Wieschaus, E. 2004. Patterned Gene Expression Directs Bipolar Planar Polarity in *Drosophila*. *Dev*. *Cell* **6**: 343 - 55.

Zerial, M.; McBride, H. 2001. Rab Proteins as Membrane Organizers. *Nat*. *Rev*. *Mol*. *Cell Biol*. **2**: 107 - 117.

Zhong, Y.; Brieher, W. M.; Gumbiner, B. M. 1999. Analysis of C-Cadherin Regulation during Tissue Morphogenesis with an Activating Antibody. *J*. *Cell Biol*. **144**: 351 - 359.

Zhou, X.; Sasaki, H.; Lowe, L.; Hogan, B. L.; Kuehn, M. R. 1993. *Nodal* is a Novel TGFβ Like Gene Expressed in the Mouse Node during Gastrulation. *Nature* **361**: 543 - 547.

Hiermit versichere ich, daß ich die vorliegende Arbeit ohne unzulässige Hilfe Dritter und ohne Benutzung anderer als der angegebenen Hilfsmittel angefertigt habe; die aus fremden Quellen direkt oder indirekt übernommenen Gedanken sind als solche kenntlich gemacht. Die Arbeit wurde bisher weder im Inland noch im Ausland in gleicher oder ähnlicher Form einer anderen Prüfungsbehörde vorgelegt.

Die Arbeit wurde vom 01.07.2001 bis zum 30.06.2005 im Labor von Dr. Carl-Philipp Heisenberg, Max-Planck-Institut für Molekulare Zellbiologie und Genetik, angefertigt. Der betreuende Hochschullehrer an der Technischen Universität Dresden war Herr Prof. Dr. Herwig O. Gutzeit.

Dresden, den 30.06.05

Florian Ulrich, Dipl. Biochem.